

**Phenoxide Chelated Ir(III) N-Heterocyclic Carbene Complexes :  
Synthesis, Characterization, and Evaluation of the in Vitro Anticancer  
Activity**

Yujiao Zhang, Shumiao Zhang\*, Zhenzhen tian, Juanjuan Li, Zhishan Xu, Shanshan Li, Zhe Liu\*

**Supporting Information**

Experimental Section .....	<b>S2-S8</b>
Figure S1-S26.....	<b>S9-S23</b>
Table S1-S17 .....	<b>S24-S28</b>
Figure S27-S62.....	<b>S29-S46</b>

## Experimental Section

### General

All air-sensitive manipulations were performed under a nitrogen atmosphere.  $\text{IrCl}_3 \cdot n\text{H}_2\text{O}$ ,  $\text{Ag}_2\text{O}$ , 1H-imidazole, 1-H-benzimidazole, 2-bromoanisole, n-butyl bromide, benzyl chloride, 4-fluoro-1-(chloromethyl)benzene, 1-chloro-4-(chloromethyl)-benzene, 9-ethylguanine, and 9-methyladenine were purchased from Sigma-Aldrich. All the solvents were of analytical grade. For the biological experiments, DMEM medium, trypsin/EDTA, cisplatin, MTT, MTDR, LTDR, CCCP, chloroquine, AO and phosphate-buffered saline (PBS) were purchased from Sangon Biotech. Tested compounds were dissolved in DMSO, stored at  $-20^\circ\text{C}$ , thawed and diluted with culture medium prior to each experiment.

$^1\text{H}$  NMR spectra and  $^{13}\text{C}$  NMR spectra were acquired at 298 K on Bruker DPX 500 ( $^1\text{H}= 500.13$  MHz and  $^{13}\text{C}=126$  MHz) spectrometers relative to the signal of tetramethylsilane. All data processing was carried out using XWINNMR version 3.6 (Bruker UK Ltd.). The UV-Vis spectra were recorded by TU-1901 UV spectrophotometer and processed using UVWinlab software.

## **X-ray Crystallography**

Single yellow block-shaped crystals of complexes **1** and **10** were obtained by diffusion of n-hexane into CH<sub>2</sub>Cl<sub>2</sub> solutions. A suitable crystal was selected and mounted on a suitable support on an CCD area detector diffractometer. The crystal was kept at a steady T = 298(2) K during data collection. The structure was solved with the ShelXS-97 (Sheldrick, 1990) structure solution program using the direct solution method and by using ShelXTL (Bruker) as the graphical interface. The model was refined with version of ShelXL-2014/7(Sheldrick, 2014) and ShelXL(Sheldrick, 2015) using full matrix least squares on F<sup>2</sup> minimisation. SADABS 2015/1 (Bruker,2015) was used for absorption correction. For complex **1**, R(int) was 0.1334 before and 0.0359 after correction, the Ratio of minimum to maximum transmission is 0.107390, the Lambda/2 correction factor is 0.0015. CCDC-1544033 (**1**) and CCDC-1852809 (**10**) include the detailed crystallographic data for this paper.

## **Hydrolysis Studies**

Solutions of complexes **2**, **4**, **5** and **6** with concentration of 1 mM were formulated in 80% MeOD-d<sub>4</sub>/20% D<sub>2</sub>O (v/v), noting that after the addition of MeOD-d<sub>4</sub> dissolved, D<sub>2</sub>O was added to rapidly dilute. <sup>1</sup>H NMR spectra were recorded after various time intervals at 310 K. Solutions of complexes **2**, **4**, **5** and **6** with final concentrations of 50 μM were prepared in 20% MeOH/80% H<sub>2</sub>O (v/v). UV-vis spectrophotometers were used to monitor the changes in solutions at different time intervals at 298 K.

## **Solubility Experiment**

The solution of complexes were prepared in DMSO with the concentration of 10 mM. The stock solutions were diluted in concentrations ranging from 5×10<sup>-6</sup> to 5×10<sup>-4</sup> mol/L in 80% HEPES (pH=7.2-7.4) and 20% acetonitrile. The saturated solutions were obtained and the spectra were collected from 230 to 800 nm.

## **Interaction with Nucleobases**

A solution containing 1 mol equiv of nucleobase to an solution of complexes **2**, **4**, **5**, and **6** (1 mM) in 80 %MeOD/20 % D<sub>2</sub>O (v/v). <sup>1</sup>H NMR spectra were recorded changes of the reaction of complexes **2**, **4**, **5**, and **6** with nucleobases at 310 K after various time intervals.

## **Cleavage of Plasmid DNA**

Different concentrations of compounds **2**, **4**, **5**, and **6** and pBR322 DNA were incubated for 24 hours at 37°C. The pBR322 DNA was stained with 0.5 mg ml<sup>-1</sup> of GelRed and the cleavage reactions were quenched by the addition of bromophenol blue. Gel electrophoresis experiments

were carried out with pBR322 DNA, in 0.8% agarose solution, at 5 V cm<sup>-1</sup> for 1 h using TAE buffer (40 mM Tris, 1 mM EDTA (disodium salt), Ph=8.3). Gel electrophoresis experiments were operated on a DYY-12C gel electrophoresis spectrometer. A gel imaging system (Smart Gel 600, China) was showed the result of agarose gel electrophoresis of pBR322 DNA.

### **DNA Binding Studies**

Stock solutions of the complexes were prepared by dissolving the complex in DMSO and diluting with 50mM Tris/50mM HCl buffer solution (pH=7.2) to required concentrations. Interaction of complexes with ctDNA was investigated by the absorption and luminescence titrations. Absorption titration experiments were performed by maintaining a constant metal complex concentration (20 μM) and varying the ctDNA (0–108μM) in the buffer at ambient temperature with 5 min equilibration time.

### **Reaction with NADH**

NADH (3.5 mol equiv.) was added to a 1 mM solution of complexes **2**, **4**, **5**, and **6** in 80% MeOD /20% D<sub>2</sub>O (v/v), and the <sup>1</sup>H NMR spectra of these solutions were recorded at 298 K after various time intervals. The reaction of complexes **2**, **4**, **5**, and **6** (ca. 1 μM) with NADH (ca. 100 μM) in 10% MeOH /90% H<sub>2</sub>O (v/v) was monitored by UV-Vis at 298 K after various time intervals. TON was calculated from the difference in NADH absorbance at 339 nm after 8 h multiplied by the ratio of NADH concentration to iridium catalyst. The concentration of NADH was obtained using the extinction coefficient  $\epsilon_{339} = 6220 \text{ M}^{-1}\text{cm}^{-1}$ .

### **Cell Culture**

Lung cancer A549 cells, BEAS-2B human normal lung epithelial cells and HeLa cervical cancer cells were purchased from Shanghai Institute of Biochemistry and Cell Biology (SIBCB) and grew in Dulbecco's Modified Eagle's Medium (DMEM). All media were supplemented with 10% fetal bovine serum, and 1% penicillin–streptomycin solution. All cells grew at 310 K in a humidified incubator under a 5% CO<sub>2</sub> atmosphere.

### **Viability Assay (MTT assay)**

The all complexes were dissolved in DMSO in order to prepare a stock solution of the drug. After inoculation of 5000 cells per well into a 96-well plate, the cells were pre-incubated in a drug-free medium at 310K for 24 hours. The stock solution were further diluted using cell culture medium until the working concentrations, then different concentrations of the complexes were added to cells. The drug exposure period was 24 h. 15 μL of 5 mg/mL MTT solution was added to form a purple formazan. Subsequently, 100 μL of dimethyl sulfoxide (DMSO) was transferred into each well to dissolve the purple formazan. The results were monitored by a microplate reader (DNM-9606,

Perlong Medical, Beijing, China) at an absorbance of 570 nm. Each well was performed in triplicate and each experiment was repeated at least three times. The IC<sub>50</sub> values quoted are mean ± SEM.

### **Cell Cycle Analysis**

The A549 cancer cells were seeded in a six well plate at  $1.5 \times 10^6$  per well and preincubated in drug-free medium at 310 K for 24 h. Complexes **2**, **4**, **6** and **12** were added against A549 cancer cells at concentrations of  $0.25 \times IC_{50}$ ,  $0.5 \times IC_{50}$  and  $1 \times IC_{50}$ . Supernatants were removed by suction after 24h. Finally, cells were harvested by trypsin-EDTA and fixed for 24 h using cold 70 % ethanol. In PBS containing propidium iodide (PI) and RNase, DNA staining was achieved by resuspending the cell pellets. Cell pellets were washed and resuspended in PBS and then analyzed in a flow cytometer (ACEA NovoCyte, Hangzhou, China) using excitation of DNA-bound PI at 488 nm, with emission at 585 nm. Data were processed by NovoExpress™ software. The cell cycle distribution was shown as the percentage of cells containing G<sub>0</sub>/G<sub>1</sub>, S and G<sub>2</sub>/M DNA as identified by propidium iodide staining.

### **Induction of Apoptosis**

Flow cytometry analysis of apoptotic populations of A549 cells caused by exposure to iridium complexes was carried out using an Annexin V-FITC Apoptosis Detection Kit (Beyotime Institute of Biotechnology, China) according to the supplier's instructions. Briefly, A549 cells ( $1.5 \times 10^6/2$  ml per well) were seeded into a six-well plate and were preincubated in drug-free medium at 310 K for 24 h. Complexes **2**, **4**, **6** and **12** were added into cells at concentrations of  $0.5 \times IC_{50}$ ,  $1 \times IC_{50}$ ,  $2 \times IC_{50}$  and  $3 \times IC_{50}$ . After 24 h of drug exposure, the cells were collected, washed once with PBS, and resuspended in 195 µl of annexin V-FITC binding buffer, which was then added to 5 µl of annexin V-FITC and 10 µl of PI, and then incubated at room temperature in the dark for 15 min. Subsequently, the buffer was placed in an ice bath in the dark. The samples were analyzed by a flow cytometer (ACEA NovoCyte, Hangzhou, China). In addition, complex **6** was exposed to cells for 12 hours and the remaining steps were the same.

### **ROS Determination**

Flow cytometry analysis of ROS generation in A549 cells caused by exposure to iridium complexes was carried out using a Reactive Oxygen Species Assay Kit (Beyotime Institute of Biotechnology, Shanghai, China) according to the supplier's instructions. Briefly,  $1.5 \times 10^6$  A549 cells per well were seeded into a six-well plate. The cells were preincubated in drug-free medium at 310 K for 24 h in a 5% CO<sub>2</sub> humidified atmosphere, and then drugs were added at concentrations of  $0.25 \times IC_{50}$  and  $0.5 \times IC_{50}$ . After 24 h of drug exposure, the cells were washed twice with PBS and then incubated with the DCFH-DA probe (10 µM) at 37 °C for 30 min. The cells were then immediately washed three times with PBS. The fluorescence intensity was analyzed by flow

cytometry (ACEA NovoCyte, Hangzhou, China). The data were processed using NovoExpress™ software. At all times, the samples were kept in the dark to avoid light-induced ROS production.

#### **Mitochondrial Membrane Assay**

A549 cells were seeded at a density of  $1.5 \times 10^6$  cells/well in six-well plates and kept for 24 h in drug-free medium at 310 K in a humidified atmosphere. Then A549 cells were treated with  $0.25 \times IC_{50}$ ,  $0.5 \times IC_{50}$ ,  $1 \times IC_{50}$  and  $2 \times IC_{50}$  of complexes **2**, **4**, **6** and **12** for 24 h under similar conditions and were treated in triplicate. Supernatants were removed by suction, and each well was washed with PBS before detaching the cells using trypsin-EDTA. The samples were stained in flow cytometry tubes protected from light, keeping for 30 min at room temperature and immediately analyzing by a flow cytometer (ACEA Novo Cyte, Hangzhou, China). For positive controls, the cells were exposed to carbonyl cyanide 3-chlorophenylhydrazone (CCCP) with  $5 \mu\text{M}$  for 20 min. Data were processed using Novo Express™ software.

#### **Lysosomal damage**

A549 cells was cultured at 35 mm dishes, and exposed to complex **6** at indicated concentrations for 6 h. Then A549 cells was irradiated with a 425 nm LED light array ( $40 \text{ mW}/\text{cm}^2$ ) for 15 min ( $36 \text{ J}/\text{cm}^2$ ). The cells were washed twice with PBS, and incubated with AO ( $5 \mu\text{M}$ ) at  $37^\circ\text{C}$  for 15 min. The cells were washed twice with PBS, and observed immediately under a confocal microscope. Green fluorescence was acquired with excitation at 488 nm and emission at 490-530 nm; red fluorescence was acquired with excitation at 488nm and emission at 605-645 nm.

#### **Synthesis of the ligands (L1-L8).**

General method: The first step: 2-bromoanisole (10.0 mmol), 1-H-imidazole (15.0 mmol), CuO (1.0 mmol),  $\text{K}_2\text{CO}_3$  (50.0 mmol) were stirred in dimethyl sulfoxide (DMSO) (15mL) at  $150^\circ\text{C}$  for 10 h. However, a mixture of 1-H-benzimidazole (15.0 mmol), 2-bromoanisole (10.0 mmol), KOH (10.0mmol), and  $\text{Cu}_2\text{O}$  (1.0mmol) was suspended 15 mL of DMSO and stirred at  $150^\circ\text{C}$  for 24 h. These two reactions are different in using bases and catalysts but are both catalytic N-arylation of nitrogen-containing heterocycles with aryl halides. The mixture was cooled, diluted with  $\text{CH}_2\text{Cl}_2$  (20 mL) and water (20 mL), stirred for 1 hour, and filtered. The filtrate was washed with water ( $3 \times 20 \text{ mL}$ ) and dried over anhydrous  $\text{Na}_2\text{SO}_4$ . The crude product was purified by column chromatography (silica gel, petroleum ether/ ethyl acetate).

The second step: to the product of the first step was added a solution of 48% HBr and the mixture were refluxed under  $\text{N}_2$  for 12 h. The solution was cooled and added  $\text{KHCO}_3$  for neutralization until complete release of  $\text{CO}_2$  and precipitate formed. Then the precipitate was filtered and dried in vacuo to obtain solid product.

The third step: the product of the previous step and a series of halogenated hydrocarbons were refluxed under N<sub>2</sub> atmosphere overnight to obtain the target product.

3-Butyl-1-(2-hydroxyphenyl)-1-H-imidazolium bromide (**L1**) Yield: 94%, yellow liquid. <sup>1</sup>H NMR (500.13 MHz, DMSO-d<sub>6</sub>): δ 10.85 (s, 1H), 9.57 (s, 1H), 8.06 (t, J = 1.7 Hz, 1H), 8.00 (t, J = 1.7 Hz, 1H), 7.54 (dd, J = 7.9, 1.5 Hz, 1H), 7.44 – 7.39 (td, J = 7.9, 1.1 Hz, 1H), 7.14 (dd, J = 8.2, 0.9 Hz, 1H), 7.03 (td, J = 7.8, 1.1 Hz, 1H), 4.27 (t, J = 7.2 Hz, 2H), 1.89 – 1.81 (m, 2H), 1.28-1.36 (m, 2H), 0.93 (t, J = 7.4 Hz, 3H).

3-Benzyl-1-(2-hydroxyphenyl)-1-H-imidazolium chloride (**L2**) Yield: 47%, colorless solid. <sup>1</sup>H NMR (500.13 MHz, DMSO-d<sub>6</sub>) δ 10.98 (s, 1H), 9.76 (s, 1H), 8.07 (t, J = 1.8 Hz, 1H), 8.00 (t, J = 1.7 Hz, 1H), 7.55 (dd, J = 8.0, 1.5 Hz, 1H), 7.53 – 7.48 (m, 2H), 7.48 – 7.35 (m, 4H), 7.18 (dd, J = 8.2, 0.9 Hz, 1H), 7.02– 7.00 (m, 1H), 5.53 (s, 2H).

3-(4-chloro-1-benzyl)-1-(2-hydroxyphenyl)-1-H-imidazolium chloride (**L3**) Yield: 72%, colorless solid. <sup>1</sup>H NMR (500.13 MHz, DMSO-d<sub>6</sub>) δ 11.04 (s, 1H), 9.76 (s, 1H), 8.08 (t, J = 1.8 Hz, 1H), 8.00 (t, J = 1.8 Hz, 1H), 7.61 – 7.50 (m, 5H), 7.42 – 7.38 (m, 1H), 7.20 (dd, J = 8.2, 1.1 Hz, 1H), 7.02 (td, J = 7.9, 1.2 Hz, 1H), 5.53 (s, 2H).

3-(4-fluoro-1-benzyl)-1-(2-hydroxyphenyl)-1-H-imidazolium chloride (**L4**) Yield: 54%, colorless solid. <sup>1</sup>H NMR (500.13 MHz, DMSO-d<sub>6</sub>) δ 11.00 (s, 1H), 10.36 (s, 1H), 8.07 (d, J = 7.8 Hz, 1H), 7.73 – 7.65 (m, 2H), 7.66 (dd, J = 7.2, 1.0 Hz, 1H); 7.63 – 7.58 (m, 2H), 7.56 – 7.51 (m, 1H), 7.47 – 7.37 (m, 1H), 7.29 (dd, J = 8.3, 0.9 Hz, 1H), 7.11 (td, J = 7.8, 1.1 Hz, 1H), 5.89 (s, 2H).

3-Butyl-1-(2-hydroxyphenyl)-1-H-benzimidazolium bromide (**L5**) Yield: 92%, brick red liquid. <sup>1</sup>H NMR (500.13 MHz, DMSO-d<sub>6</sub>) δ 10.75 (s, 1H), 10.13 (s, 1H), 8.22 (d, J = 8.3 Hz, 1H), 7.77 – 7.74 (m, 1H), 7.68 (ddd, J = 9.4, 8.1, 1.1 Hz, 2H), 7.58 (d, J = 8.3 Hz, 1H), 7.56 – 7.52 (m, 1H), 7.23 (dd, J = 8.3, 1.0 Hz, 1H), 7.12 (td, J = 7.8, 1.1 Hz, 1H), 4.61 (t, J = 7.2 Hz, 2H), 2.02 – 1.94 (m, 2H), 1.37-1.44 (m, 2H), 0.96 (t, J = 7.4 Hz, 3H).

3-Benzyl-1-(2-hydroxyphenyl)-1-H-benzimidazolium chloride (**L6**) Yield: 57%, light red solid. <sup>1</sup>H NMR (500.13 MHz, DMSO-d<sub>6</sub>) δ 10.99 (s, 1H), 10.36 (s, 1H), 8.07 (d, J = 7.7 Hz, 1H), 7.70 (dtd, J = 7.9, 3.4, 1.2 Hz, 2H), 7.66 (dd, J = 7.2, 1.0 Hz, 1H), 7.63 – 7.58 (m, 3H), 7.56 – 7.52 (m, 1H), 7.44 (d, J = 14.5 Hz, 2H), 7.40 (d, J = 7.2 Hz, 1H), 7.28 (dd, J = 8.3, 0.9 Hz, 1H), 7.11 (td, J = 7.8, 1.1 Hz, 1H), 5.88 (d, J = 10.2 Hz, 2H).

3-(4-chloro-1-benzyl)-1-(2-hydroxyphenyl)-1-H-benzimidazolium chloride (**L7**) Yield: 58%, brown solid. <sup>1</sup>H NMR (500.13 MHz, DMSO-d<sub>6</sub>) δ 11.26 (s, 1H), 10.41 (s, 1H), 8.07 (d, J = 7.8 Hz, 1H), 7.72 – 7.65 (m, 5H), 7.59 (d, J = 7.7 Hz, 1H), 7.54 – 7.50 (m, 3H), 7.33 (d, J = 8.2 Hz, 1H), 7.09 (td, J = 7.9, 1.0 Hz, 1H), 5.92 (s, 2H).

3-(4-fluoro-1-benzyl)-1-(2-hydroxyphenyl)-1-H-benzimidazolium chloride (**L8**) Yield: 58%, brown solid. <sup>1</sup>H NMR (500.13 MHz, DMSO) δ 11.00 (s, 1H), 10.32 (s, 1H), 8.09 (d, *J* = 8.2 Hz, 1H), 7.74 – 7.65 (m, 5H), 7.59 (d, *J* = 8.2 Hz, 1H), 7.56 – 7.51 (m, 1H), 7.31 – 7.26 (m, 3H), 7.11 (t, *J* = 7.6 Hz, 1H), 5.88 (s, 2H).

#### Synthesis of [(η<sup>5</sup>-Cp\*)Ir(C<sup>^</sup>O)Cl]

General method: the respective ligand (0.12 mmol) and Ag<sub>2</sub>O (0.144 mmol) in 10 mL CH<sub>2</sub>Cl<sub>2</sub> were stirred 2 h at room temperature. Then K<sub>2</sub>CO<sub>3</sub> (0.12 mmol) and [IrCp\*Cl<sub>2</sub>]<sub>2</sub> (0.06 mmol) were added to the mixture and reacted for 4 h. The mixture was filtered through celite and purified by recrystallization.

[(η<sup>5</sup>-C<sub>5</sub>Me<sub>5</sub>)Ir(L1)Cl] (**1**) Yield: 52 %, yellow solid. <sup>1</sup>H NMR (500.13 MHz, CD<sub>3</sub>OD-d<sub>4</sub>): δ 7.80 (d, *J* = 2.1 Hz, 1H), 7.49 (d, *J* = 2.1 Hz, 1H), 7.36 (dd, *J* = 7.9, 1.5 Hz, 1H), 7.05 (td, *J* = 8.0, 1.5 Hz, 1H), 6.92 (dd, *J* = 8.1, 1.2 Hz, 1H), 6.69 (td, *J* = 7.8, 1.2 Hz, 1H), 4.43 – 4.36 (m, 1H), 3.96-4.04 (m, 1H), 2.07 – 1.90 (m, 2H), 1.55 – 1.49 (m, 2H), 1.48 (s, 15H), 1.04 (t, *J* = 7.4 Hz, 3H). <sup>13</sup>C NMR (126 MHz, CDCl<sub>3</sub>) δ 160.95, 160.84, 130.63, 126.94, 122.25, 120.81, 119.08, 117.76, 115.30, 87.42 (5C), 50.48, 33.00, 20.32, 13.90, 8.75 (5C). Anal. Calcd. For: [(η<sup>5</sup>-C<sub>5</sub>Me<sub>5</sub>)Ir(L1)Cl] (578.17) C, 47.78; H, 5.23; N, 4.85. Found: C, 48.04; H, 5.17; N, 4.80. MS: 542.1992 [(η<sup>5</sup>-C<sub>5</sub>Me<sub>5</sub>) Ir(L1)]<sup>+</sup>.

[(η<sup>5</sup>-C<sub>5</sub>Me<sub>5</sub>)Ir(L2)Cl] (**2**) Yield: 63%, yellow solid. <sup>1</sup>H NMR (500.13 MHz, CD<sub>3</sub>OD-d<sub>4</sub>): δ 7.76 (d, *J* = 2.2 Hz, 1H), 7.57 (d, *J* = 7.2 Hz, 2H), 7.42 – 7.33 (m, 4H), 7.07 (td, *J* = 8.5, 1.5 Hz 1H), 7.02 (d, *J* = 2.2 Hz, 1H), 6.96 (dd, *J* = 8.1, 1.2 Hz, 1H), 6.71 (td, *J* = 7.8, 1.3 Hz, 1H), 5.85 (d, *J* = 14.2 Hz, 1H), 5.17 (d, *J* = 14.2 Hz, 1H), 1.50 (s, 15H). <sup>13</sup>C NMR (126 MHz, CDCl<sub>3</sub>) δ 161.42, 160.93, 135.48, 130.54, 129.05 (2C), 128.88 (2C), 128.40, 127.12, 122.41, 121.45, 119.05, 117.72, 115.33, 87.74 (5C), 54.24, 8.89 (5C). Anal. Calcd. For: [(η<sup>5</sup>-C<sub>5</sub>Me<sub>5</sub>)Ir(L2)Cl] (612.15) C, 51.01; H, 4.61; N, 4.58. Found: C, 51.25; H, 4.59; N, 4.53. MS: 577.1776 [(η<sup>5</sup>-C<sub>5</sub>Me<sub>5</sub>) Ir(L2)]<sup>+</sup>.

[(η<sup>5</sup>-C<sub>5</sub>Me<sub>5</sub>)Ir(L3)Cl] (**3**) Yield: 87%, yellow solid. <sup>1</sup>H NMR (500.13 MHz, CD<sub>3</sub>OD-d<sub>4</sub>) δ 7.77 (d, *J* = 2.1 Hz, 1H), 7.58 (d, *J* = 8.4 Hz, 2H), 7.37 (dd, *J* = 11.3, 4.9 Hz, 3H), 7.06 (td, *J* = 8.3, 1.5 Hz, 1H), 7.04 (d, *J* = 2.2 Hz, 1H), 6.95 (dd, *J* = 8.1, 1.1 Hz, 1H), 6.70 (td, *J* = 7.9, 1.2 Hz, 1H), 5.83 (d, *J* = 14.2 Hz, 1H), 5.14 (d, *J* = 14.2 Hz, 1H), 1.49 (s, 15H). <sup>13</sup>C NMR (126 MHz, CDCl<sub>3</sub>) δ 161.58, 160.95, 134.48, 134.00, 130.59 (2C), 130.43, 129.07 (2C), 127.22, 122.50, 121.15, 119.00, 117.96, 115.39, 87.80 (5C), 53.49, 8.90 (5C). Anal. Calcd. For: [(η<sup>5</sup>-C<sub>5</sub>Me<sub>5</sub>)Ir(L3)Cl] (646.11) C, 48.29; H, 4.21; N, 4.33. Found: C, 49.03; H, 4.25; N, 4.26. MS: 611.1362 [(η<sup>5</sup>-C<sub>5</sub>Me<sub>5</sub>) Ir(L3)]<sup>+</sup>.

[(η<sup>5</sup>-C<sub>5</sub>Me<sub>5</sub>) Ir(L4)Cl] (**4**) Yield: 62%, yellow solid. <sup>1</sup>H NMR (500.13 MHz, CD<sub>3</sub>OD-d<sub>4</sub>) δ 7.79 (d, *J* = 2.0 Hz, 1H), 7.66 (dd, *J* = 8.4, 5.5 Hz, 2H), 7.40 (dd, *J* = 7.9, 1.2 Hz, 1H), 7.14 (t, *J* = 8.7 Hz, 2H), 7.11 – 7.07 (m, 1H), 7.04 (d, *J* = 2.1 Hz, 1H), 6.98 (dd, *J* = 8.1, 0.9 Hz, 1H), 6.75 – 6.71 (m, 1H), 5.87 (d, *J* = 14.0 Hz, 1H), 5.15 (d, *J* = 14.0 Hz, 1H), 1.53 (s, 15H). <sup>13</sup>C NMR (126 MHz,

CDCl<sub>3</sub>)  $\delta$  163.79, 161.83, 161.14 (d,  $^1J_{CF}$ =34.0 Hz), 131.26 (d,  $^4J_{CF}$ =3.28 Hz), 131.15 (d,  $^3J_{CF}$ =8.3 Hz), 130.46, 127.15, 122.49, 121.11, 119.01, 117.87, 115.79 (d,  $^2J_{CF}$ =21.6 Hz), 115.32, 87.76 (5C), 53.44, 8.89 (5C). Anal. Calcd. For:  $[(\eta^5\text{-C}_5\text{Me}_5)\text{Ir}(\text{L4})\text{Cl}]$  (630.14) C, 49.56; H, 4.32; N, 4.45. Found: C, 50.12; H, 4.29; N, 4.47. MS: 595.1931  $[(\eta^5\text{-C}_5\text{Me}_5)\text{Ir}(\text{L4})]^+$ .

**$[(\eta^5\text{-C}_5\text{Me}_5)\text{Ir}(\text{L5})\text{Cl}]$  (5)** Yield: 33%, yellow solid.  $^1\text{H}$  NMR (500.13 MHz, CDCl<sub>3</sub>):  $\delta$  7.87 – 7.84 (m, 1H), 7.55 (dd,  $J$  = 7.8, 1.5 Hz, 1H), 7.50 – 7.48 (m, 1H), 7.30 – 7.28 (m, 2H), 7.13–7.06 (m, 2H), 6.66 (td,  $J$  = 7.9, 1.7 Hz, 1H), 4.57 (td,  $J$  = 12.9, 4.6 Hz, 1H), 4.38 (td,  $J$  = 12.7, 4.9 Hz, 1H), 2.39 – 2.29 (m, 1H), 2.07–1.98 (m, 1H), 1.61 – 1.54 (m, 2H), 1.52 (s, 15H), 1.06 (t,  $J$  = 7.4 Hz, 3H).  $^{13}\text{C}$  NMR (126 MHz, CDCl<sub>3</sub>)  $\delta$  176.72, 163.47, 135.00, 132.46, 130.35, 126.91, 123.24 (2C), 122.26, 121.13, 114.91, 112.88, 111.28, 88.38 (5C), 49.70, 31.79, 20.64, 13.93, 8.73 (5C). Anal. Calcd. For:  $[(\eta^5\text{-C}_5\text{Me}_5)\text{Ir}(\text{L5})\text{Cl}]$  (630.14) C, 51.62; H, 5.13; N, 4.46. Found: C, 50.96; H, 5.18; N, 4.35. MS: 593.1952  $[(\eta^5\text{-C}_5\text{Me}_5)\text{Ir}(\text{L5})]^+$ .

**$[(\eta^5\text{-C}_5\text{Me}_5)\text{Ir}(\text{L6})\text{Cl}]$  (6)** Yield: 35%, yellow solid.  $^1\text{H}$  NMR (500.13 MHz, MeOD-*d*<sub>4</sub>):  $\delta$  7.91 (d,  $J$  = 8.3 Hz, 1H), 7.75 (dd,  $J$  = 7.9, 1.5 Hz, 1H), 7.39 – 7.29 (m, 6H), 7.21 – 7.16 (m, 2H), 7.08 (dd,  $J$  = 12.8, 4.7 Hz, 2H), 6.89 – 6.84 (m, 1H), 6.01 – 5.93 (m, 2H), 1.45 (s, 15H).  $^{13}\text{C}$  NMR (126 MHz, CDCl<sub>3</sub>)  $\delta$  178.09, 163.62, 135.71, 135.53, 132.59, 130.17, 128.69 (2C), 127.60, 127.22, 126.58 (2C), 123.52, 123.48, 122.34, 121.49, 115.00, 112.65, 112.39, 88.72 (5C), 53.07, 8.84 (5C). Anal. Calcd. For:  $[(\eta^5\text{-C}_5\text{Me}_5)\text{Ir}(\text{L6})\text{Cl}]$  (662.17) C, 54.41; H, 4.57; N, 4.23. Found: C, 54.56; H, 4.62; N, 4.20. MS: 627.5  $[(\eta^5\text{-C}_5\text{Me}_5)\text{Ir}(\text{L6})]^+$ .

**$[(\eta^5\text{-C}_5\text{Me}_5)\text{Ir}(\text{L7})\text{Cl}]$  (7)** Yield: 38%, yellow solid.  $^1\text{H}$  NMR (500.13 MHz, CDCl<sub>3</sub>).  $^1\text{H}$  NMR (500 MHz, CD<sub>3</sub>OD-*d*<sub>4</sub>)  $\delta$  7.91 (d,  $J$  = 8.3 Hz, 1H), 7.74 (dd,  $J$  = 7.9, 1.5 Hz, 1H), 7.38 – 7.28 (m, 5H), 7.21 – 7.16 (m, 2H), 7.08 – 7.05 (m, 2H), 6.85 (td,  $J$  = 7.8, 1.3 Hz, 1H), 6.00 (d,  $J$  = 16.2 Hz, 1H), 5.87 (d,  $J$  = 16.2 Hz, 1H), 1.46 (s, 15H).  $^{13}\text{C}$  NMR (126 MHz, CDCl<sub>3</sub>)  $\delta$  178.15, 163.65, 135.17, 134.21, 133.54, 132.64, 130.12, 128.91 (2C), 128.21 (2C), 127.29, 123.60 (2C), 122.44, 121.40, 115.02, 112.82, 112.21, 88.74 (5C), 52.65, 8.85 (5C). Anal. Calcd. For:  $[(\eta^5\text{-C}_5\text{Me}_5\text{C}_6\text{H}_4\text{C}_6\text{H}_5)\text{Ir}(\text{L1})\text{Cl}]$  (696.16) C, 51.72; H, 4.20; N, 4.02. Found: C, 51.79; H, 4.22; N, 4.09. MS: 661.5  $[(\eta^5\text{-C}_5\text{Me}_5)\text{Ir}(\text{L7})]^+$ .

**$[(\eta^5\text{-C}_5\text{Me}_5)\text{Ir}(\text{L8})\text{Cl}]$  (8)** Yield: 36%, yellow solid.  $^1\text{H}$  NMR (500.13 MHz, CD<sub>3</sub>OD-*d*<sub>4</sub>)  $\delta$  7.90 (d,  $J$  = 8.3 Hz, 1H), 7.74 (dd,  $J$  = 7.9, 1.6 Hz, 1H), 7.42 – 7.38 (m, 2H), 7.35 – 7.31 (m, 1H), 7.20 – 7.15 (m, 2H), 7.10 – 7.03 (m, 4H), 6.85 (td,  $J$  = 7.7, 1.4 Hz, 1H), 6.01 (d,  $J$  = 16.1 Hz, 1H), 5.85 (d,  $J$  = 16.0 Hz, 1H), 1.46 (s, 15H).  $^{13}\text{C}$  NMR (126 MHz, CDCl<sub>3</sub>)  $\delta$  178.01, 163.43 (d,  $^1J_{CF}$ =55.4 Hz), 135.25, 132.67, 131.37 (d,  $^4J_{CF}$ =3.2 Hz), 130.15, 128.59 (d,  $^3J_{CF}$ =8.1 Hz), 127.27, 123.55, 122.43, 121.41, 115.67 (d,  $^2J_{CF}$ =21.5 Hz), 115.02, 112.81, 112.27, 88.73 (5C), 52.65, 8.85 (5C). Anal. Calcd. For:  $[(\eta^5\text{-C}_5\text{Me}_5)\text{Ir}(\text{L8})\text{Cl}]$  (680.16) C, 52.97; H, 4.30; N, 4.12. Found: C, 52.79; H, 4.27; N, 4.41. MS: 645.50  $[(\eta^5\text{-C}_5\text{Me}_5)\text{Ir}(\text{L8})]^+$ .

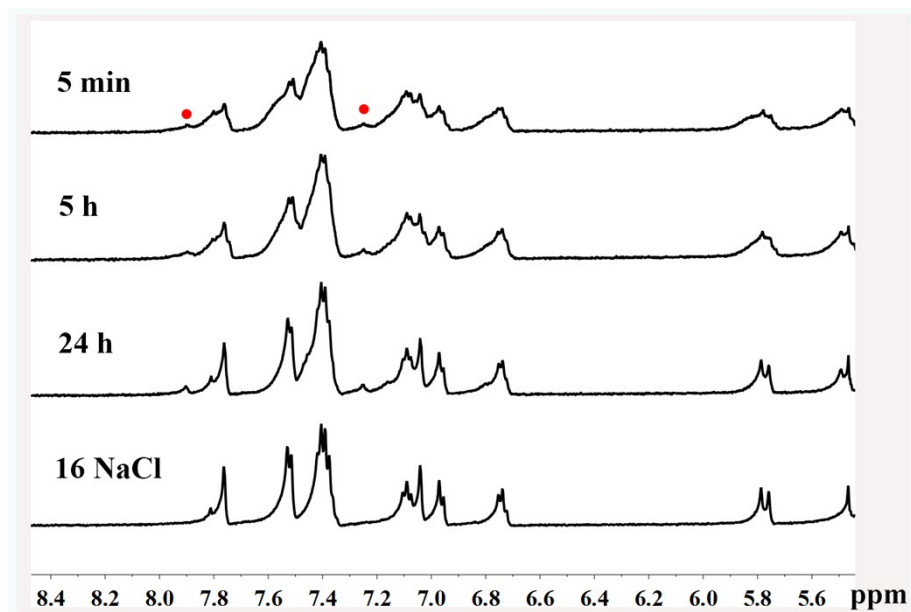
**[( $\eta^5$ -C<sub>5</sub>Me<sub>4</sub>C<sub>6</sub>H<sub>4</sub>C<sub>6</sub>H<sub>5</sub>)Ir(L1)Cl] (9)** Yield: 25%, yellow solid. <sup>1</sup>H NMR (500.13 MHz, CD<sub>3</sub>OD-d<sub>4</sub>)  $\delta$  7.93 – 7.89 (m, 1H), 7.74 (dd,  $J$  = 7.9, 1.5 Hz, 1H), 7.70 – 7.51 (m, 7H), 7.44 (t,  $J$  = 7.6 Hz, 2H), 7.37 (qd,  $J$  = 7.1, 3.2 Hz, 3H), 7.15 – 7.10 (m, 1H), 7.00 (dd,  $J$  = 8.1, 1.3 Hz, 1H), 6.85 – 6.80 (m, 1H), 4.40 – 4.33 (m, 1H), 4.29 – 4.22 (m, 1H), 2.02-1.94 (m, 1H), 1.73 (d,  $J$  = 5.2 Hz, 6H), 1.53 (d,  $J$  = 8.1 Hz, 3H), 1.52 – 1.45 (m, 1H), 1.40 – 1.23 (m, 5H), 1.14-1.10 (m, 1H), 0.83 (t,  $J$  = 7.4 Hz, 3H). <sup>13</sup>C NMR (126 MHz, CDCl<sub>3</sub>)  $\delta$  174.99, 163.26, 140.59; 140.56, 135.16, 132.35, 131.28, 130.74 (2C), 130.20, 128.90 (2C), 127.54, 127.15 (2C), 127.06, 127.00 (2C), 123.39; 123.34, 122.37, 121.23, 115.19, 112.97, 111.29, 98.34, 94.30, 89.27, 83.88, 83.11, 49.10, 31.63, 20.19, 13.95, 10.97, 9.37, 8.47, 7.96. Anal. Calcd. For: [( $\eta^5$ -C<sub>5</sub>Me<sub>4</sub>C<sub>6</sub>H<sub>4</sub>C<sub>6</sub>H<sub>5</sub>)Ir(L1)Cl] (766.23) C, 59.55; H, 5.00; N, 3.66. Found: C, 60.01; H, 5.04; N, 3.62. MS: 731.204 [( $\eta^5$ -C<sub>5</sub>Me<sub>4</sub>C<sub>6</sub>H<sub>4</sub>C<sub>6</sub>H<sub>5</sub>)Ir(L1)]<sup>+</sup>.

**[( $\eta^5$ -C<sub>5</sub>Me<sub>5</sub>)Ir(L2)Cl] (10)** Yield: 41%, yellow solid. <sup>1</sup>H NMR (500.13 MHz, CDCl<sub>3</sub>)  $\delta$  7.87 (d,  $J$  = 8.3 Hz, 1H), 7.65 (dd,  $J$  = 7.7, 1.0 Hz, 1H), 7.60 (d,  $J$  = 7.4 Hz, 2H), 7.54 – 7.44 (m, 6H), 7.39 (t,  $J$  = 7.4 Hz, 1H), 7.24 (d,  $J$  = 7.9 Hz, 1H), 7.16 – 7.03 (m, 6H), 6.95 (d,  $J$  = 8.2 Hz, 1H), 6.82 (d,  $J$  = 7.5 Hz, 2H), 6.76 – 6.69 (m, 1H), 5.96 (d,  $J$  = 17.1 Hz, 1H), 5.55 (d,  $J$  = 17.1 Hz, 1H), 1.75 (s, 3H), 1.68 (s, 3H), 1.47 (s, 3H), 1.30 (s, 3H). <sup>13</sup>C NMR (126 MHz, CDCl<sub>3</sub>)  $\delta$  176.80, 163.35, 140.57, 140.45, 135.54, 135.31, 132.48, 130.86, 130.60 (2C), 130.00, 128.93 (2C), 128.29 (2C), 127.54, 127.29, 127.06, 127.02 (2C), 127.00 (2C), 126.06 (2C), 123.61, 123.54, 122.59, 121.40, 115.24, 112.80, 112.43, 98.36, 92.10, 91.44, 85.36, 82.74, 52.91, 10.97, 9.54, 8.70, 8.24. Anal. Calcd. For: [( $\eta^5$ -C<sub>5</sub>Me<sub>4</sub>C<sub>6</sub>H<sub>4</sub>C<sub>6</sub>H<sub>5</sub>)Ir(L2)Cl] (800.21) C, 61.52; H, 4.53; N, 3.56. Found: C, 61.61; H, 4.49; N, 3.59. MS: 765.220[( $\eta^5$ -C<sub>5</sub>Me<sub>4</sub>C<sub>6</sub>H<sub>4</sub>C<sub>6</sub>H<sub>5</sub>)Ir(L2)]<sup>+</sup>.

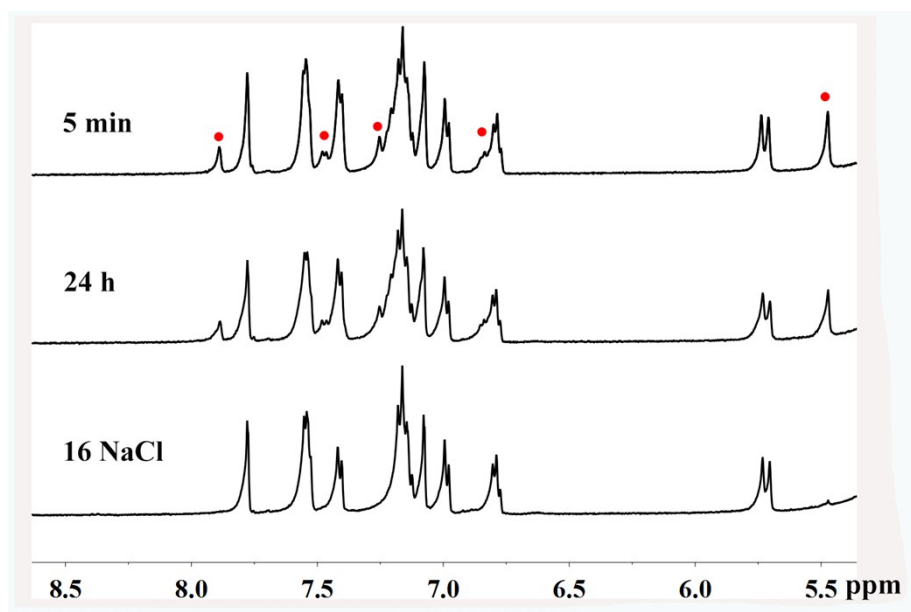
**[( $\eta^5$ -C<sub>5</sub>Me<sub>5</sub>)Ir(L2)Cl] (11)** Yield: 19 %, yellow solid. <sup>1</sup>H NMR (500.13 MHz, CDCl<sub>3</sub>)  $\delta$  7.87 (d,  $J$  = 8.3 Hz, 1H), 7.64 (dd,  $J$  = 7.8, 1.2 Hz, 1H), 7.62 – 7.58 (m, 2H), 7.48 (dd,  $J$  = 12.0, 8.5 Hz, 6H), 7.40 (t,  $J$  = 7.4 Hz, 1H), 7.28-7.25 (m, 2H), 7.16 – 7.08 (m, 3H), 7.04 (d,  $J$  = 8.4 Hz, 2H), 6.89 (d,  $J$  = 8.1 Hz, 1H), 6.78 (d,  $J$  = 8.4 Hz, 2H), 6.76 – 6.71 (m, 1H), 5.80 (d,  $J$  = 17.0 Hz, 1H), 5.55 (d,  $J$  = 17.1 Hz, 1H), 1.78 (s, 3H), 1.72 (s, 3H), 1.48 (s, 3H), 1.28 (s, 3H). <sup>13</sup>C NMR (126 MHz, CDCl<sub>3</sub>)  $\delta$  176.88, 163.31, 140.51, 140.35, 135.20, 133.79, 132.92, 132.48, 130.90, 130.57 (2C), 129.93, 129.00 (2C), 128.46 (2C), 127.65, 127.55 (2C), 127.38, 127.01 (2C), 126.97 (2C), 123.72, 123.68, 122.65, 121.35, 115.33, 112.94, 112.18, 99.06, 92.97, 90.87, 84.35, 82.88, 52.35, 11.15, 9.53, 8.61, 8.14. Anal. Calcd. For: [( $\eta^5$ -C<sub>5</sub>Me<sub>4</sub>C<sub>6</sub>H<sub>4</sub>C<sub>6</sub>H<sub>5</sub>)Ir(L3)Cl] (834.18) C, 58.99; H, 4.23; N, 3.26. Found: C, 58.37; H, 4.27; N, 3.38. MS: 799.216 [( $\eta^5$ -C<sub>5</sub>Me<sub>4</sub>C<sub>6</sub>H<sub>4</sub>C<sub>6</sub>H<sub>5</sub>)Ir(L3)]<sup>+</sup>.

**[( $\eta^5$ -C<sub>5</sub>Me<sub>5</sub>)Ir(L2)Cl] (12)** Yield: 17 %, yellow solid. <sup>1</sup>H NMR (500.13 MHz, CDCl<sub>3</sub>)  $\delta$  7.87 (d,  $J$  = 8.3 Hz, 1H), 7.64 (d,  $J$  = 7.4 Hz, 1H), 7.60 (d,  $J$  = 7.4 Hz, 2H), 7.56 – 7.44 (m, 6H), 7.40 (t,  $J$  = 7.4 Hz, 1H), 7.27-7.24 (m, 1H), 7.15-7.08(m, 3H), 6.91 (d,  $J$  = 8.2 Hz, 1H), 6.86 – 6.80 (m, 2H), 6.80 – 6.68 (m, 3H), 5.78 (d,  $J$  = 16.8 Hz, 1H), 5.58 (d,  $J$  = 16.8 Hz, 1H), 1.78 (s, 3H), 1.72 (s, 3H), 1.48 (s, 3H), 1.28 (s, 3H). <sup>13</sup>C NMR (126 MHz, CDCl<sub>3</sub>)  $\delta$  176.77, 163.03 (d, <sup>1</sup> $J_{CF}$  = 63.0 Hz), 140.48, 140.38, 135.26, 132.49, 130.97(d, <sup>4</sup> $J_{CF}$  = 3.0 Hz), 130.91, 130.59 (2C), 129.93, 128.99

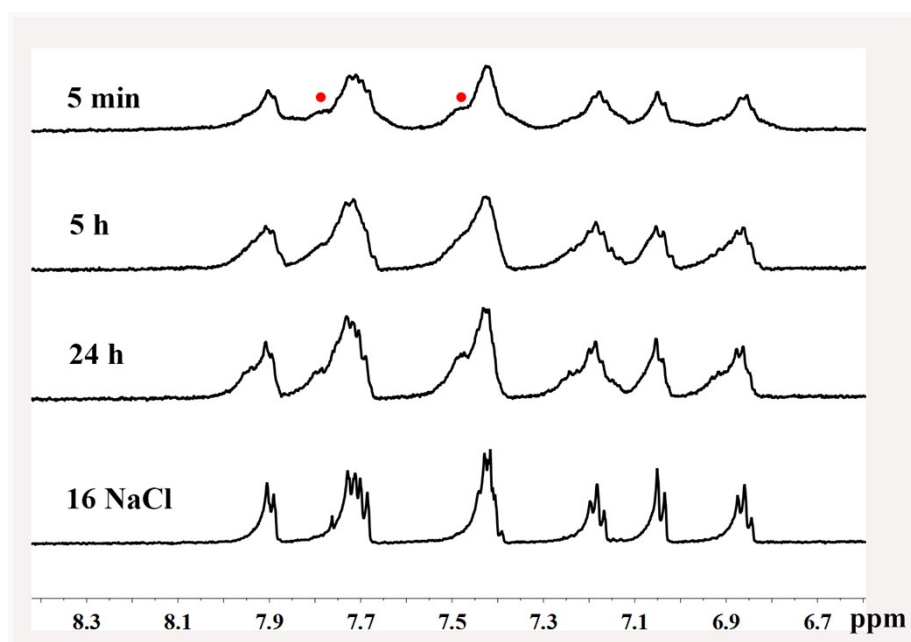
(2C), 128.45, 127.88 (d,  $^3J_{CF}=8.1$  Hz), 127.64, 127.54, 127.34, 127.00 (2C), 126.93 (2C), 123.66, 123.62, 122.62, 121.34, 115.22(d,  $^2J_{CF}=22.7$  Hz), 112.91, 112.24, 99.01, 92.71, 90.87, 84.62, 82.82, 52.37, 11.06, 9.51, 8.61, 8.15. Anal. Calcd. For:  $[(\eta^5\text{-C}_5\text{Me}_4\text{C}_6\text{H}_4\text{C}_6\text{H}_5)\text{Ir}(\text{L4})\text{Cl}]$  (818.21) C, 60.17; H, 4.31; N, 3.42. Found: C, 60.29; H, 4.27; N, 3.35. MS: 783.314  $[(\eta^5\text{-C}_5\text{Me}_4\text{C}_6\text{H}_4\text{C}_6\text{H}_5)\text{Ir}(\text{L4})]^+$ .



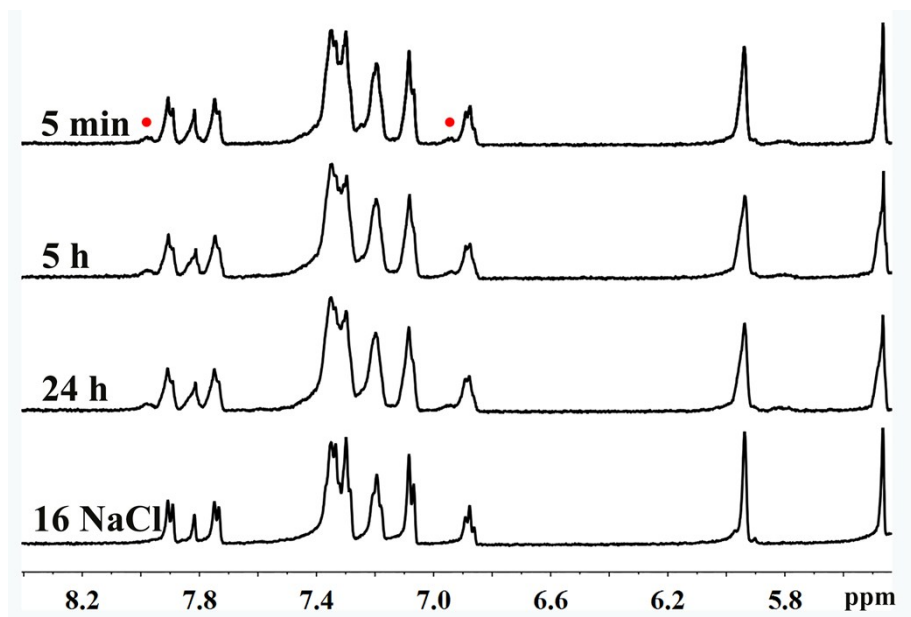
**Figure S1.**  $^1\text{H}$  NMR spectra of Complex  $[(\eta^5\text{-C}_5\text{Me}_5)\text{Ir}(\text{L}2)\text{Cl}]$  (**2**) (1 mM) hydrolyzed in 80%  $\text{MeOD-d}_4$  / 20%  $\text{D}_2\text{O}$  (v / v) at 310K for 5 min, 5h, 24h and addition of 16 mol equiv of NaCl. Peaks labeled  $\bullet$  correspond to the aqua complex  $[(\eta^5\text{-C}_5\text{Me}_5)\text{Ir}(\text{L}2)\text{D}_2\text{O}]^+$ .



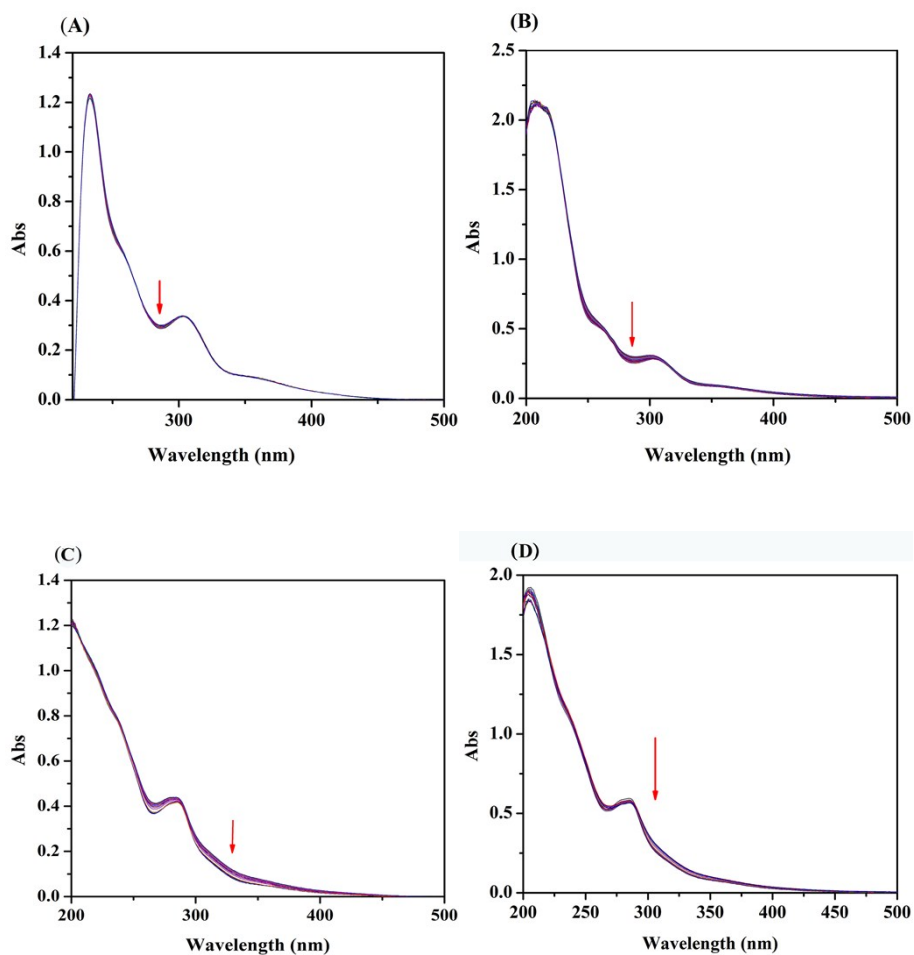
**Figure S2.**  $^1\text{H}$  NMR spectra of Complex  $[(\eta^5\text{-C}_5\text{Me}_5)\text{Ir}(\text{L}4)\text{Cl}]$  (**4**) (1 mM) hydrolyzed in 80%  $\text{MeOD-d}_4$  / 20%  $\text{D}_2\text{O}$  (v / v) at 310K for 5 min, 5h, 24h and addition of 16 mol equiv of NaCl. Peaks labeled  $\bullet$  correspond to the aqua complex  $[(\eta^5\text{-C}_5\text{Me}_5)\text{Ir}(\text{L}4)\text{D}_2\text{O}]^+$ .



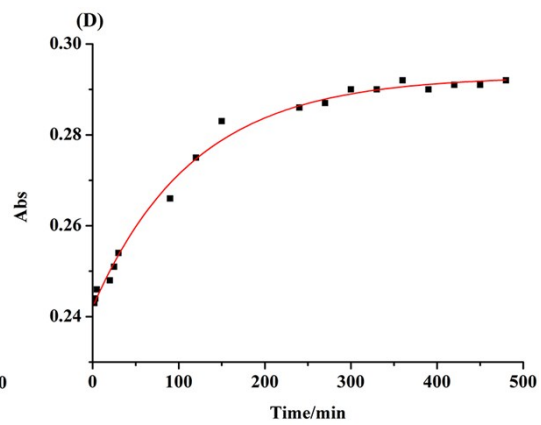
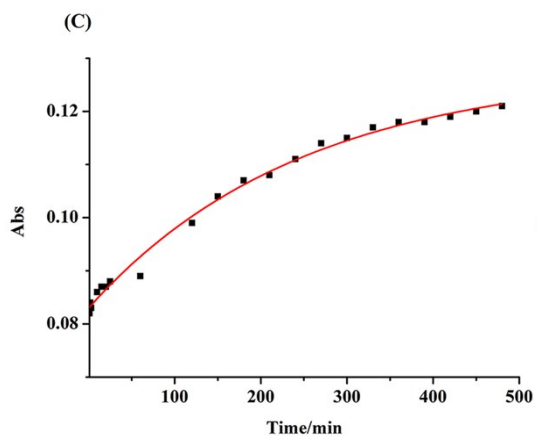
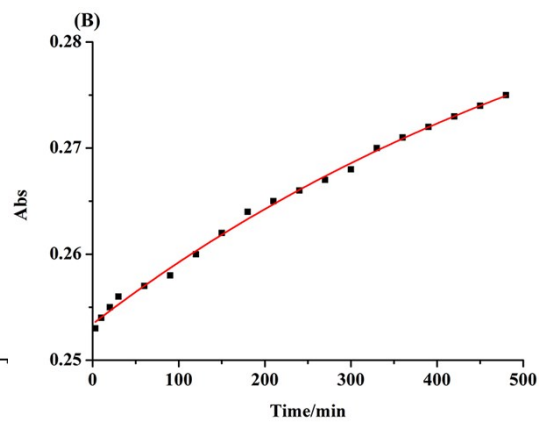
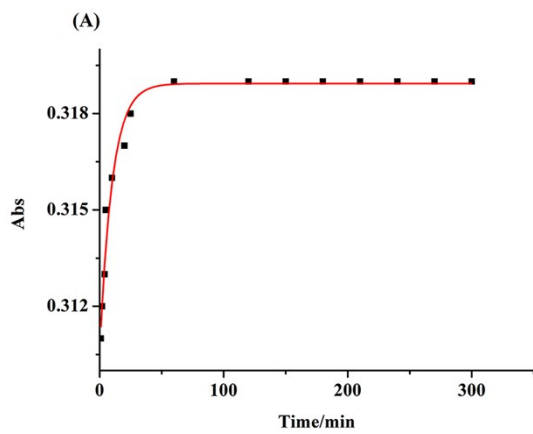
**Figure S3.**  $^1\text{H}$  NMR spectra of Complex  $[(\eta^5\text{-C}_5\text{Me}_5)\text{Ir}(\text{L}5)\text{Cl}]$  (**5**) (1 mM) hydrolyzed in 80%  $\text{MeOD-d}_4/20\%$   $\text{D}_2\text{O}$  (v/v) at 310K for 5 min, 5h, 24h and addition of 16 mol equiv of NaCl. Peaks labeled  $\bullet$  correspond to the aqua complex  $[(\eta^5\text{-C}_5\text{Me}_5)\text{Ir}(\text{L}5)\text{D}_2\text{O}]^+$ .



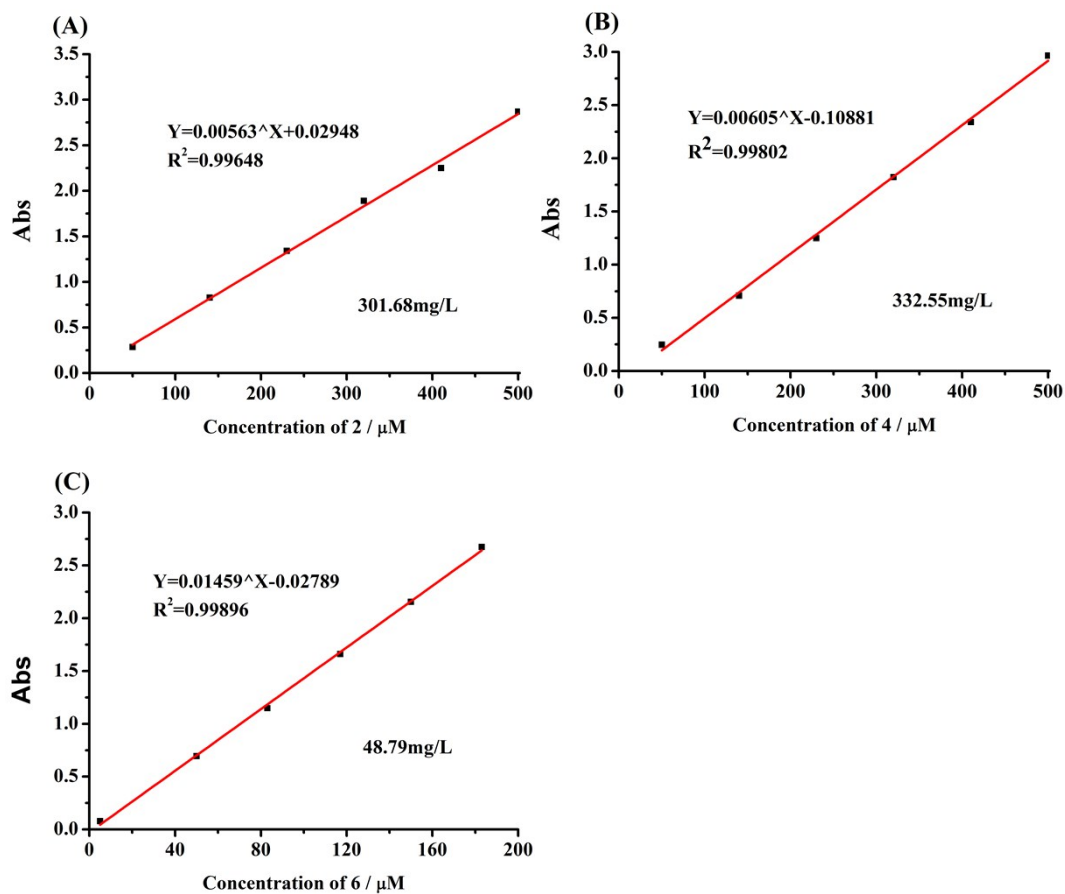
**Figure S4.**  $^1\text{H}$  NMR spectra of Complex  $[(\eta^5\text{-C}_5\text{Me}_5)\text{Ir}(\text{L}6)\text{Cl}]$  (**6**) (1 mM) hydrolyzed in 80%  $\text{MeOD-d}_4/20\%$   $\text{D}_2\text{O}$  (v/v) at 310K for 5 min, 5h, 24h and addition of 16 mol equiv of NaCl. Peaks labeled  $\bullet$  correspond to the aqua complex  $[(\eta^5\text{-C}_5\text{Me}_5)\text{Ir}(\text{L}6)\text{D}_2\text{O}]^+$ .



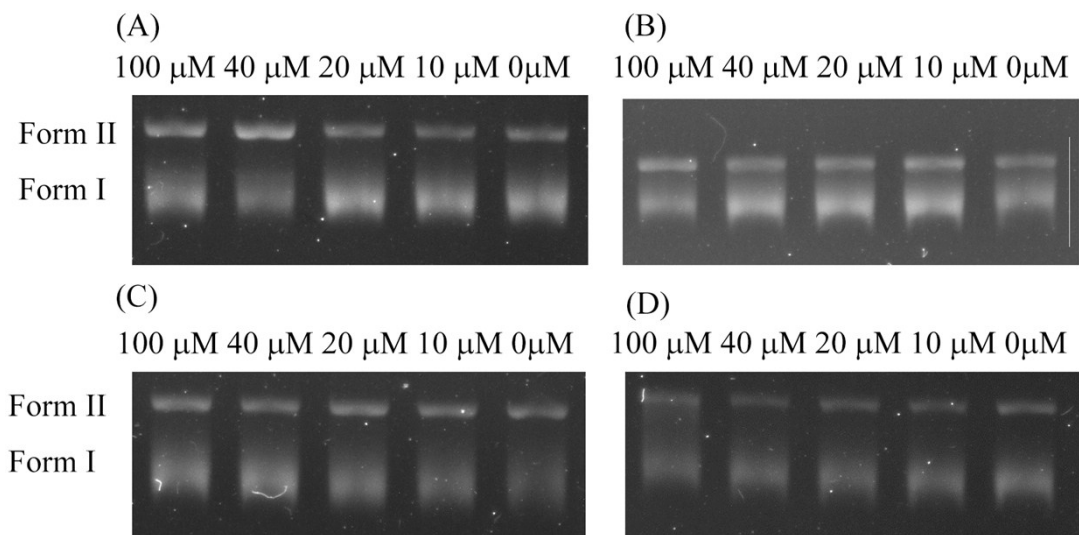
**Figure S5.** UV-Vis spectrum for a 50  $\mu\text{M}$  solution of complexes (A) 2, (B) 4, (C) 5 and (D) 6 in 20% MeOH/80% H<sub>2</sub>O (v/v) recorded over a period of 8 h at 298 K.



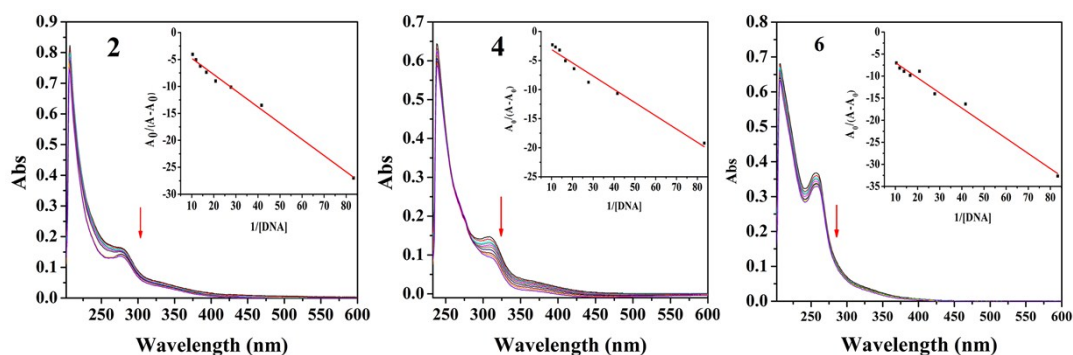
**Figure S6.** Time dependence of hydrolysis of (A) complex **2**, (B) complex **4**, (C) complex **5** and (D) complex **6** in 20% MeOH/80% H<sub>2</sub>O (v/v) at 298 K based on UV-Vis spectrum by measuring the absorption difference at 295 nm, 286 nm, 329 nm and 308 nm, respectively.



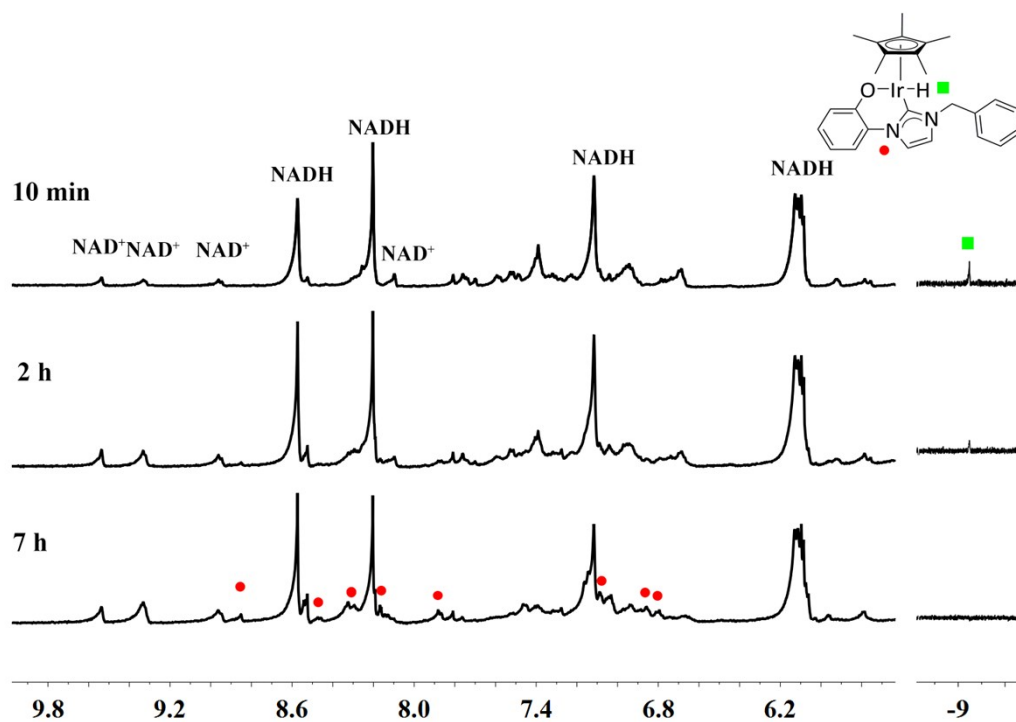
**Figure S7.** Calibration of UV-spectroscopic measurement for solubility of complex 2 (a), 4 (b) and 6 (c) by the UV-spectroscopic assay at 302nm, 302nm and 280 nm, respectively.



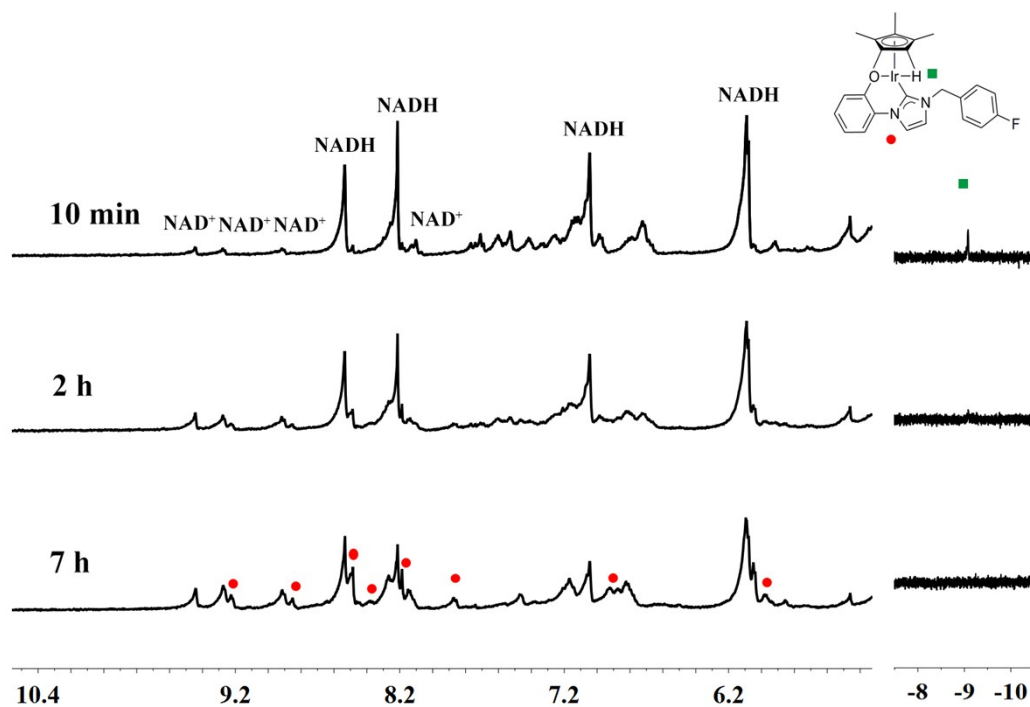
**Figure S8.** Agarose gel electrophoresis patterns for the cleavage of pBR322 DNA by different concentrations of (A) complex **2**, (B) complex **4**, (C) complex **5** and (D) complex **6**.



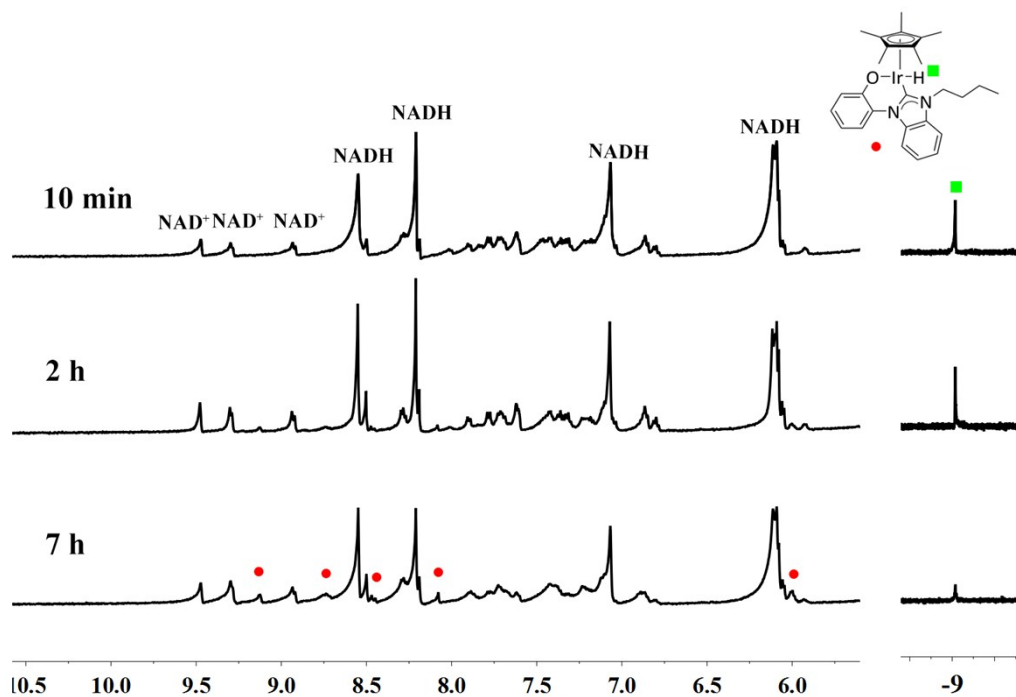
**Figure S9.** Absorption spectra showed the changes of complex **2**, **4**, and **6** (20  $\mu\text{M}$ ) in 50mM Tris-HCl/50mM NaCl buffer after adding to CT-DNA (0–108 $\mu\text{M}$ ). Inset plots of  $A_0/(A - A_0)$  vs.  $1/[DNA]$  for the titration of complex **2**, **4**, and **6** with DNA. The arrow indicated that the absorbance decreased as the DNA concentration increases.



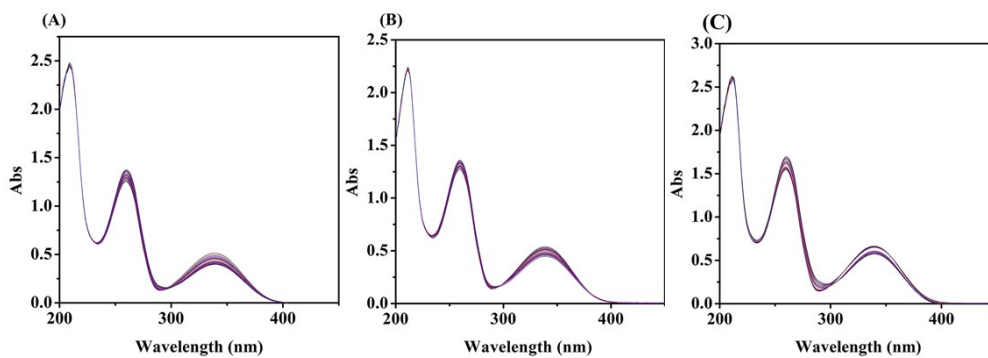
**Figure S10.**  $^1\text{H}$  NMR spectra of the reaction for complex **2** (1 mM) and NADH (3.5 mM) in 80%MeOD- $\text{d}_4$ /20%  $\text{D}_2\text{O}$  (v/v) at 310 K after 10 min, 2 h and 7 h. Peaks labeled  $\bullet$  correspond to the formed Ir-H complex and  $\blacksquare$  correspond to the Ir-H bond; hydride peak at  $-9.09$  ppm.



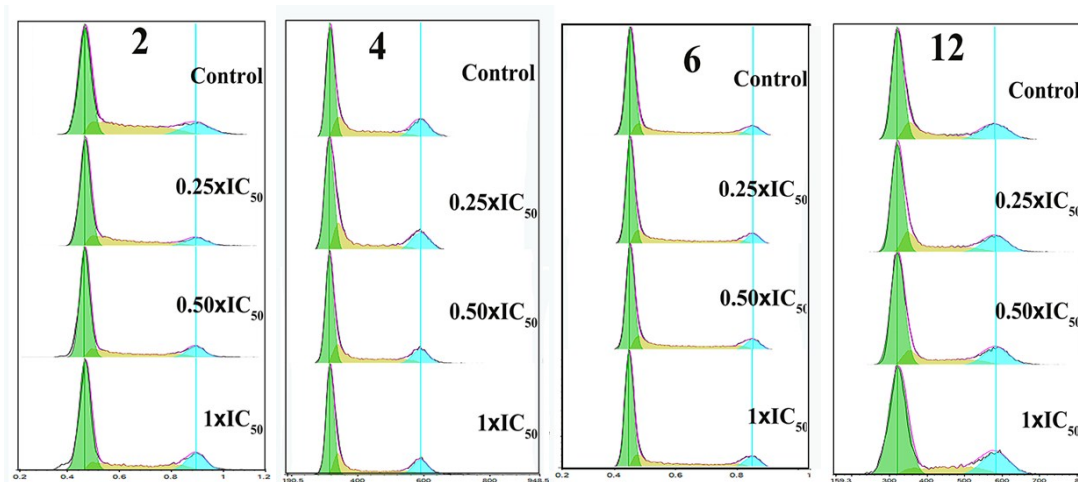
**Figure S11.**  $^1\text{H}$  NMR spectra of the reaction for complex **4** (1 mM) and NADH (3.5 mM) in 80%MeOD- $d_4$ /20%  $\text{D}_2\text{O}$  (v/v) at 310 K after 10 min, 2 h and 7 h. Peaks labeled  $\bullet$  correspond to the formed Ir–H complex and  $\blacksquare$  correspond to the Ir–H bond; hydride peak at  $-9.08$  ppm.



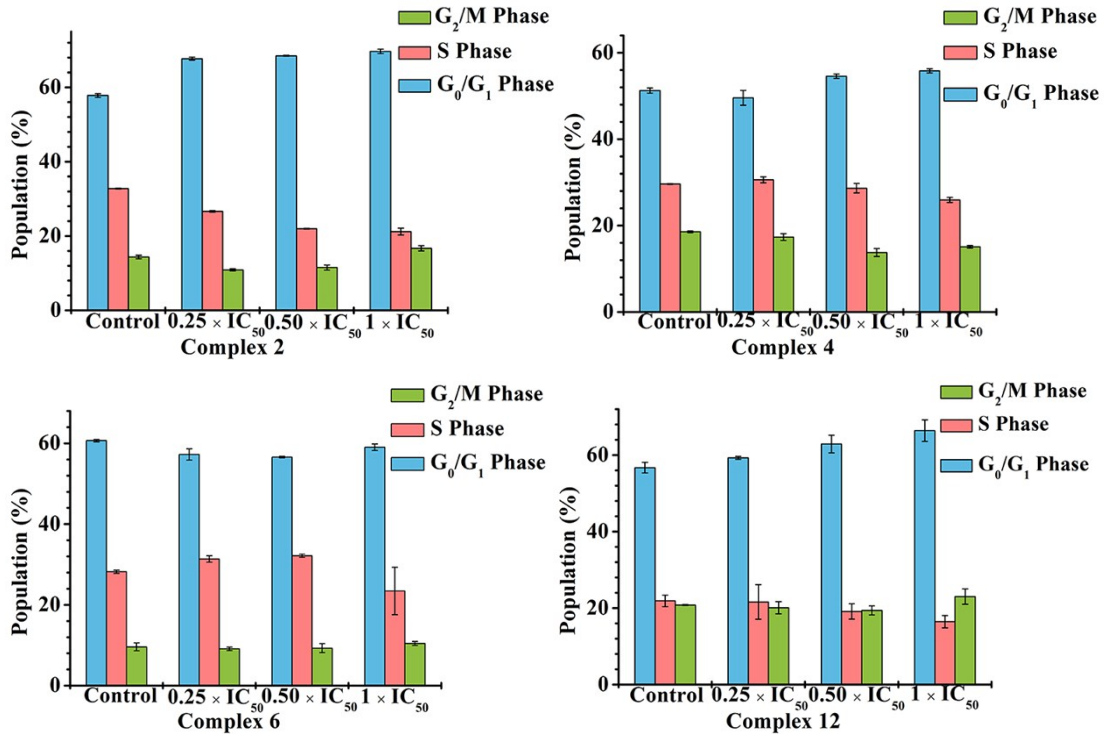
**Figure S12.**  $^1\text{H}$  NMR spectra of the reaction for complex **5** (1 mM) and NADH (3.5 mM) in 80%MeOD- $d_4$ /20%  $\text{D}_2\text{O}$  (v/v) at 310 K after 10 min, 2 h and 7 h. Peaks labeled  $\bullet$  correspond to the formed Ir–H complex and  $\blacksquare$  correspond to the Ir–H bond; hydride peak at  $-9.07$  ppm.



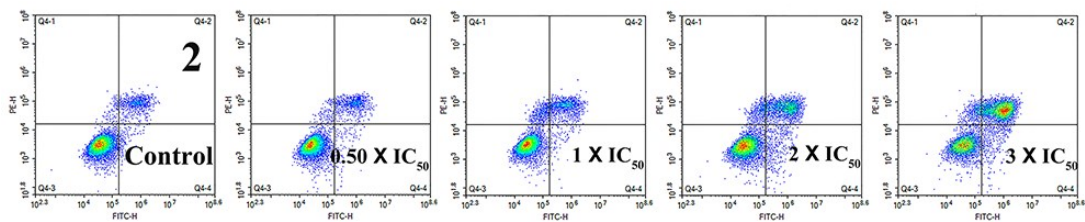
**Figure S13.** UV-Vis spectra of the reaction of NADH (100  $\mu$ M) with complex **2**, **4** and **5** (1  $\mu$ M) in 10% MeOH/90% H<sub>2</sub>O (v/v) at 298 K for 8 h. (A) complex **2**; (B) complex **4**; (C) complex **5**.

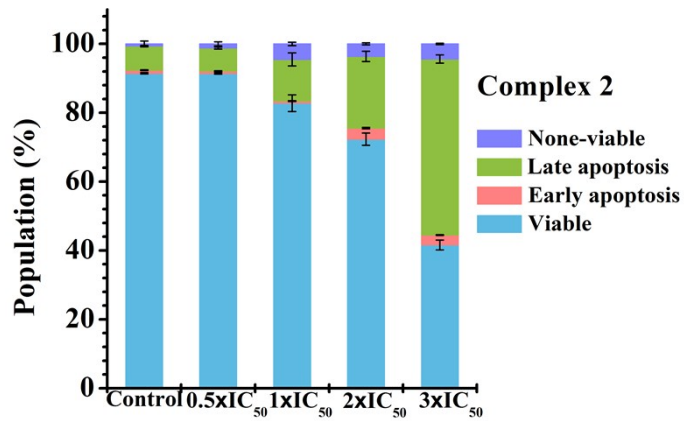


**Figure S14.** Flow cytometry analysis for cell cycle arrest of A549 cancer cells caused by complexes **2**, **4**, **6** and **12** at various concentrations after 24 h of exposure at 310 K.

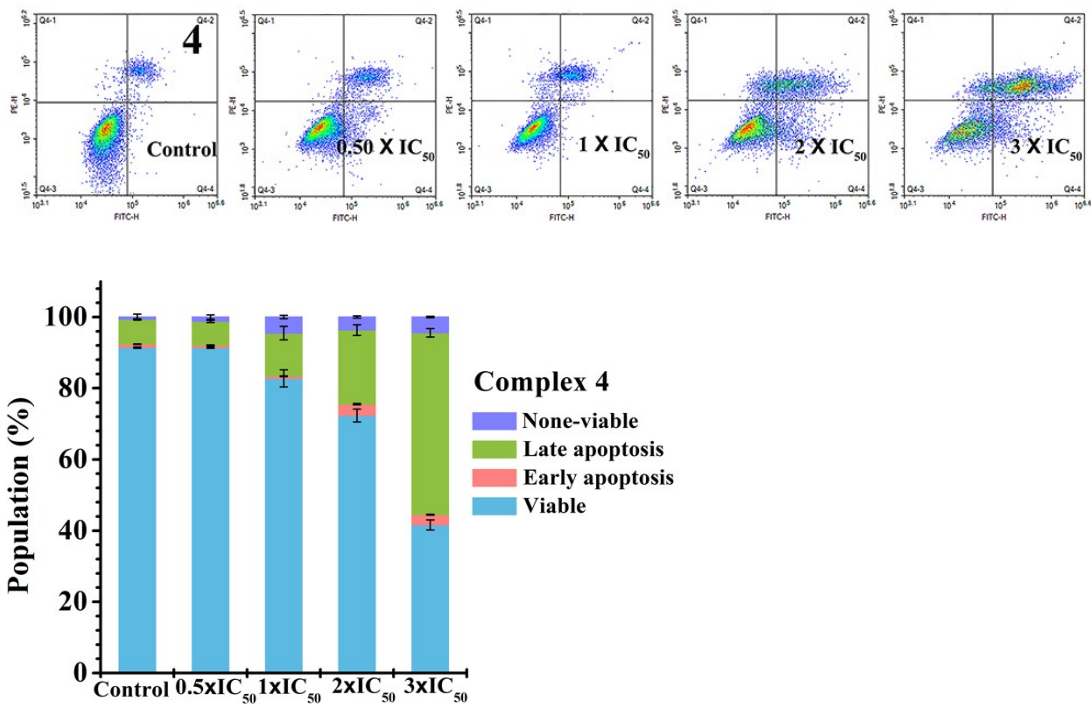


**Figure S15.** Cell cycle analyzed A549 cells exposing to complexes 2, 4, 6 and 12 after 24h by flow cytometer.

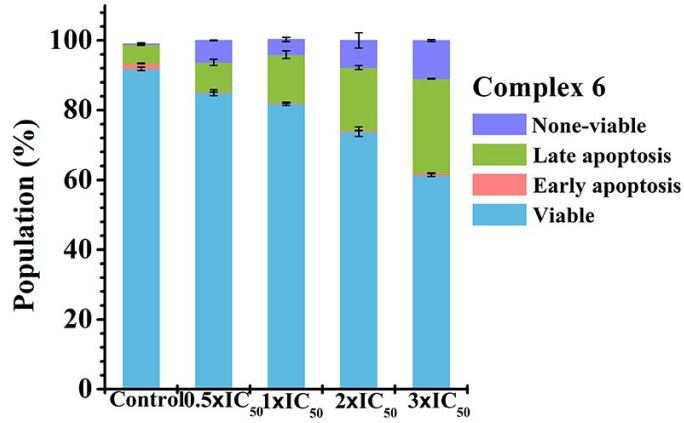




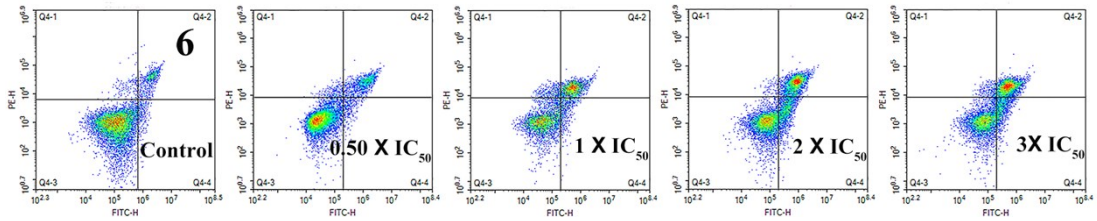
**Figure S16.** Apoptosis analysis of A549 cancer cells of exposure to complex 2 after 24 h at 310 K determined by flow cytometry using annexin VFITC vs PI staining.

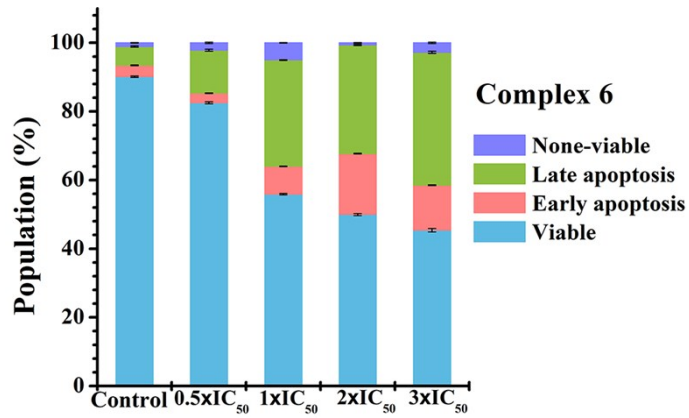


**Figure S17.** Apoptosis analysis of A549 cancer cells of exposure to complex 4 after 24 h at 310 K determined by flow cytometry using annexin VFITC vs PI staining.

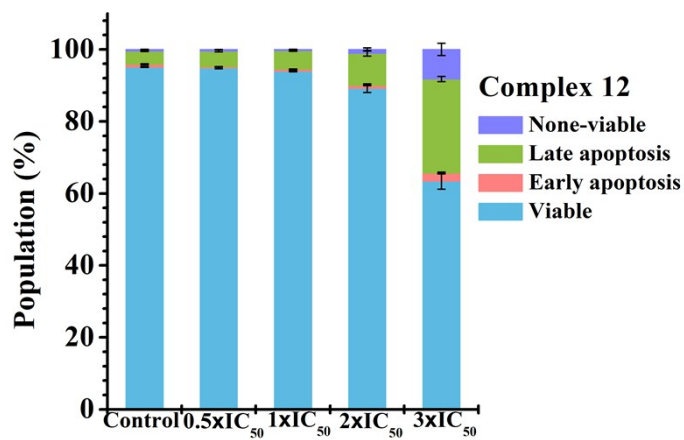
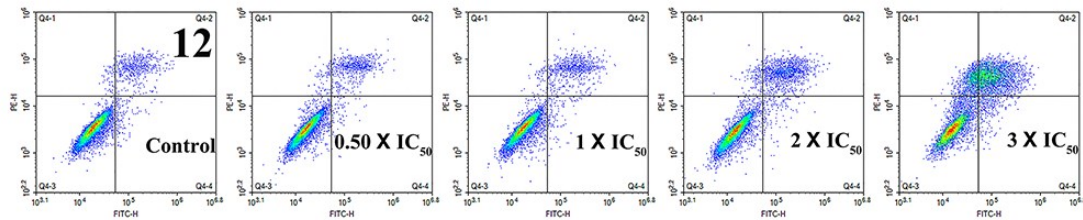


**Figure S18.** Apoptosis analysis of A549 cancer cells of exposure to complex **6** after 24 h at 310 K determined by flow cytometry using annexin VFITC vs PI staining.

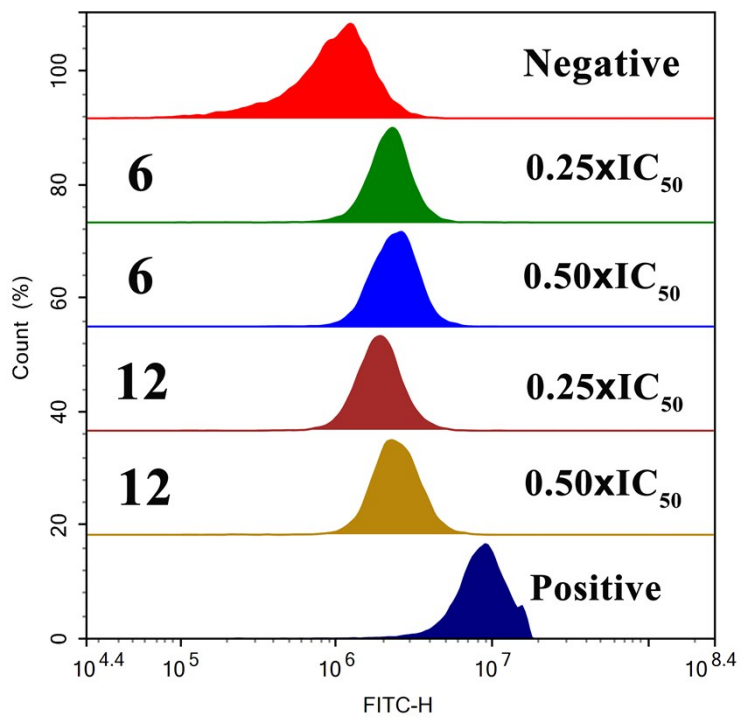




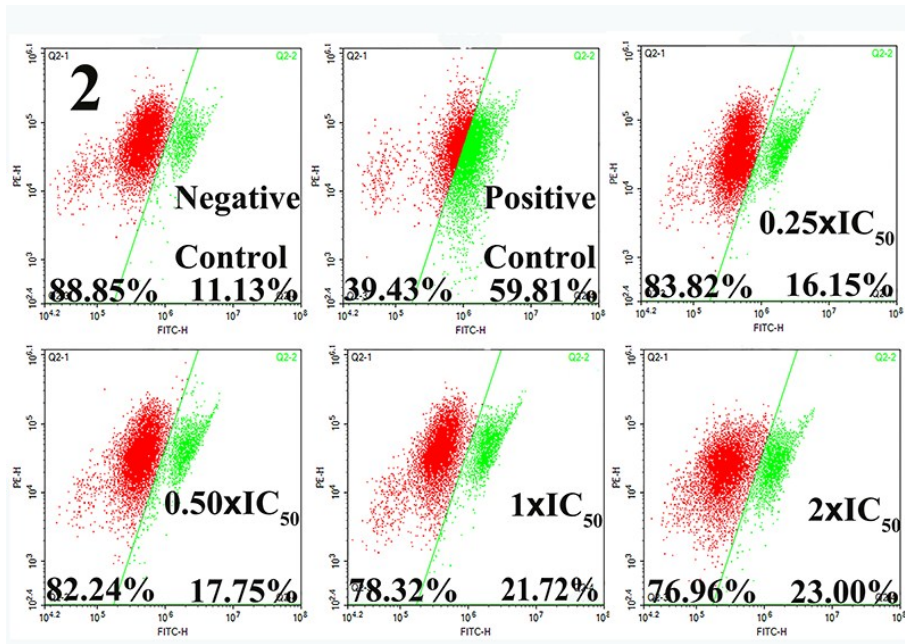
**Figure S19.** Apoptosis analysis of A549 cancer cells of exposure to complex 6 after 12 h at 310 K determined by flow cytometry using annexin V-FITC vs PI staining.



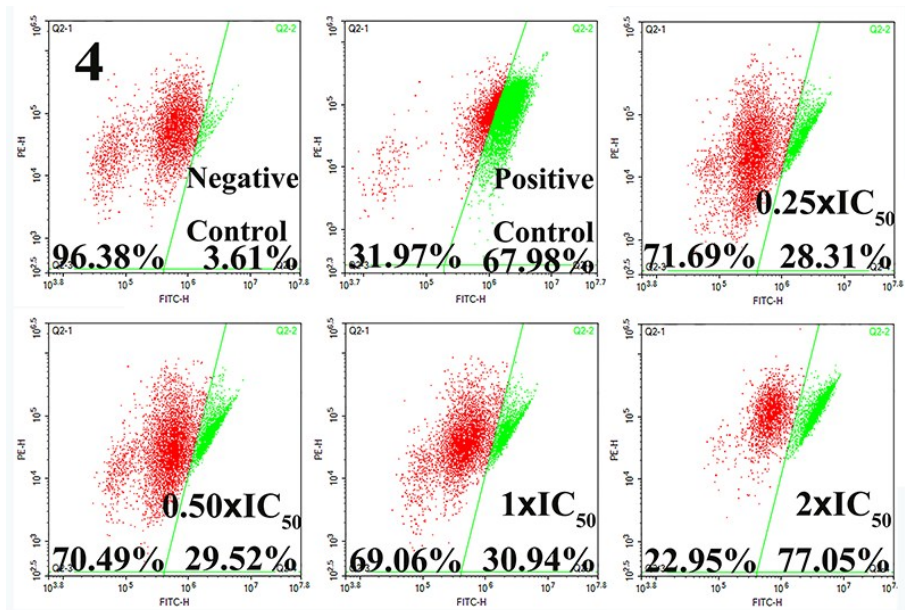
**Figure S20.** Apoptosis analysis of A549 cancer cells of exposure to complex **12** after 24 h at 310 K determined by flow cytometry using annexin VFITC vs PI staining.



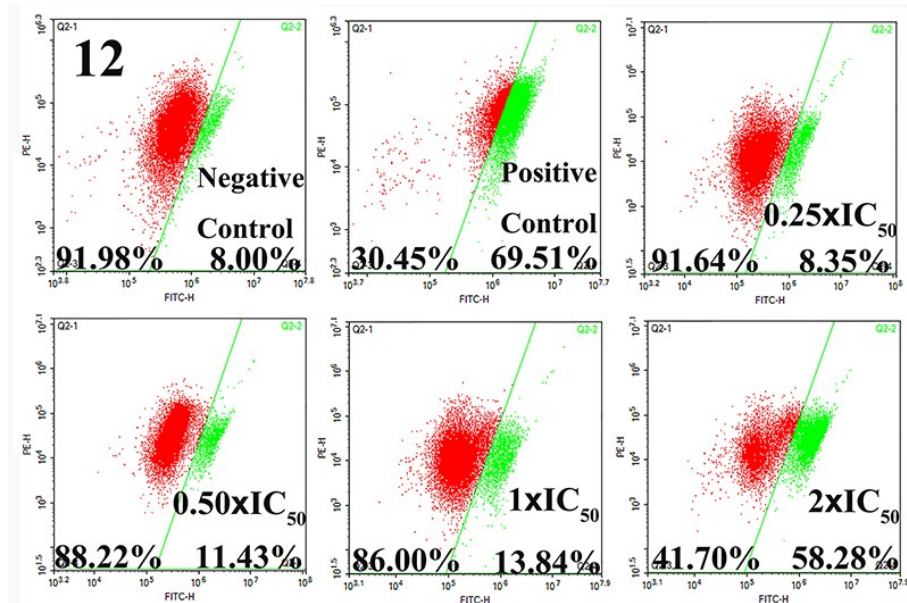
**Figure S21.** ROS of induction in A549 cancer cells treated with complexes **6** and **12** at concentration of  $0.25 \times IC_{50}$  and  $0.5 \times IC_{50}$ .



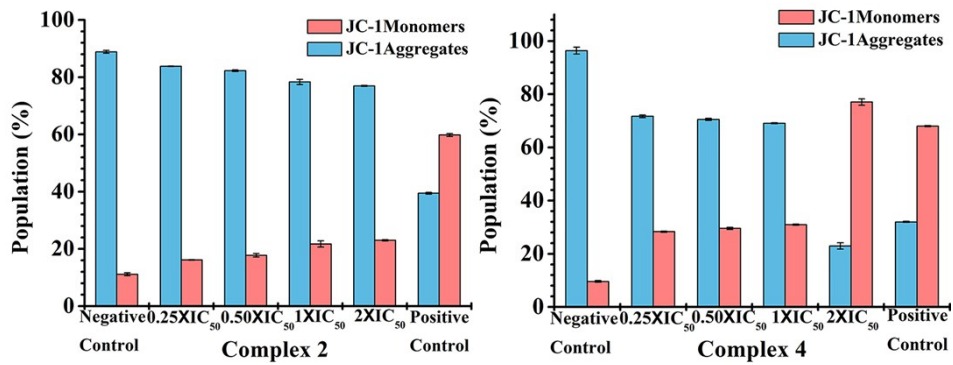
**Figure S22.** Mitochondrial membrane potential analysis of A549 cancer cells induced by complex 2.



**Figure S23.** Mitochondrial membrane potential analysis of A549 cancer cells induced by complex 4.



**Figure S24.** Mitochondrial membrane potential analysis of A549 cancer cells induced by complex 12.



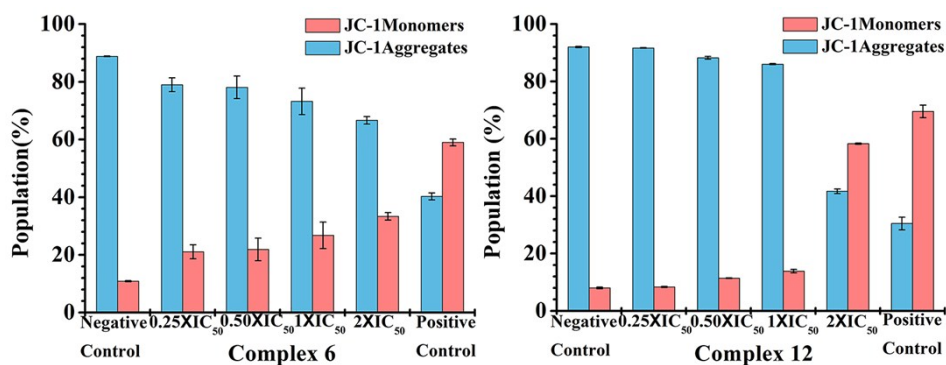


**Figure S25.** The histogram picture of mitochondrial membrane potential analysis in A549 cancer cells induced by complexes 2, 4, 6 and 12, respectively.

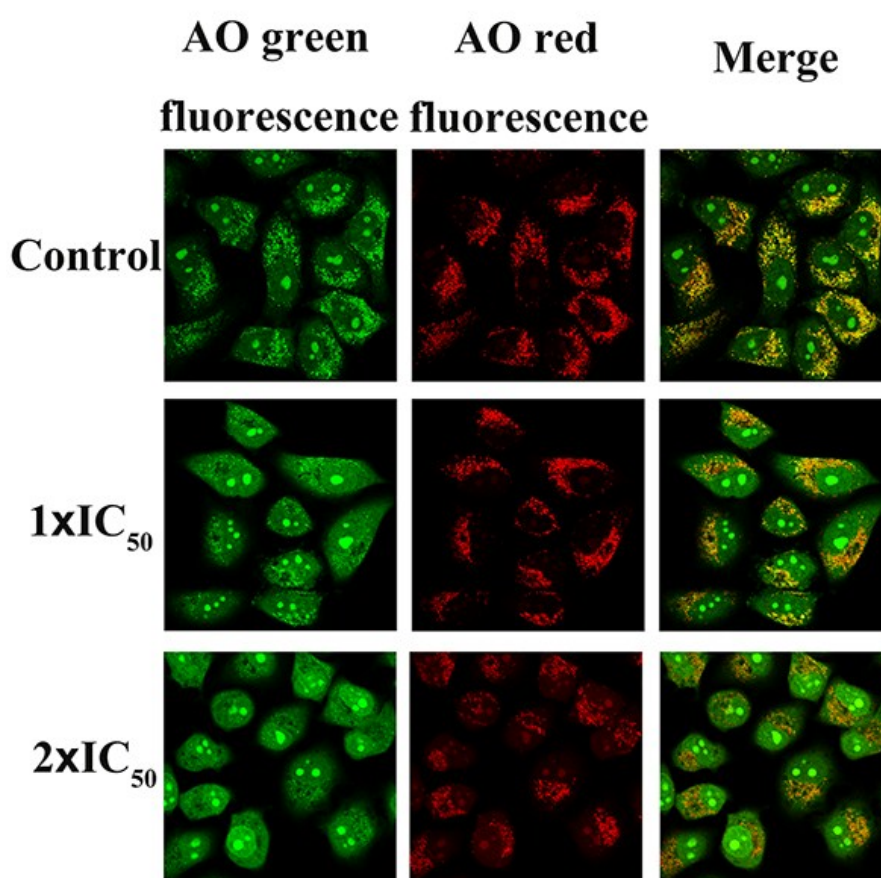


**Figure S26.** Lysosomes damaged in A549 cells was observed by AO (5  $\mu$ M) staining. Emission was collected at  $510 \pm 20$  nm (green fluorescence) and  $625 \pm 20$  nm (red fluorescence) upon excitation at 488 nm. Scale bars: 20  $\mu$ M.

**Table S1.** Hydrolysis data of complexes **2**, **4**, **5** and **6** monitored by UV-Vis at 298 K

Complex	K (min <sup>-1</sup> )	t <sub>1/2</sub> (min)
<b>2</b>	0.10	7.0
<b>4</b>	0.0015	462.1
<b>5</b>	0.0040	80.6
<b>6</b>	0.0086	173.3

---

**Table S2.** The <sup>1</sup>H NMR spectrum showed the extent of adducts formation for complexes **2**, **4**, **5** and **6** and 9-EtG and 9-EtA after 24 h.

Complex	G adduct (%)	A adduct (%)
<b>2</b>	0%	0%
<b>4</b>	0%	0%
<b>5</b>	0%	0%
<b>6</b>	0%	0%

**Table S3.** Absorption spectroscopic properties of the Ir (III) complexes on binding to DNA

Absorption $\lambda_{max}$ (nm)	Hypochromicity
---------------------------------	----------------

Complex	Free	Bound	$\Delta\lambda$	(%)	$K_b$ (mM <sup>-1</sup> )
<b>2</b>	272	276	4	17.0%	4.60
<b>4</b>	306	309	3	35.4%	3.60
<b>6</b>	257	260	3	10.6%	10.22

**Table S4.** Cell cycle analyzed A549 cells exposing to complexes **2** after 24h by flow cytometer.

complex	Ir concentration	Population (%)		
		G <sub>0</sub> /G <sub>1</sub> phase	S phase	G <sub>2</sub> /M phase
Control		57.81±0.5	32.77±0.1	14.36±0.5
<b>2</b>	0.25 × IC <sub>50</sub>	67.70±0.4	26.63±0.2	10.89±0.3
	0.50 × IC <sub>50</sub>	68.49±0.1	21.97±0.1	11.52±0.7
	1 × IC <sub>50</sub>	69.67±0.6	21.19±0.9	16.70±0.7

**Table S5.** Cell cycle analyzed A549 cells exposing to complexes **4** after 24h by flow cytometer

complex	Ir concentration	Population (%)		
		G <sub>0</sub> /G <sub>1</sub> phase	S phase	G <sub>2</sub> /M phase
Control		51.24±0.6	29.62±0.1	18.55±0.2
<b>4</b>	0.25 × IC <sub>50</sub>	49.56±1.7	30.59±0.7	17.33±0.8

	$0.50 \times IC_{50}$	54.56±0.5	28.63±1.1	13.77±0.9
	$1 \times IC_{50}$	55.81±0.5	25.93±0.6	15.07±0.3

**Table S6.** Cell cycle analyzed A549 cells exposing to complexes **6** after 24h by flow cytometer

complex	Ir concentration	Population (%)		
		G <sub>0</sub> /G <sub>1</sub> phase	S phase	G <sub>2</sub> /M phase
Control		60.68±0.3	28.21±0.4	9.59±1.0
<b>6</b>	$0.25 \times IC_{50}$	57.23±1.4	31.35±0.8	9.12±0.4
	$0.50 \times IC_{50}$	56.62±0.2	32.17±0.8	9.26±1.1
	$1 \times IC_{50}$	59.05±0.8	23.43±5.9	10.42±0.5

**Table S7.** Cell cycle analyzed A549 cells exposing to complexes **12** after 24h by flow cytometer

complex	Ir concentration	Population (%)		
		G <sub>0</sub> /G <sub>1</sub> phase	S phase	G <sub>2</sub> /M phase
Control		56.71±1.4	21.88±1.5	20.80±0.1
<b>12</b>	$0.25 \times IC_{50}$	59.28±0.4	21.59±4.5	20.08±1.6
	$0.50 \times IC_{50}$	62.89±2.3	19.12±2.0	19.38±1.2
	$1 \times IC_{50}$	66.40±2.8	16.44±1.6	22.98±2.0

**Table S8.** The percentages of apoptotic cells were determined exposing to complex **2** after 24h by flow cytometer

Complex	Ir concentration	Population (%)			
		Viable	Early apoptosis	Late apoptosis	Non-viable
<b>2</b>	$0.5 \times IC_{50}$	91.41±0.2	0.68±0.1	6.71±0.3	1.21±0.6
	$1 \times IC_{50}$	82.79±2.4	0.61±0.1	12.08±1.9	4.53±0.5
	$2 \times IC_{50}$	72.35±1.8	3.20±0.2	20.80±1.5	3.67±0.3
	$3 \times IC_{50}$	41.59±1.4	2.89±0.1	51.11±1.2	4.42±0.2
Control		91.45±0.2	0.94±0.1	6.96±0.2	0.70±0.1

**Table S9.** The percentages of apoptotic cells were determined exposing to complex **4** after 24h by flow cytometer

Complex	Ir concentration	Population (%)			
		Viable	Early apoptosis	Late apoptosis	Non-viable
<b>4</b>	$0.5 \times IC_{50}$	86.97±0.1	0.33±0.2	8.72±0.1	0.63±0.2
	$1 \times IC_{50}$	87.99±0.3	3.69±0.3	9.10±0.1	2.59±0.2
	$2 \times IC_{50}$	66.07±0.7	8.13±0.1	19.61±1.4	6.19±1.8
	$3 \times IC_{50}$	42.39±0.2	7.17±1.0	44.49±0.5	5.97±0.1

Control	93.65±0.7	0.45±0.2	4.22±0.1	1.69±0.1
---------	-----------	----------	----------	----------

**Table S10.** The percentages of apoptotic cells were determined exposing to complex **6** after 24h by flow cytometer

Population (%)					
Complex	Ir concentration	Viable	Early apoptosis	Late apoptosis	Non-viable
<b>6</b>	0.5×IC <sub>50</sub>	85.04±0.9	0.19±0.1	8.47±0.9	6.30±0.3
	1×IC <sub>50</sub>	81.85±0.5	0.22±0.1	13.85±1.1	4.36±0.6
	2×IC <sub>50</sub>	73.86±1.4	0.31±0.1	18.08±0.6	7.77±2.2
	3×IC <sub>50</sub>	61.38±0.4	0.54±0.1	27.13±0.1	10.92±0.3
Control		91.86±0.5	1.55±0.1	5.43±0.3	1.18±0.3

**Table S11.** The percentages of apoptotic cells were determined exposing to complex **6** after 12h by flow cytometer

Population (%)					
Complex	Ir concentration	Viable	Early apoptosis	Late apoptosis	Non-viable
<b>6</b>	0.5×IC <sub>50</sub>	82.51±0.2	2.81±0.1	12.54±0.3	2.15±0.2
	1×IC <sub>50</sub>	55.89±0.3	8.13±0.1	30.97±0.1	5.01±0.1
	2×IC <sub>50</sub>	49.98±0.2	17.74±0.1	31.65±0.2	0.63±0.1
	3×IC <sub>50</sub>	45.42±0.5	13.10±0.1	38.70±0.3	2.79±0.2
Control		90.14±0.2	3.31±0.1	5.47±0.2	1.07±0.1

**Table S12.** The percentages of apoptotic cells were determined exposing to complex **12** after 24h by flow cytometer

		Population (%)			
Complex	Ir concentration	Viable	Early apoptosis	Late apoptosis	Non-viable
<b>12</b>	$0.5 \times IC_{50}$	94.86±0.2	0.34±0.1	4.39±0.3	0.42±0.1
	$1 \times IC_{50}$	93.96±0.2	0.58±0.1	5.13±0.2	0.33±0.1
	$2 \times IC_{50}$	89.26±1.2	0.75±0.1	8.94±0.8	1.06±0.1
	$3 \times IC_{50}$	63.40±2.2	2.27±0.1	26.13±0.7	8.22±0.4
Control		95.13±0.1	0.73±0.1	3.73±0.2	0.41±0.1

**Table S13.** ROS induction in A549 cancer cells treated with complex **6** and **12**.

Complex	Ir concentration	Cells in ROS levels (%)
Untreated cells (negative control)		11.52±0.9
<b>6</b>	$0.25 \times IC_{50}$	26.23±0.5
<b>6</b>	$0.50 \times IC_{50}$	28.67±1.0

<b>12</b>	$0.25 \times IC_{50}$	22.62±0.3
<b>12</b>	$0.50 \times IC_{50}$	28.96±0.3
CCCP treated cells (positive control)		100

**Table S14.** The mitochondrial membrane polarization of A549 cells induced by complex 2

Complex	Ir concentration	Population (%)	
		JC-1 Aggregates	JC-1 Monomers
<b>2</b>	$0.25 \times IC_{50}$	83.82±0.1	16.15±0.1
	$0.50 \times IC_{50}$	82.25±0.3	17.75±0.6
	$1 \times IC_{50}$	78.32±0.9	21.72±1.1

	$2 \times IC_{50}$	76.96±0.2	23.00±0.2
Negative control		88.85±0.5	11.13±0.5
Positive control		39.43±0.3	59.81±0.5

**Table S15.** The mitochondrial membrane polarization of A549 cells induced by complex 4

		Population (%)	
Complex	Ir concentration	JC-1 Aggregates	JC-1 Monomers
<b>4</b>	$0.25 \times IC_{50}$	71.69±0.5	28.31±0.2
	$0.50 \times IC_{50}$	70.49±0.4	29.52±0.4
	$1 \times IC_{50}$	69.06±0.2	30.94±0.2
	$2 \times IC_{50}$	22.95±1.2	77.05±1.2
Negative control		96.39±1.3	9.60±0.3
Positive control		31.97±0.2	67.98±0.2

**Table S16.** The mitochondrial membrane polarization of A549 cells induced by complex 6

		Population (%)	
Complex	Ir concentration	JC-1 Aggregates	JC-1 Monomers
<b>6</b>	$0.25 \times IC_{50}$	78.93±2.4	21.08±2.4
	$0.50 \times IC_{50}$	78.07±3.9	21.90±3.9
	$1 \times IC_{50}$	73.20±4.6	26.80±4.6
	$2 \times IC_{50}$	66.64±1.3	33.36±1.3

Negative control	88.83±0.1	10.90±0.2
Positive control	40.25±1.2	58.98±1.2

**Table S17.** The mitochondrial membrane polarization of A549 cells induced by complex **12**

		Population (%)	
Complex	Ir concentration	JC-1 Aggregates	JC-1 Monomers
<b>12</b>	0.25 × IC <sub>50</sub>	91.64±0.2	8.35±0.2
	0.50 × IC <sub>50</sub>	88.22±0.1	11.43±0.1
	1 × IC <sub>50</sub>	86.00±0.5	13.84±0.6
	2 × IC <sub>50</sub>	41.70±0.2	58.28±0.2
Negative control		91.98±0.8	8.00±0.3
Positive control		30.45±2.2	69.51±2.2

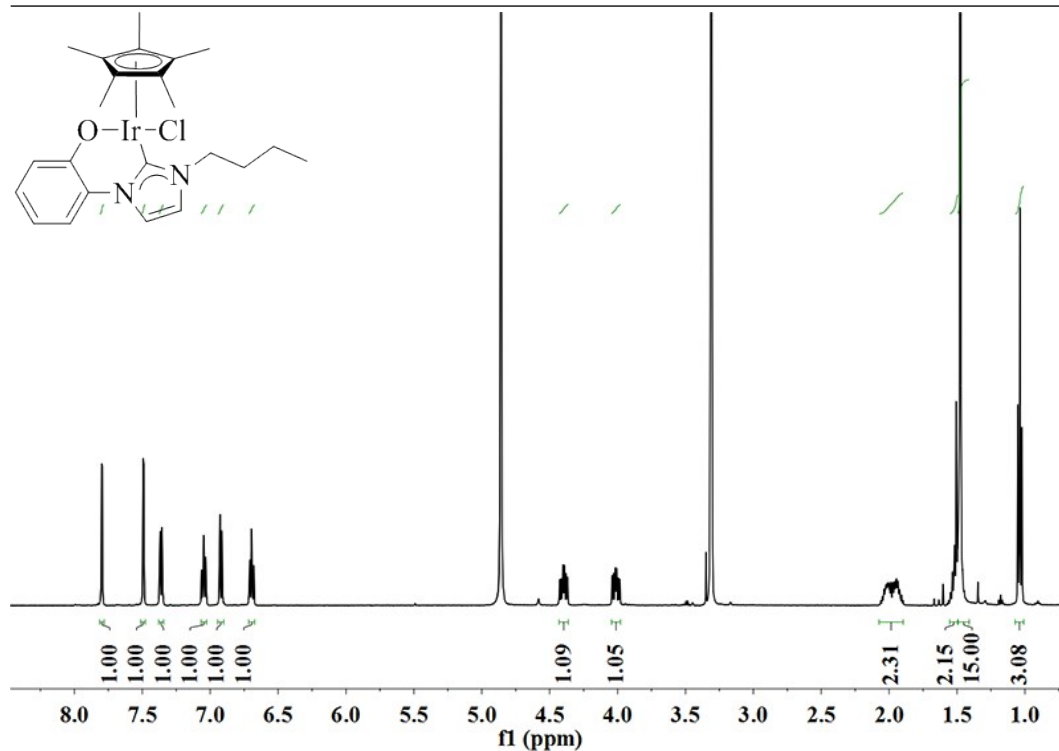


**Figure S27.** The <sup>1</sup>H NMR (500.13 MHz, MeOD-d<sub>4</sub>) peak integrals of [(η<sup>5</sup>-C<sub>5</sub>Me<sub>5</sub>)Ir(L1)Cl] (**1**).

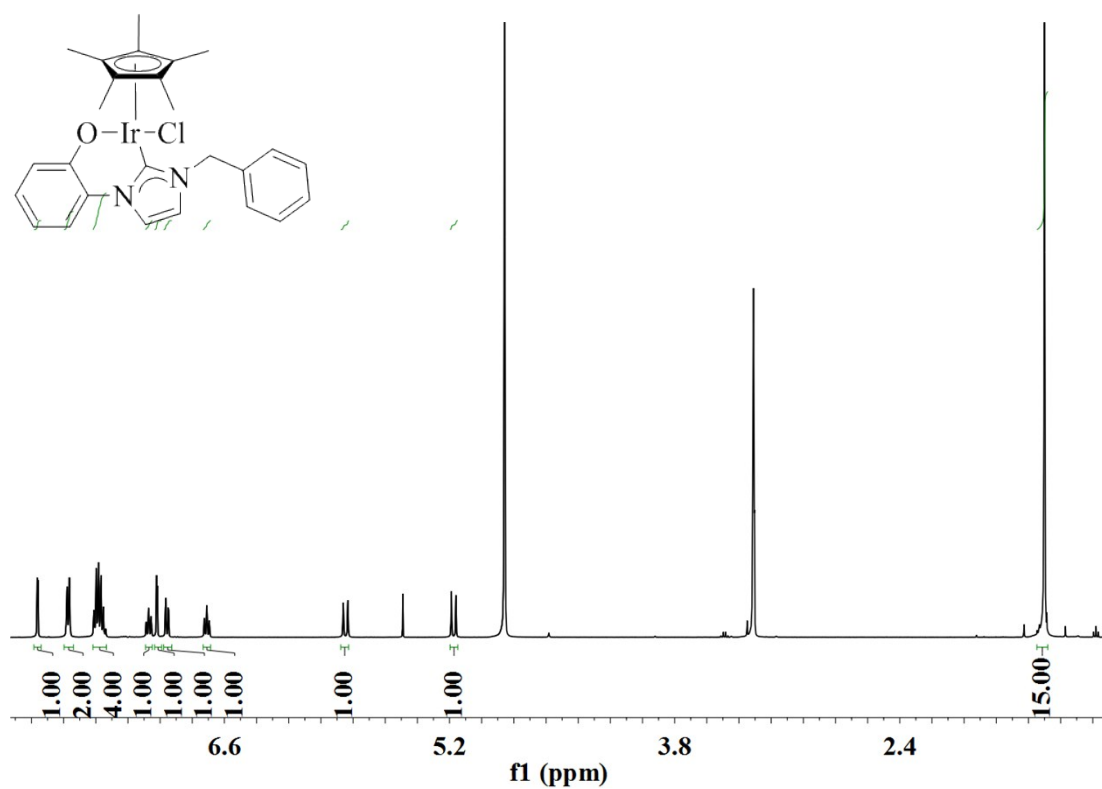


**Figure S28.** The  $^1\text{H}$  NMR (500.13 MHz, MeOD- $d_4$ ) peak integrals of  $[(\eta^5\text{-C}_5\text{Me}_5)\text{Ir}(\text{L}2)\text{Cl}]$  (2).

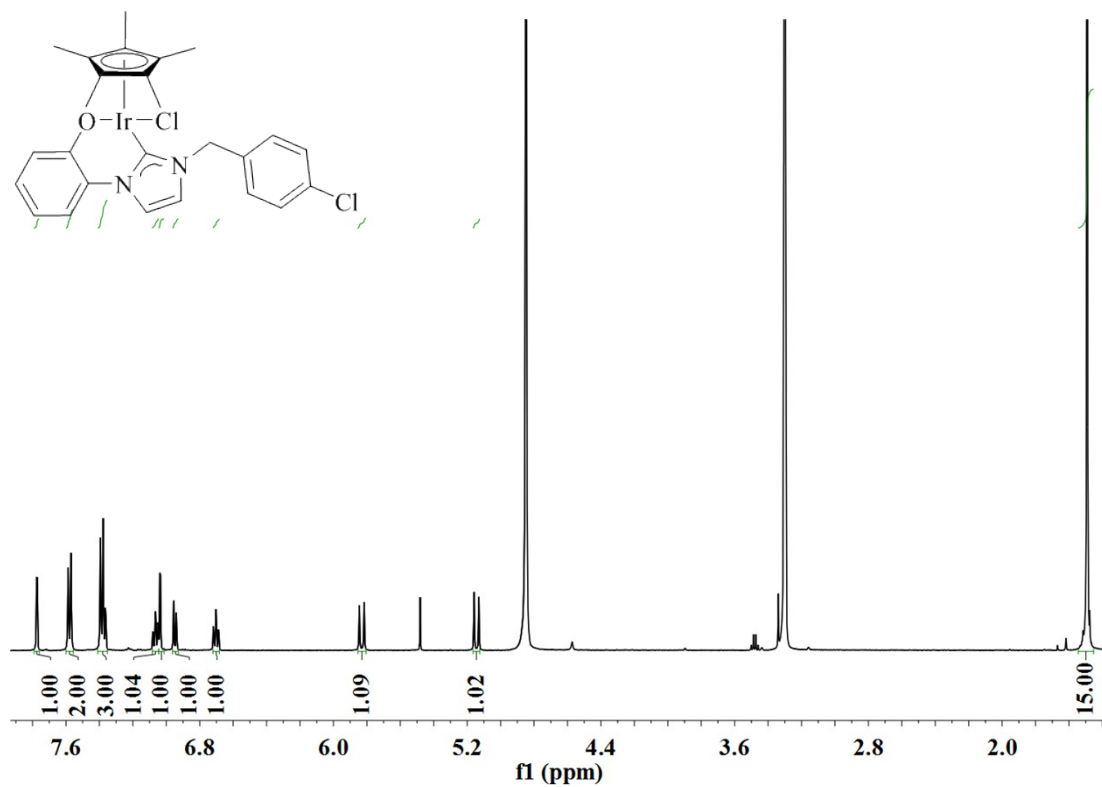


**Figure S29.** The  $^1\text{H}$  NMR (500.13 MHz, MeOD- $d_4$ ) peak integrals of  $[(\eta^5\text{-C}_5\text{Me}_5)\text{Ir}(\text{L3})\text{Cl}]$  (**3**)

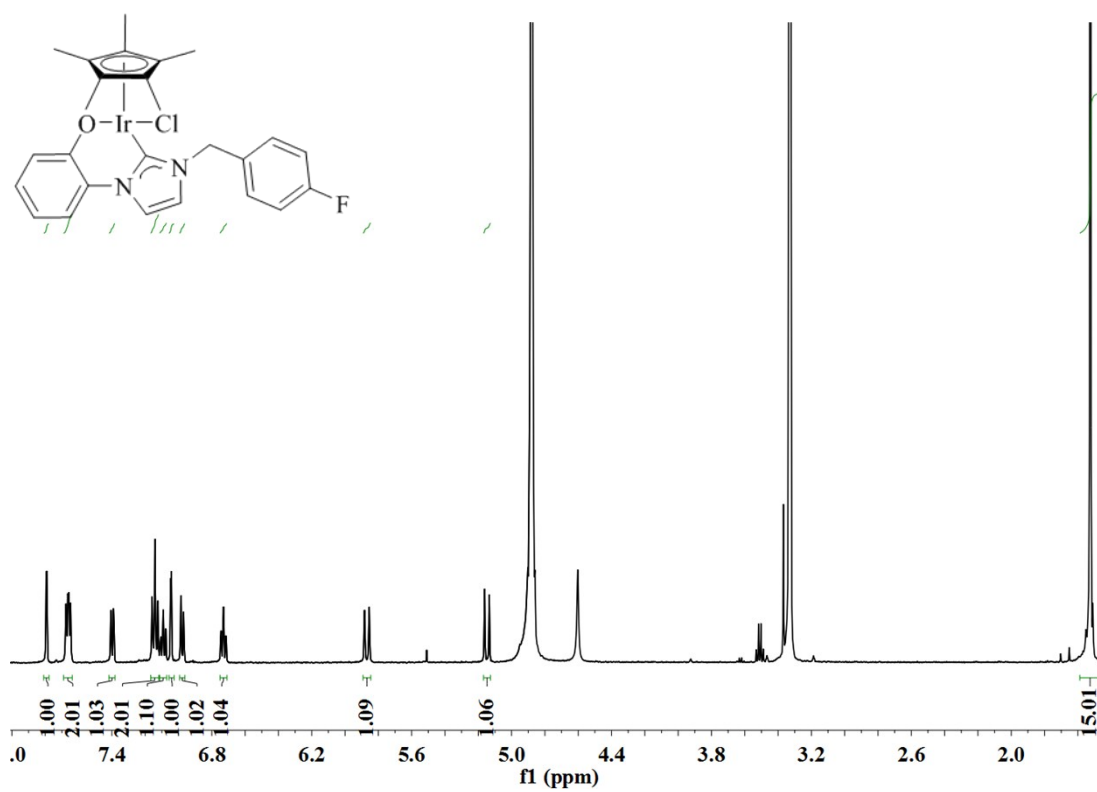


**Figure S30.** The  $^1\text{H}$  NMR (500.13 MHz, MeOD- $d_4$ ) peak integrals of  $[(\eta^5\text{-C}_5\text{Me}_5)\text{Ir}(\text{L4})\text{Cl}]$  (**4**)

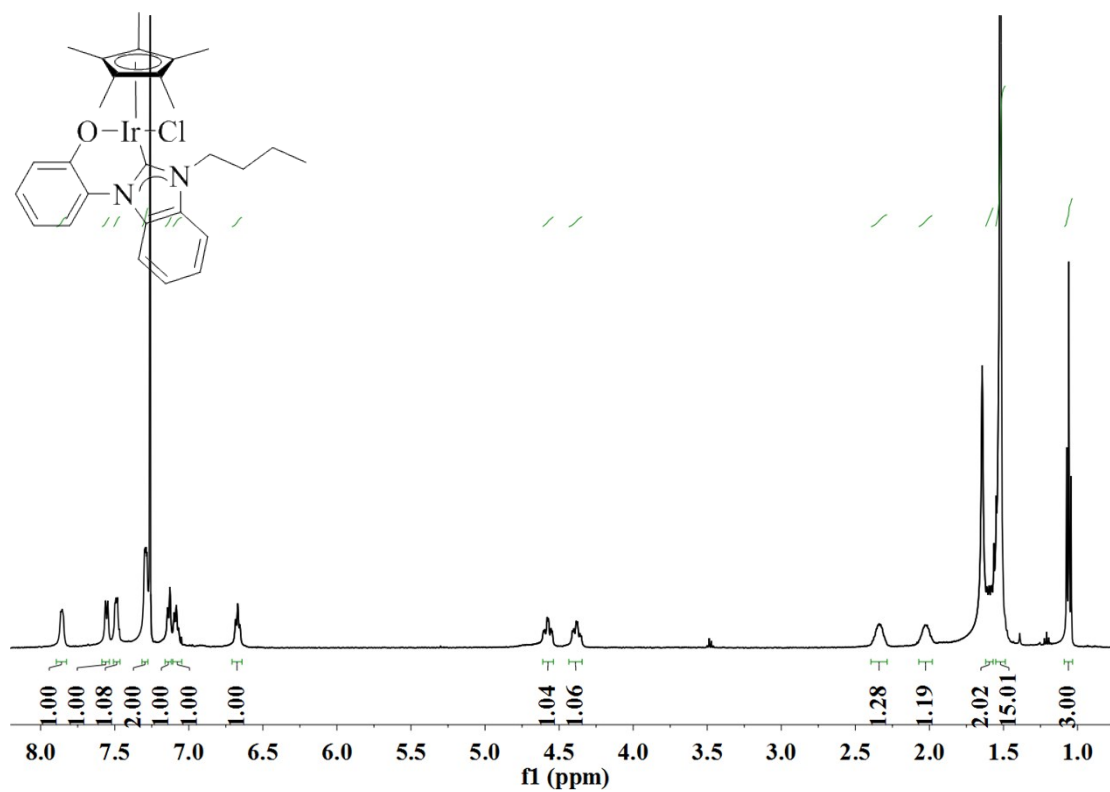


**Figure S31.** The  $^1\text{H}$  NMR (500.13 MHz,  $\text{CDCl}_3$ ) peak integrals of  $[(\eta^5\text{-C}_3\text{Me}_5)\text{Ir}(\text{L}5)\text{Cl}]$  (5).

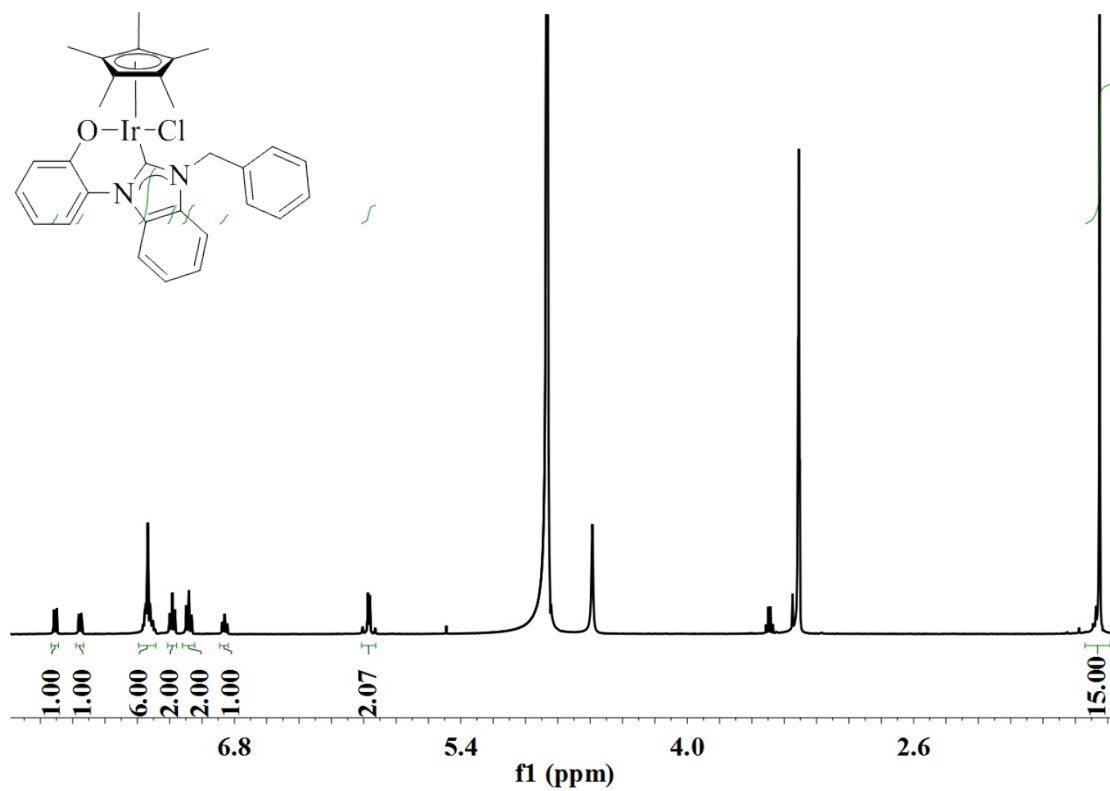


**Figure S32.** The  $^1\text{H}$  NMR (500.13 MHz, MeOD) peak integrals of  $[(\eta^5\text{-C}_5\text{Me}_5)\text{Ir}(\text{L6})\text{Cl}]$  (**6**).

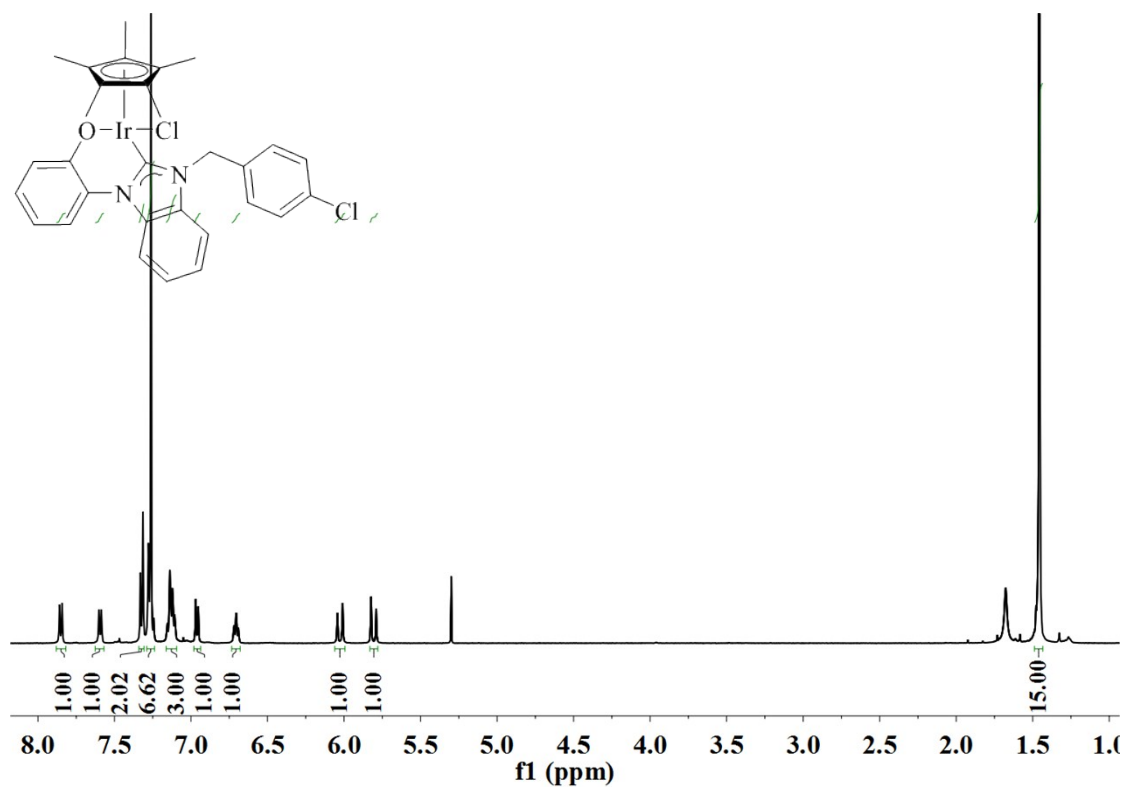


**Figure S33.** The  $^1\text{H}$  NMR (500.13 MHz,  $\text{CDCl}_3$ ) peak integrals of  $[(\eta^5\text{-C}_5\text{Me}_5)\text{Ir}(\text{L7})\text{Cl}]$  (**7**).

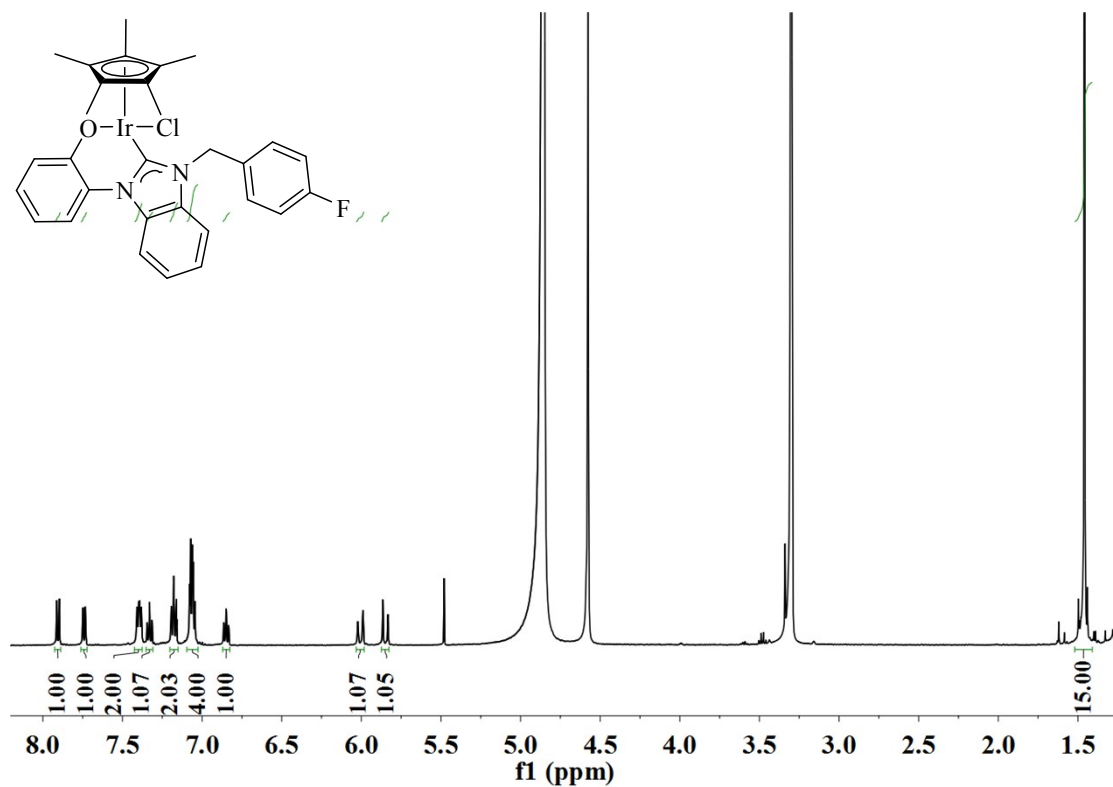


**Figure S34.** The  $^1\text{H}$  NMR (500.13 MHz, MeOD) peak integrals of  $[(\eta^5\text{-C}_5\text{Me}_5)\text{Ir}(\text{L}8)\text{Cl}]$  (**8**).

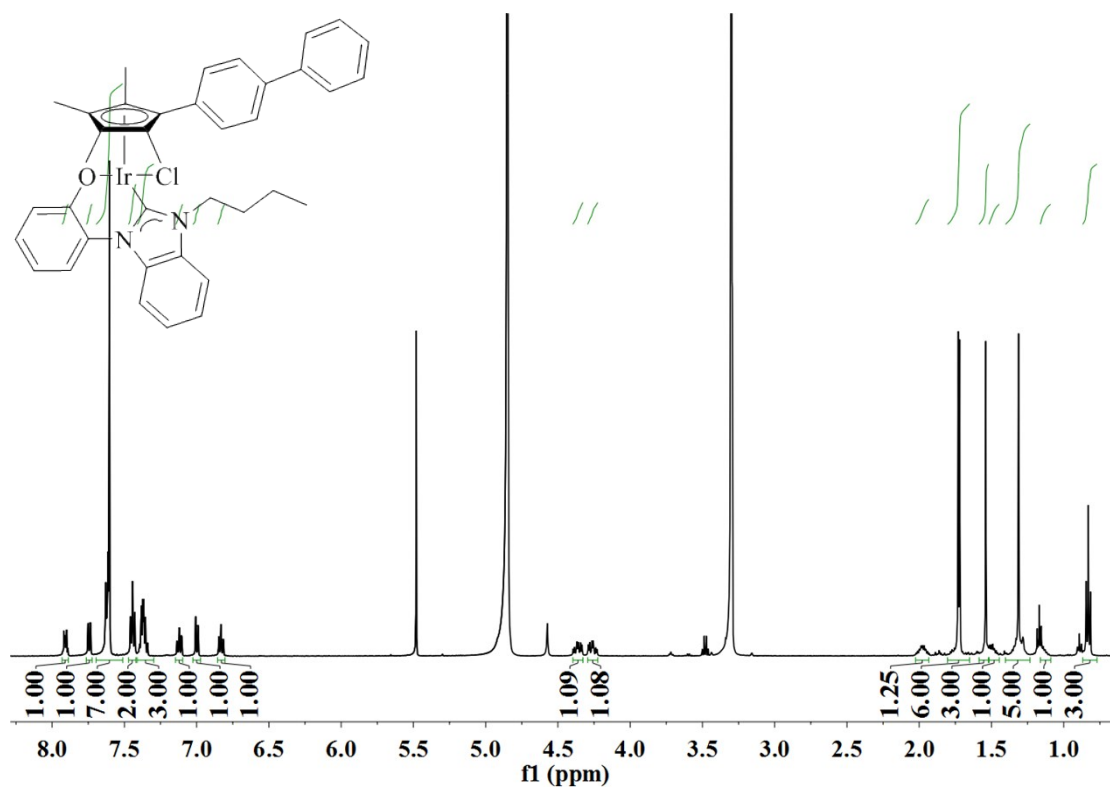


**Figure S35.** The  $^1\text{H}$  NMR (500.13 MHz, MeOD) peak integrals of  $[(\eta^5\text{-C}_5\text{Me}_4\text{C}_6\text{H}_4\text{C}_6\text{H}_5)\text{Ir}(\text{L}1)\text{Cl}]$  (**9**).

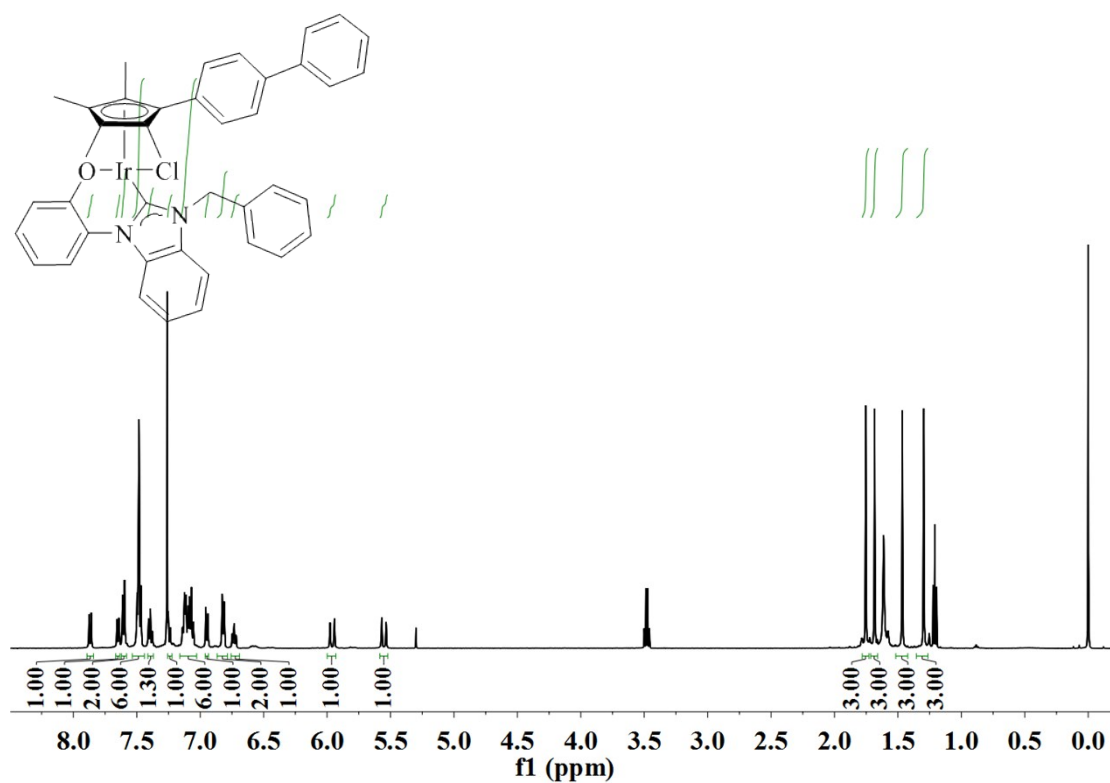


**Figure S36.** The  $^1\text{H}$  NMR (500.13 MHz,  $\text{CDCl}_3$ ) peak integrals of  $[(\eta^5\text{-C}_5\text{Me}_4\text{C}_6\text{H}_4\text{C}_6\text{H}_5)\text{Ir}(\text{L}2)\text{Cl}]$  (10).

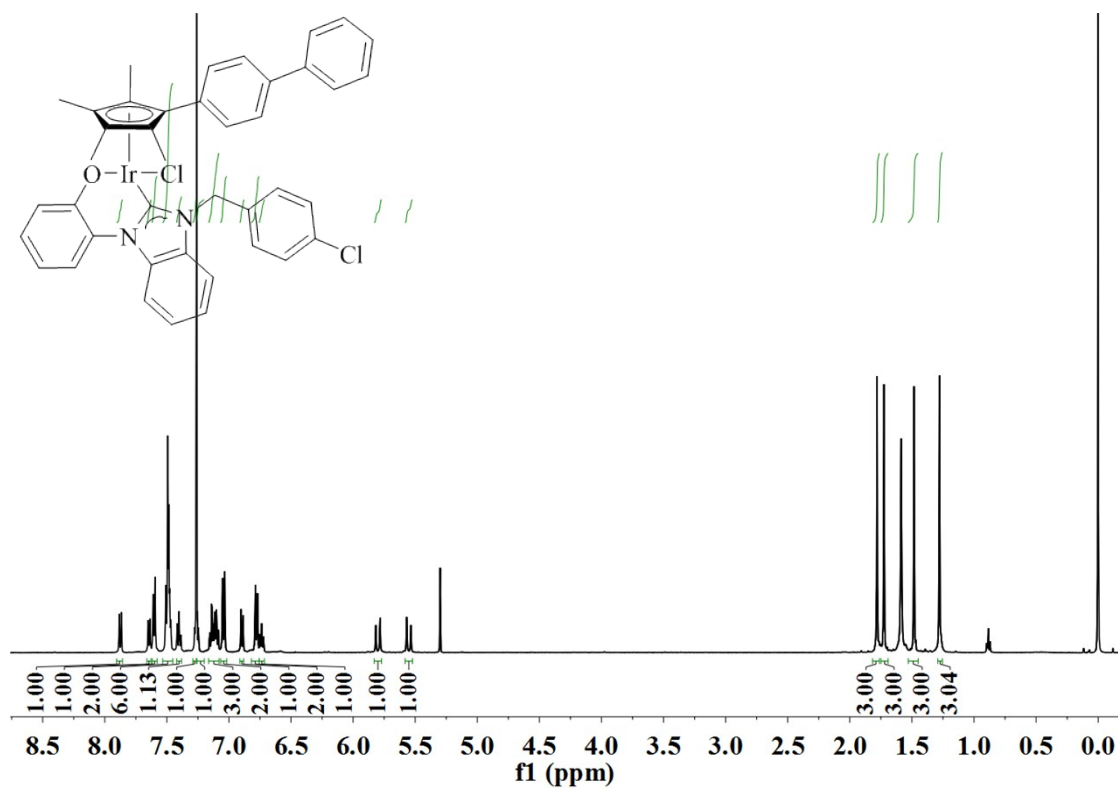


**Figure S37.** The  $^1\text{H}$  NMR (500.13 MHz,  $\text{CDCl}_3$ ) peak integrals of  $[(\eta^5\text{-C}_5\text{Me}_4\text{C}_6\text{H}_4\text{C}_6\text{H}_5)\text{Ir}(\text{L3})\text{Cl}]$  (11).

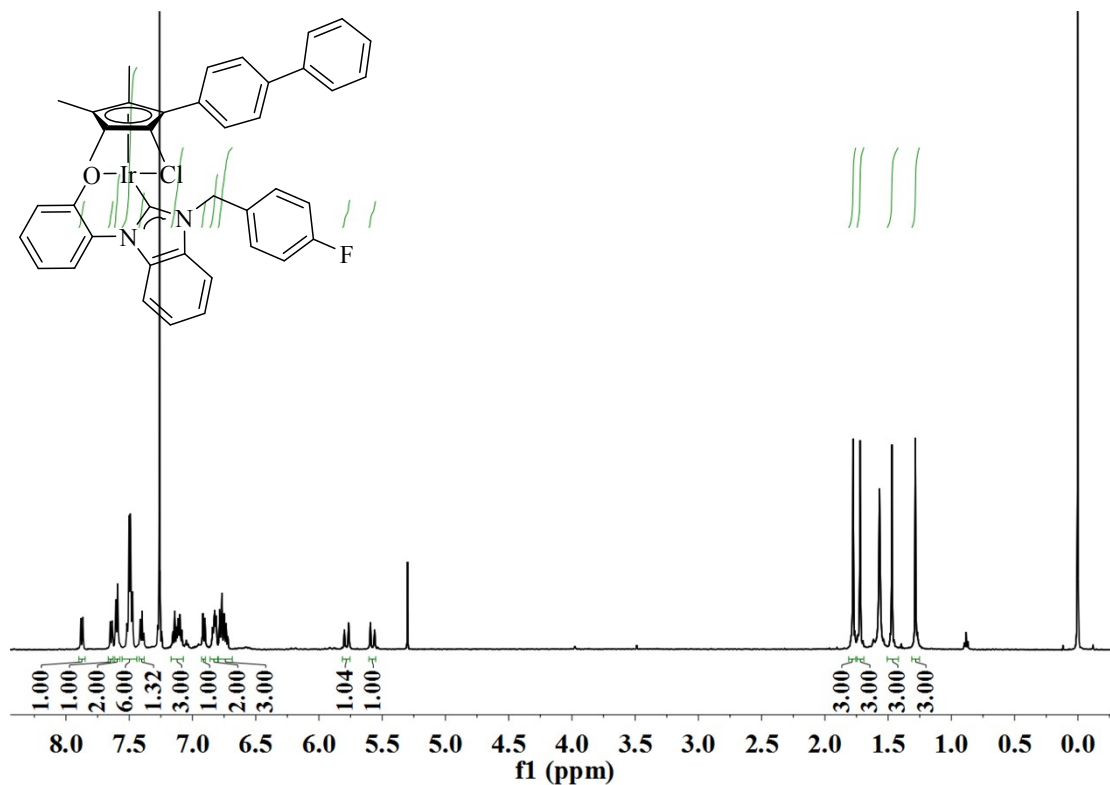


**Figure S38.** The  $^1\text{H}$  NMR (500.13 MHz,  $\text{CDCl}_3$ ) peak integrals of  $[(\eta^5\text{-C}_5\text{Me}_4\text{C}_6\text{H}_4\text{C}_6\text{H}_5)\text{Ir}(\text{L4})\text{Cl}]$  (12).

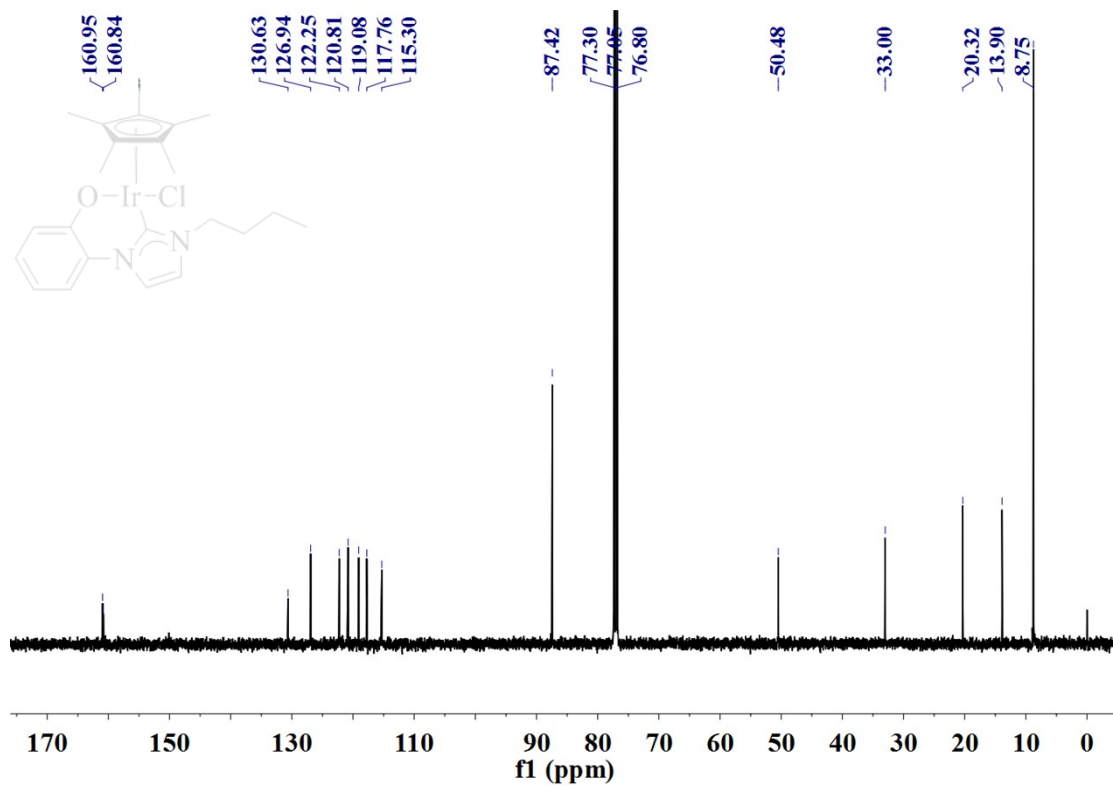
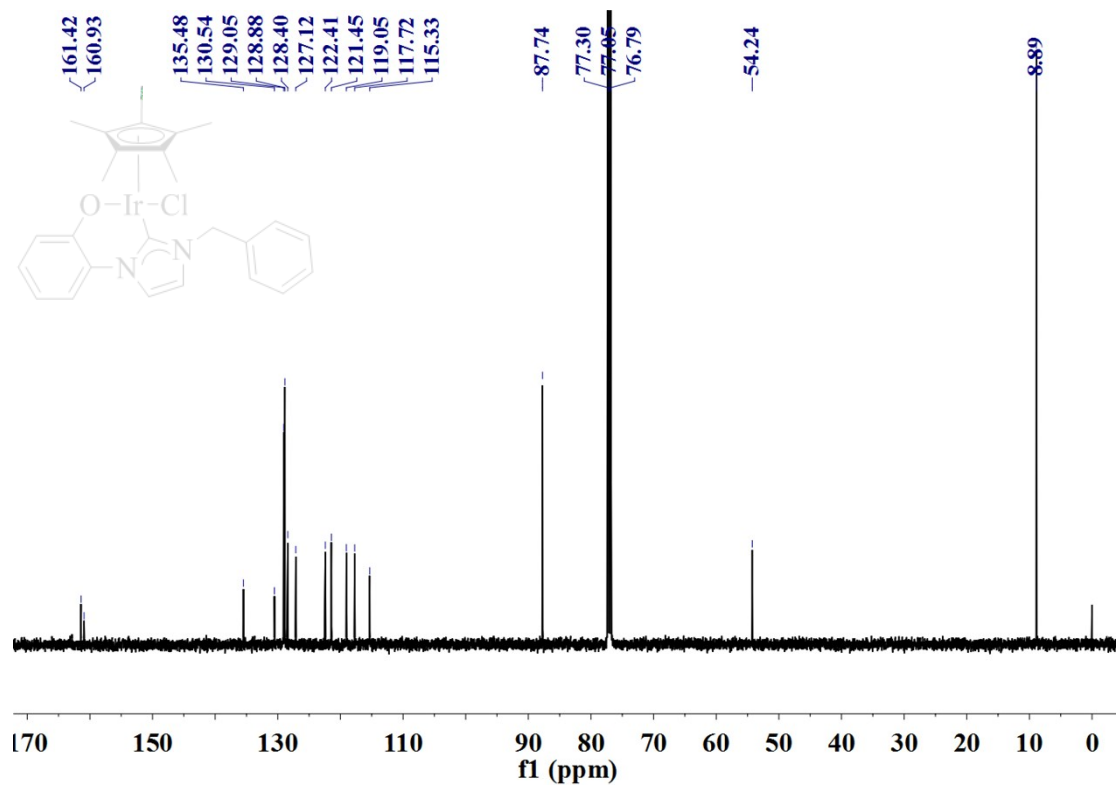
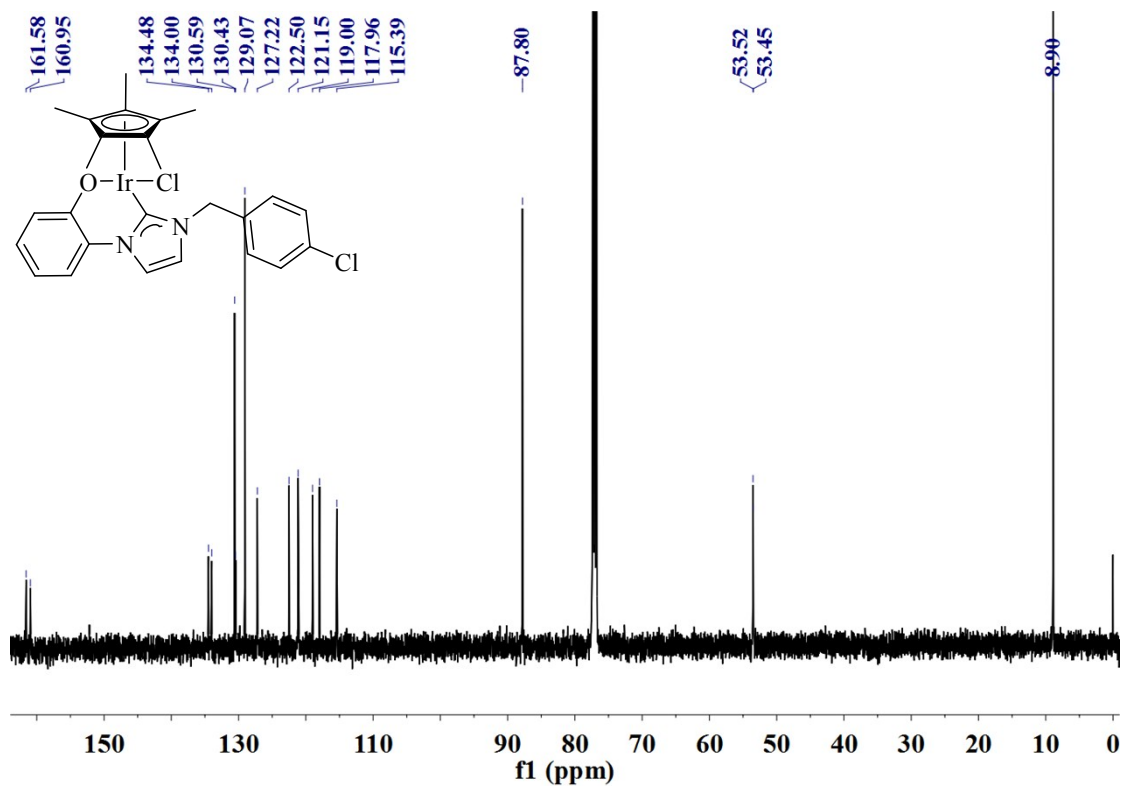


Figure S39. The  $^{13}\text{C}$  NMR (126 MHz,  $\text{CDCl}_3$ ) peak integrals of  $[(\eta^5\text{-C}_5\text{Me}_5)\text{Ir}(\text{L1})\text{Cl}]$  (1).



**Figure S40.** The  $^{13}\text{C}$  NMR (126 MHz,  $\text{CDCl}_3$ ) peak integrals of  $[(\eta^5\text{-C}_5\text{Me}_5)\text{Ir}(\text{L2})\text{Cl}]$  (**2**).



**Figure S41.** The  $^{13}\text{C}$  NMR (126 MHz,  $\text{CDCl}_3$ ) peak integrals of  $[(\eta^5\text{-C}_5\text{Me}_5)\text{Ir}(\text{L3})\text{Cl}]$  (**3**).

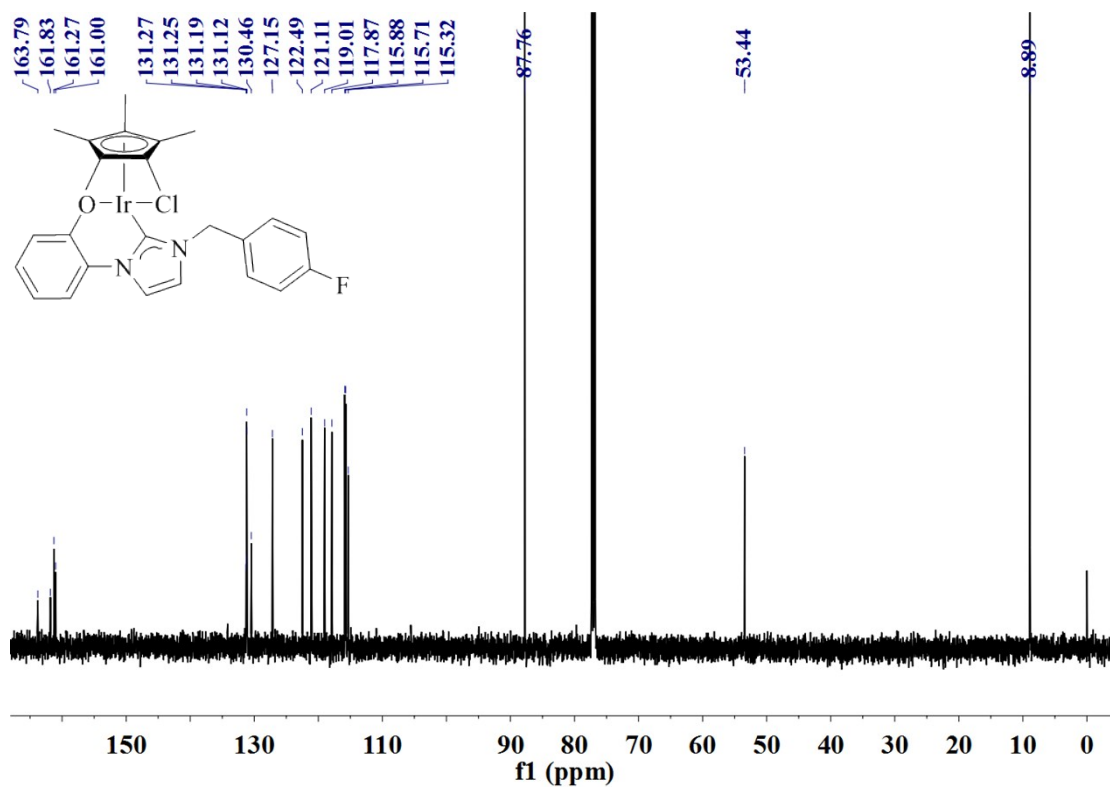


**Figure S42.** The  $^{13}\text{C}$  NMR (126 MHz,  $\text{CDCl}_3$ ) peak integrals of  $[(\eta^5\text{-C}_5\text{Me}_5)\text{Ir}(\text{L4})\text{Cl}]$  (4)

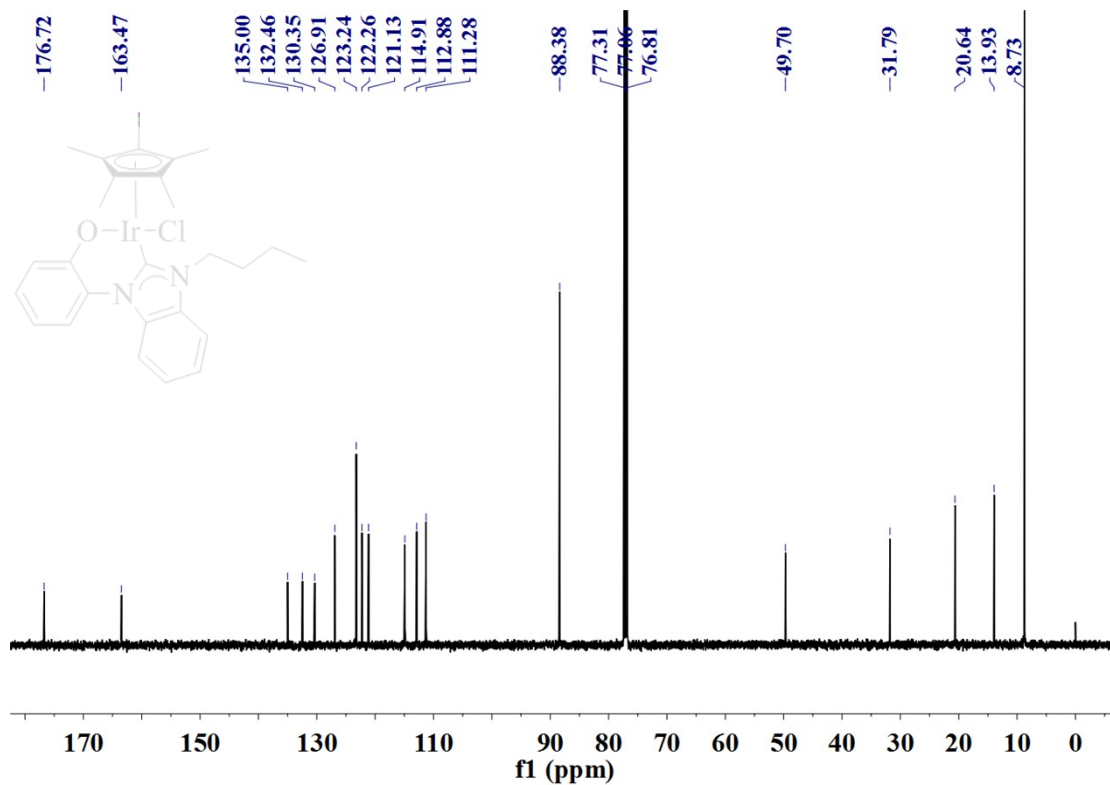


**Figure S43.** The  $^{13}\text{C}$  NMR (126 MHz,  $\text{CDCl}_3$ ) peak integrals of  $[(\eta^5\text{-C}_5\text{Me}_5)\text{Ir}(\text{L5})\text{Cl}]$  (**5**).

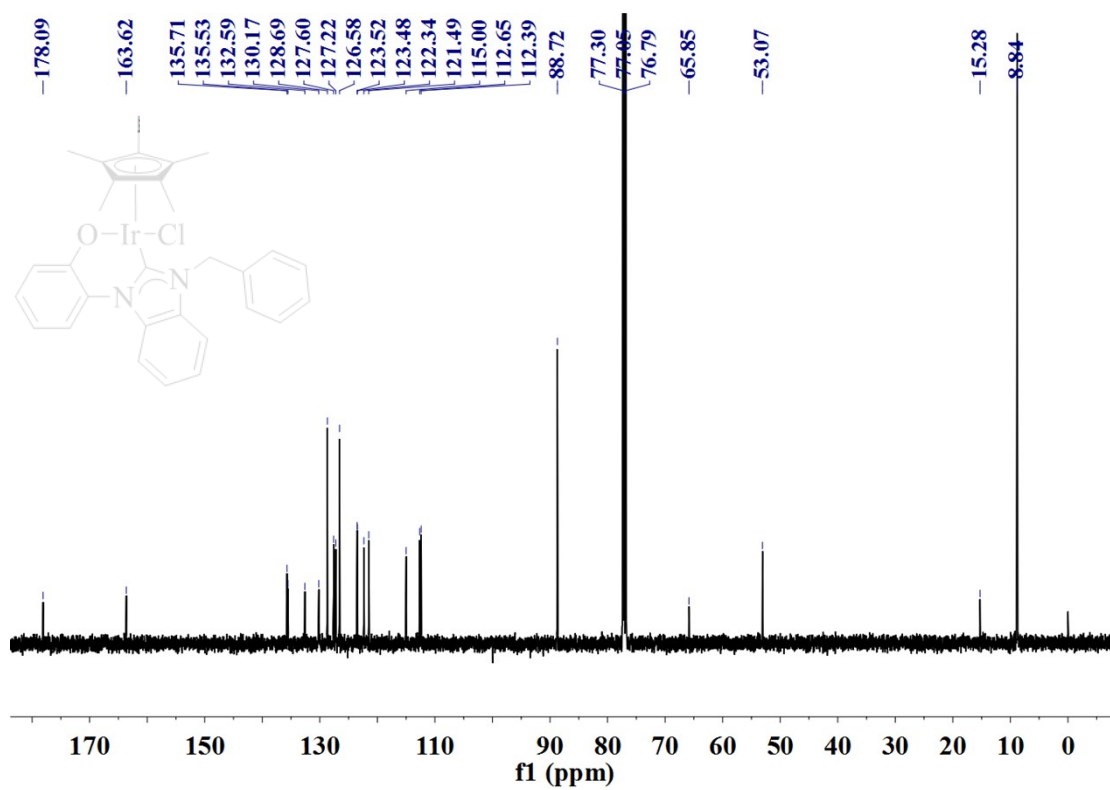


**Figure S44.** The  $^{13}\text{C}$  NMR (126 MHz,  $\text{CDCl}_3$ ) peak integrals of  $[(\eta^5\text{-C}_5\text{Me}_5)\text{Ir}(\text{L6})\text{Cl}]$  (**6**).

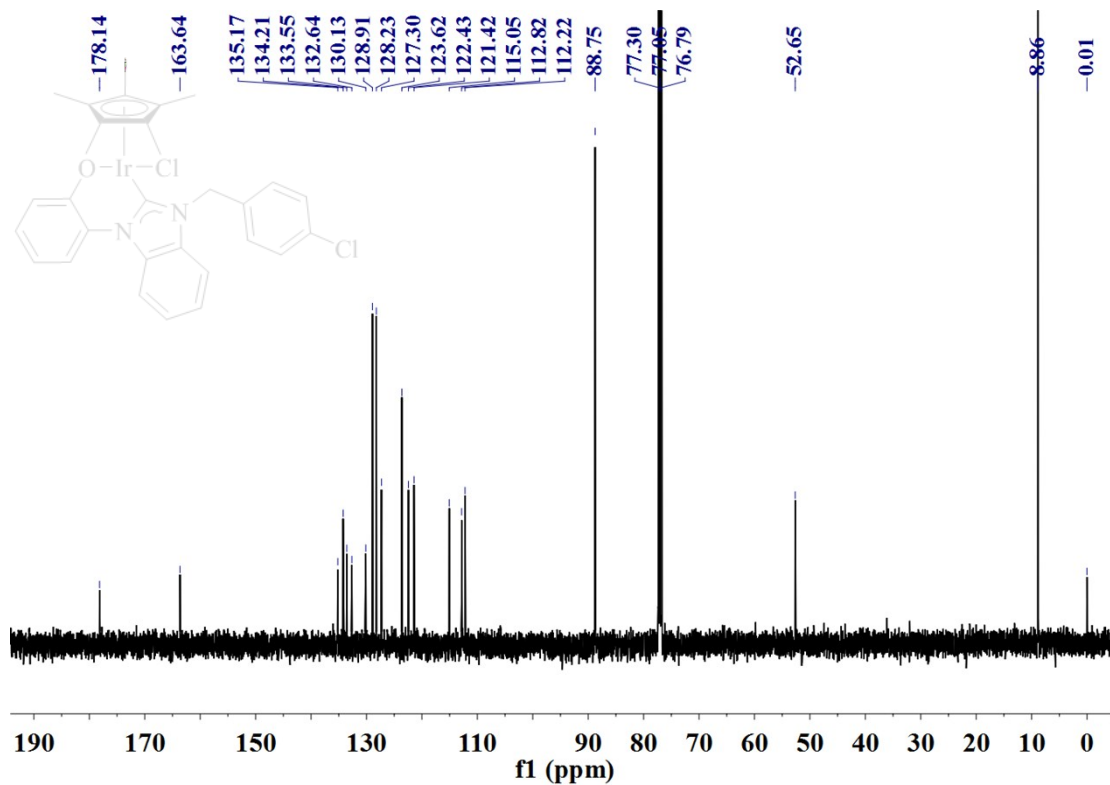
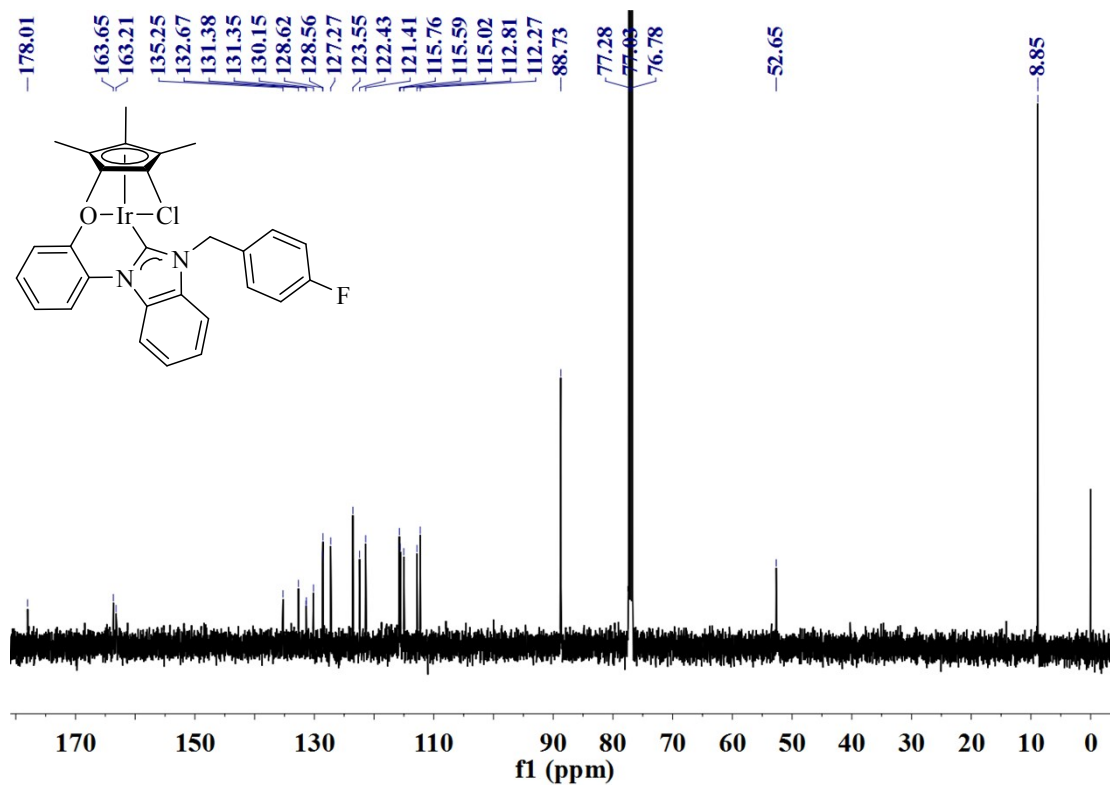
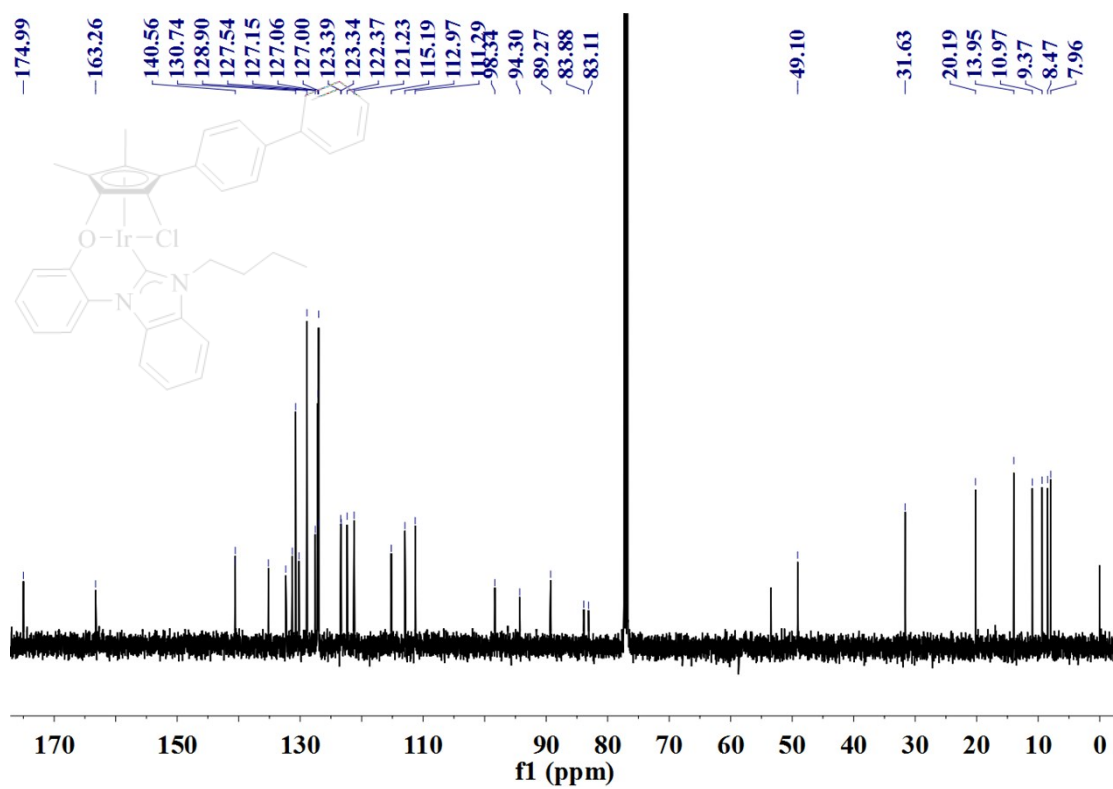


Figure S45. The  $^{13}\text{C}$  NMR (126 MHz,  $\text{CDCl}_3$ ) peak integrals of  $[(\eta^5\text{-C}_5\text{Me}_5)\text{Ir}(\text{L7})\text{Cl}]$  (7).



**Figure S46.** The  $^{13}\text{C}$  NMR (126 MHz,  $\text{CDCl}_3$ ) peak integrals of  $[(\eta^5\text{-C}_5\text{Me}_5)\text{Ir}(\text{L4})\text{Cl}]$  (**8**).



**Figure S47.** The  $^{13}\text{C}$  NMR (126 MHz,  $\text{CDCl}_3$ ) peak integrals of  $[(\eta^5\text{-C}_5\text{Me}_4\text{C}_6\text{H}_4\text{C}_6\text{H}_5)\text{Ir}(\text{L1})\text{Cl}]$  (**9**).

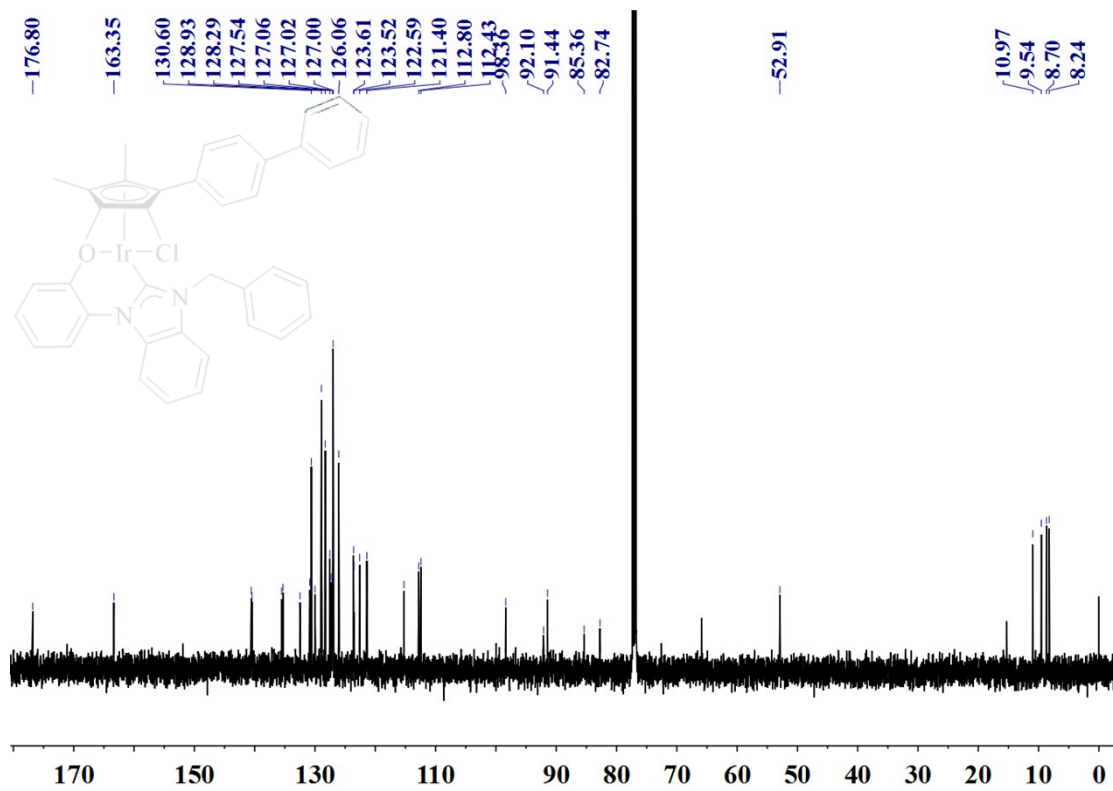


**Figure S48.** The <sup>13</sup>C NMR (126 MHz, CDCl<sub>3</sub>) peak integrals of [(η<sup>5</sup>-C<sub>5</sub>Me<sub>4</sub>C<sub>6</sub>H<sub>4</sub>C<sub>6</sub>H<sub>5</sub>)Ir(L2)Cl] (10).

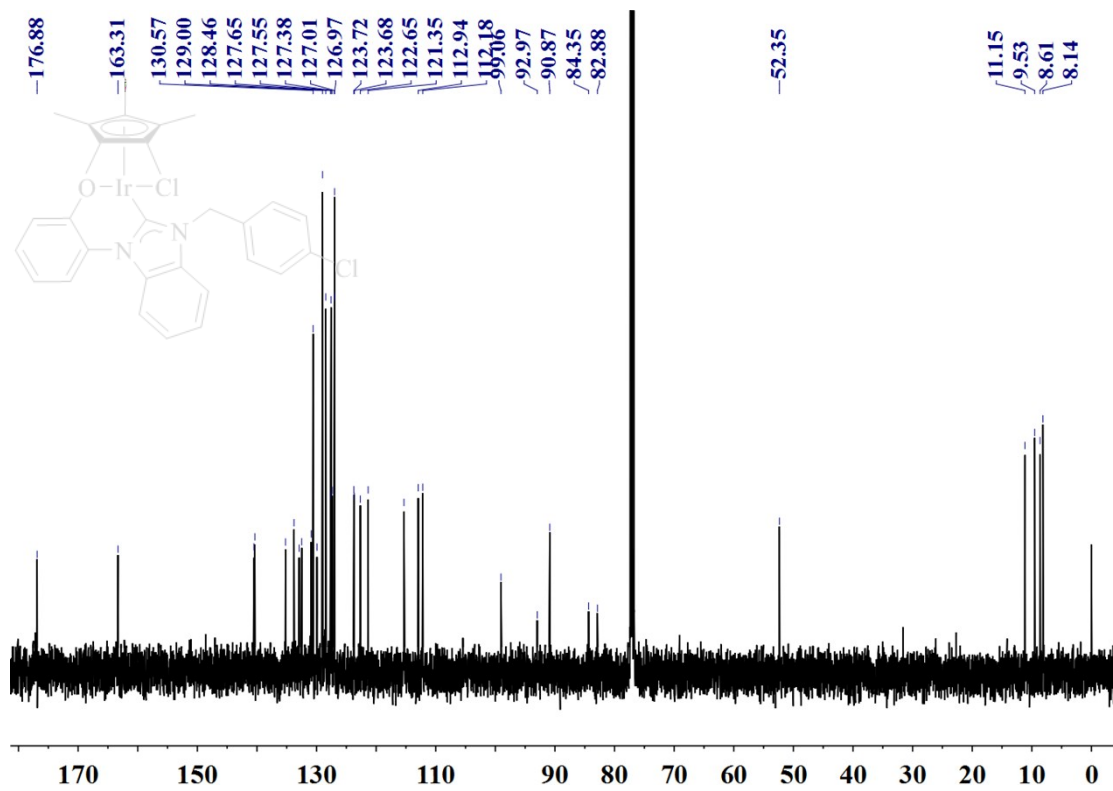


**Figure S49.** The  $^{13}\text{C}$  NMR (126 MHz,  $\text{CDCl}_3$ ) peak integrals of  $[(\eta^5\text{-C}_5\text{Me}_4\text{C}_6\text{H}_4\text{C}_6\text{H}_5)\text{Ir}(\text{L}3)\text{Cl}]$  (11).

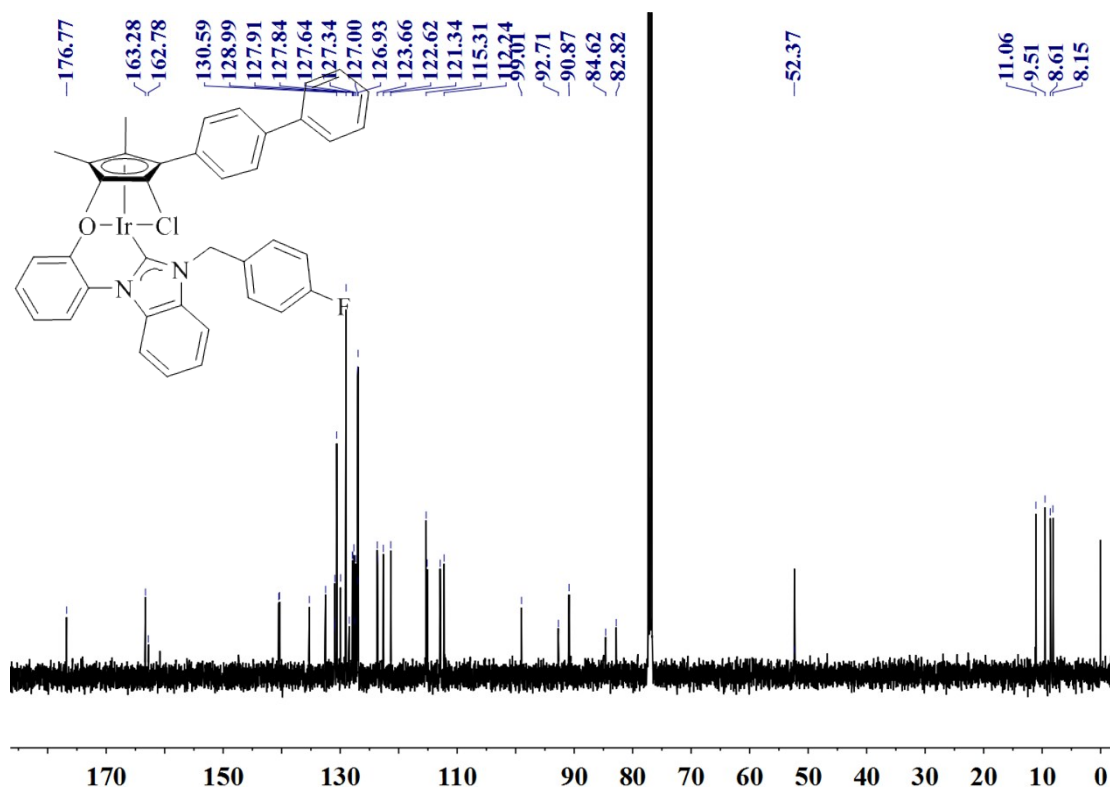


**Figure S50.** The  $^{13}\text{C}$  NMR (126 MHz,  $\text{CDCl}_3$ ) peak integrals of  $[(\eta^5\text{-C}_5\text{Me}_4\text{C}_6\text{H}_4\text{C}_6\text{H}_5)\text{Ir}(\text{L4})\text{Cl}]$  (12).

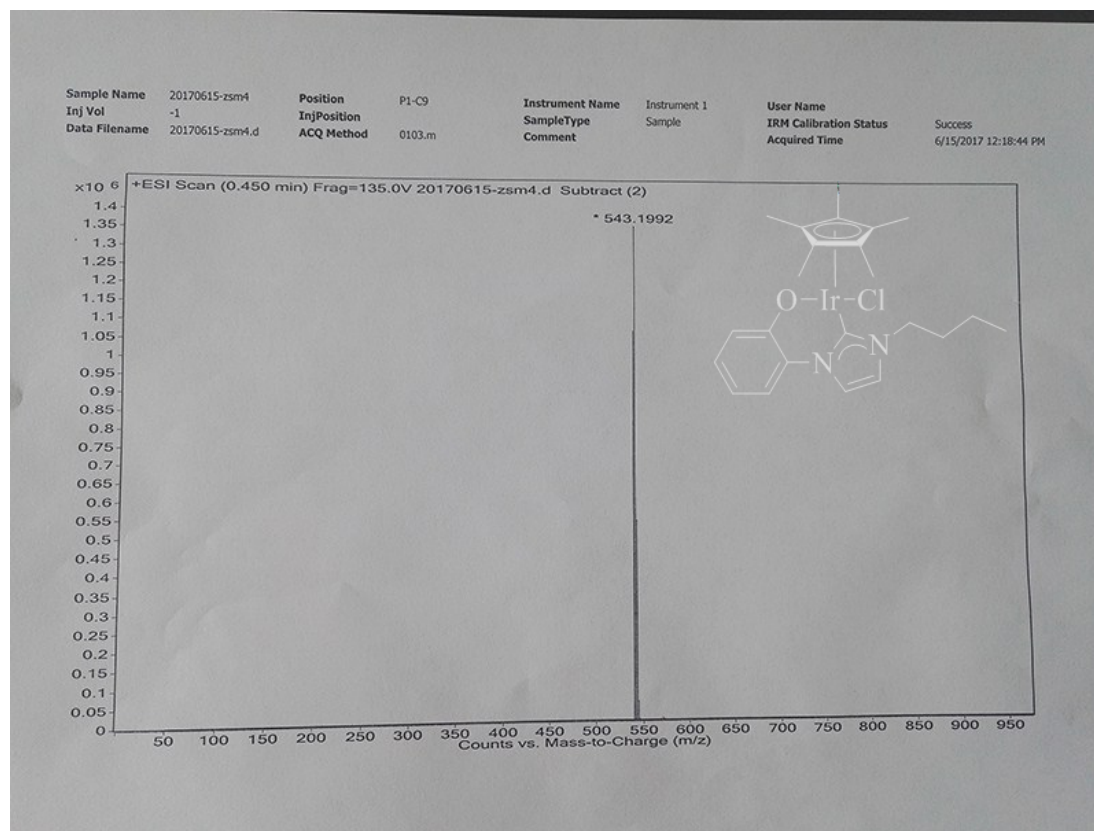


**Figure S51.** The Mass spectrometry of  $[(\eta^5\text{-C}_5\text{Me}_5)\text{Ir}(\text{L1})\text{Cl}]$  (**1**).

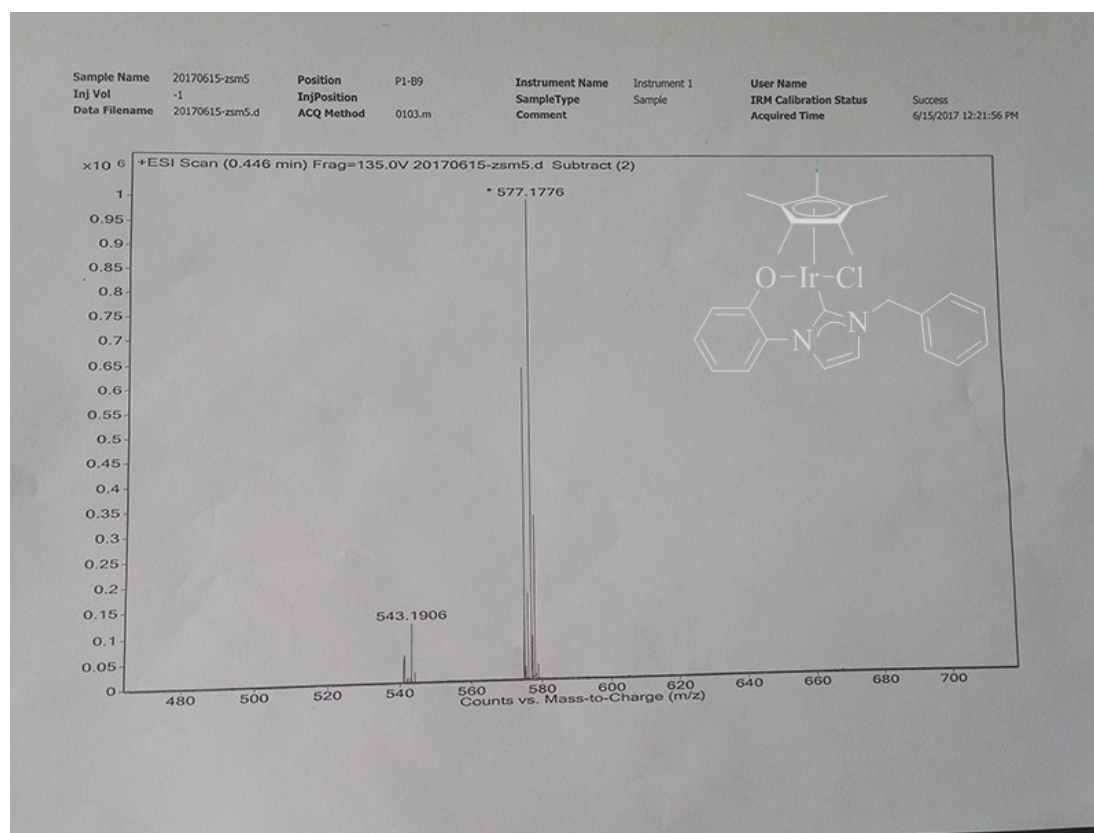


**Figure S52.** The Mass spectrometry of  $[(\eta^5\text{-C}_5\text{Me}_5)\text{Ir}(\text{L2})\text{Cl}]$  (**2**).

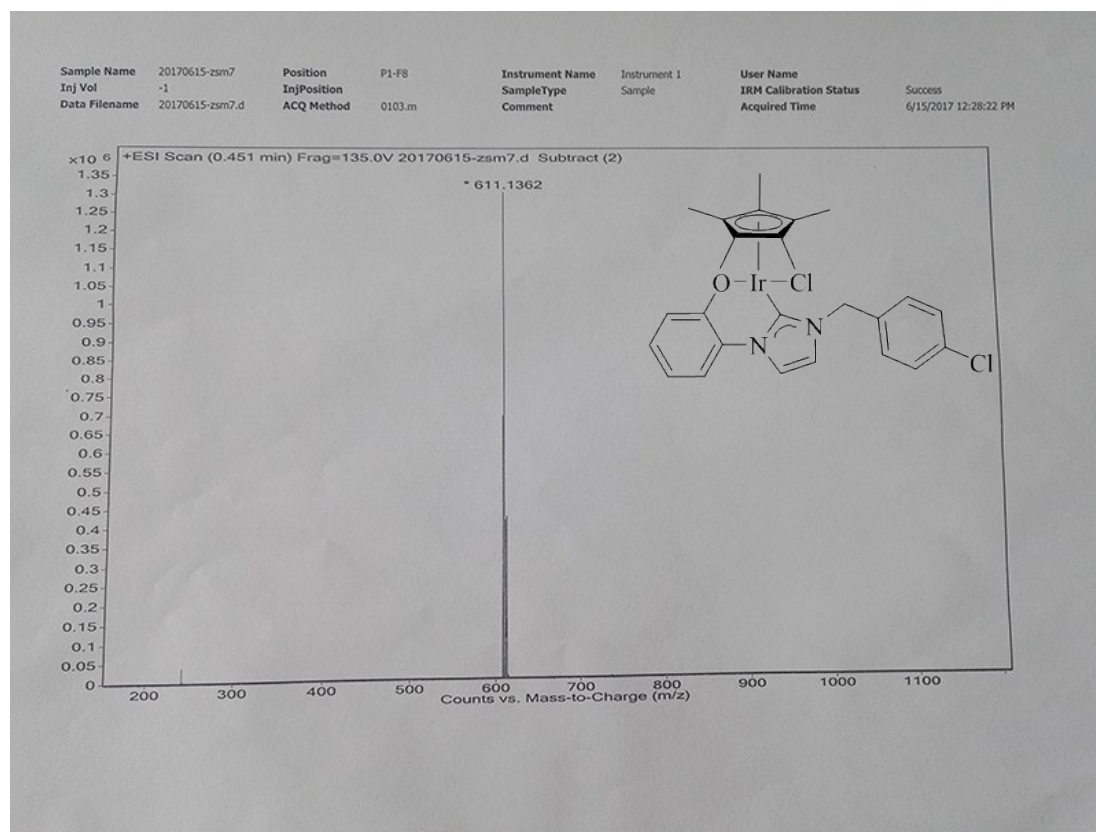


**Figure S53.** The Mass spectrometry of  $[(\eta^5\text{-C}_5\text{Me}_5)\text{Ir}(\text{L}3)\text{Cl}]$  (**3**).

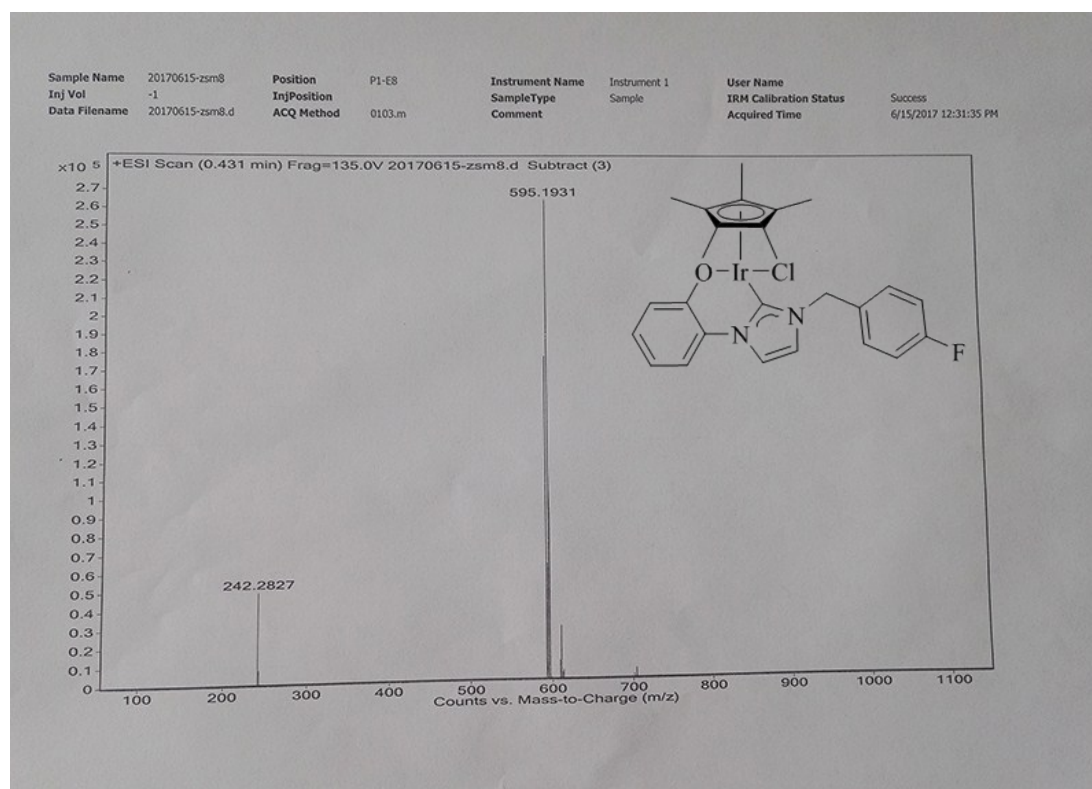


**Figure S54.** The Mass spectrometry of  $[(\eta^5\text{-C}_5\text{Me}_5)\text{Ir}(\text{L}4)\text{Cl}]$  (**4**).

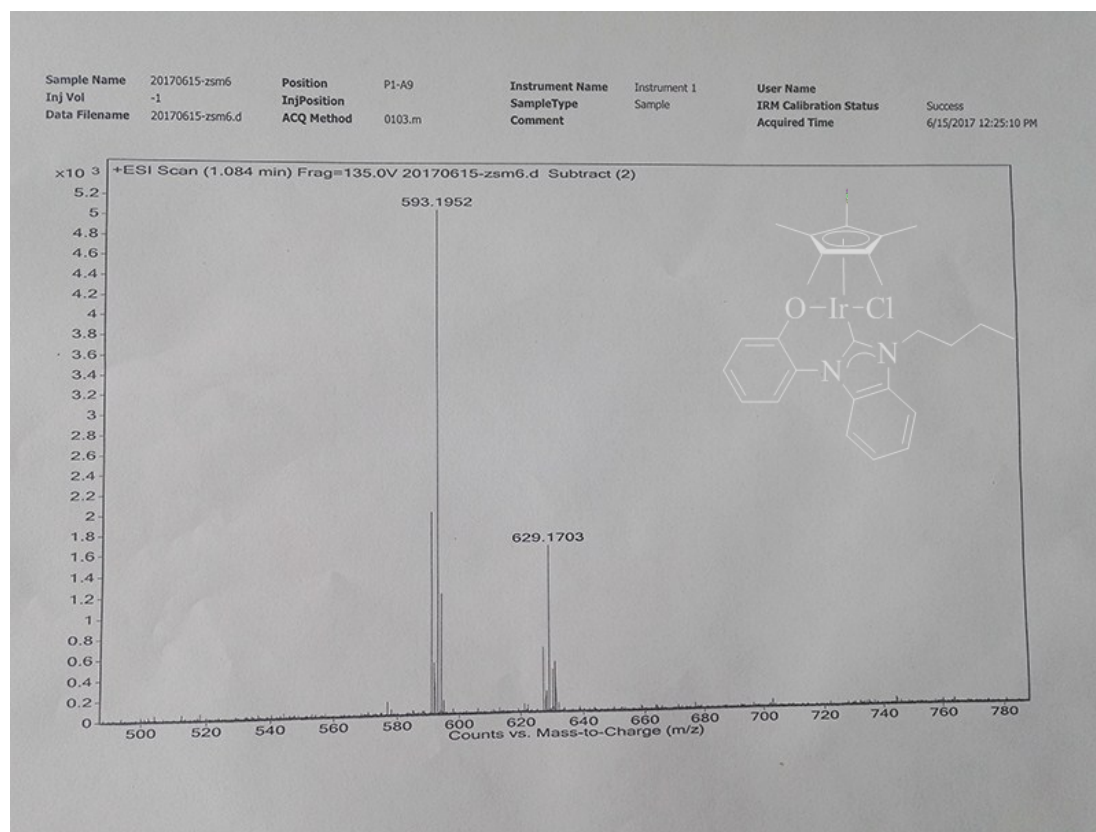
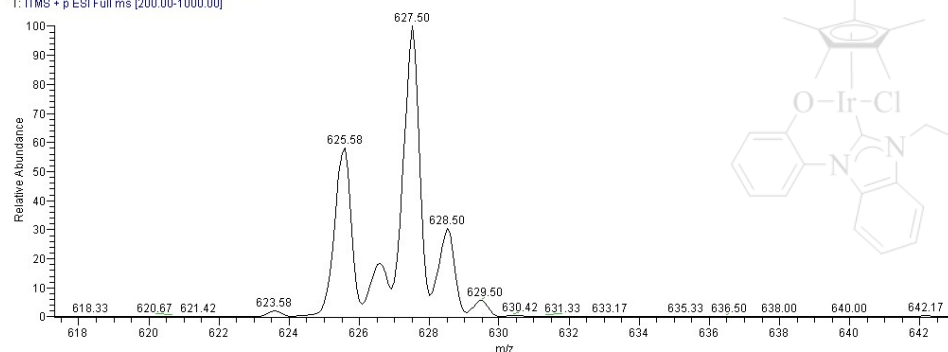


**Figure S55.** The Mass spectrometry of  $[(\eta^5\text{-C}_5\text{Me}_5)\text{Ir}(\text{L5})\text{Cl}]$  (**5**).

lz2 #27-76 RT: 0.08-0.21 AV: 50 NL: 5.35E3  
T: ITMS + p ESI Full ms [200.00-1000.00]



lz2 #27-76 RT: 0.08-0.21 AV: 50 NL: 5.35E3  
T: ITMS + p ESI Full ms [200.00-1000.00]

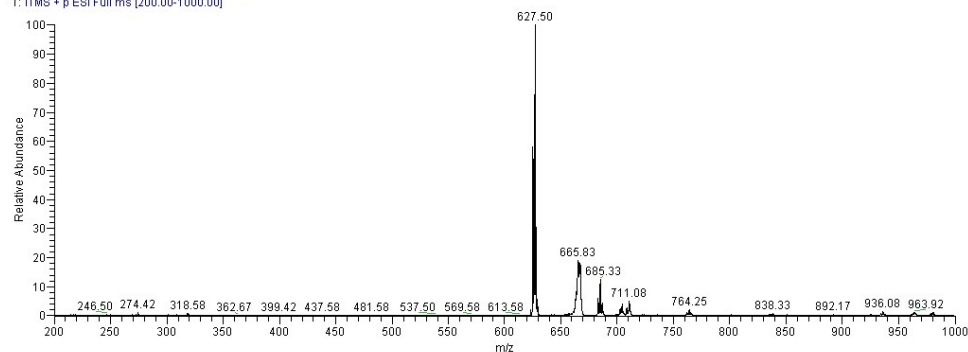
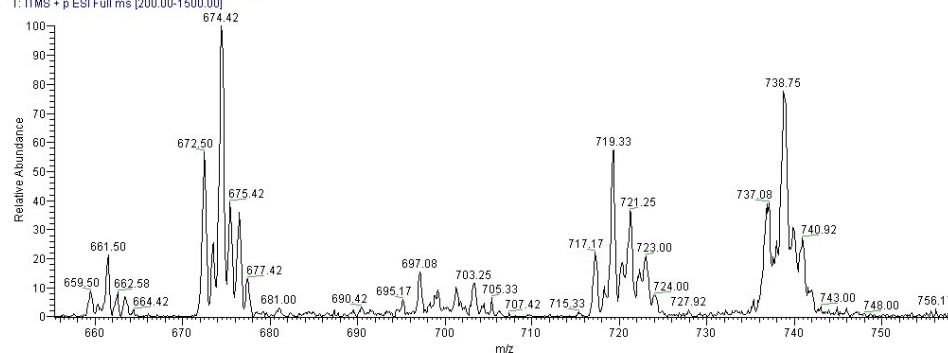


**Figure S56.** The Mass spectrometry of  $[(\eta^5\text{-C}_5\text{Me}_5)\text{Ir}(\text{L6})\text{Cl}]$  (**6**).

lz03 #89-99 RT: 0.32-0.36 AV: 11 NL: 8.83E2  
T: ITMS + p ESI Full ms [200.00-1500.00]



lz03 #89-99 RT: 0.32-0.36 AV: 11 NL: 8.83E2  
T: ITMS + p ESI Full ms [200.00-1500.00]

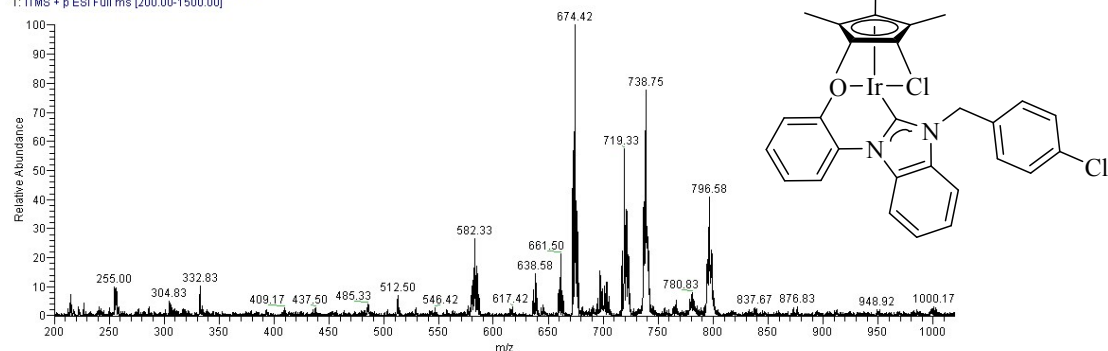


**Figure S57.** The Mass spectrometry of  $[(\eta^5\text{-C}_5\text{Me}_5)\text{Ir}(\text{L7})\text{Cl}]$  (**7**).

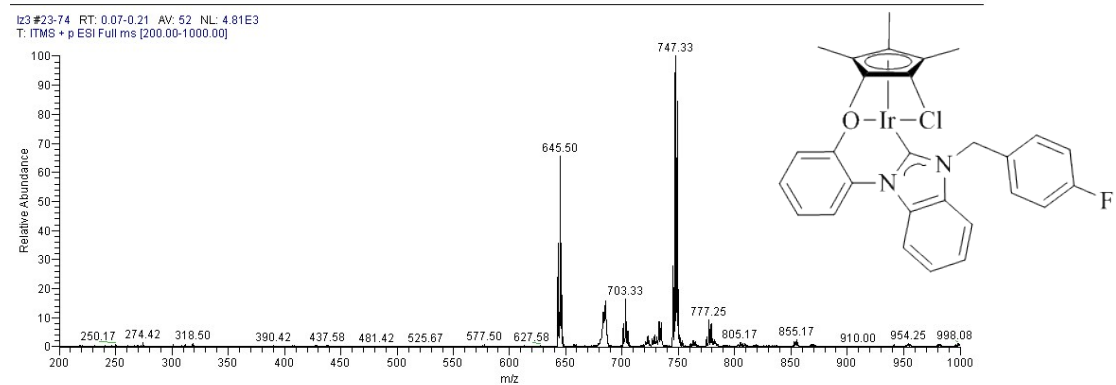
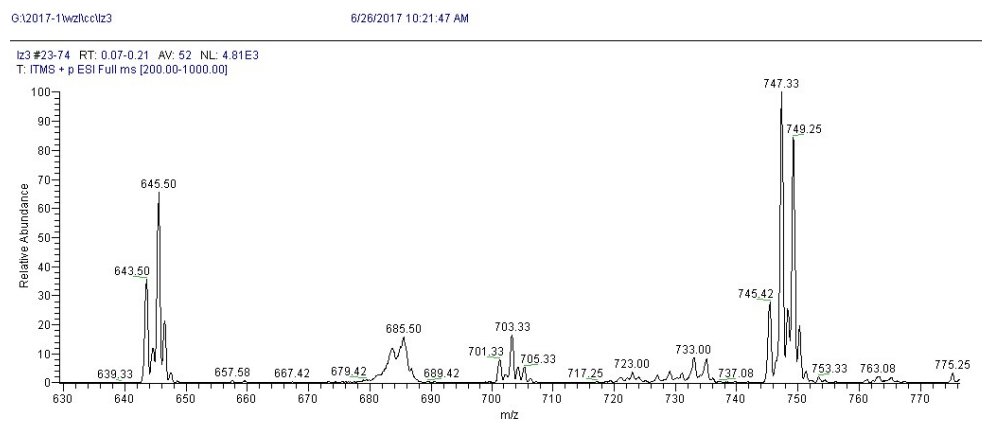


**Figure S58.** The Mass spectrometry of  $[(\eta^5\text{-C}_5\text{Me}_5)\text{Ir}(\text{L8})\text{Cl}]$  (**8**).

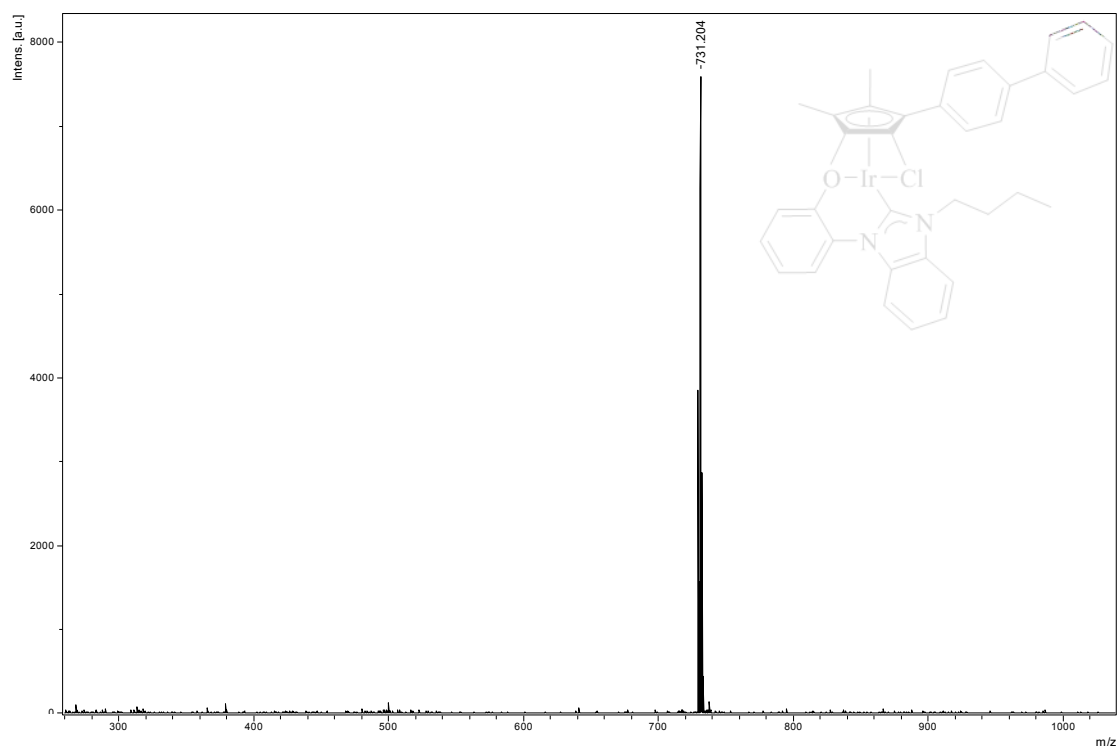


**Figure S59.** The Mass spectrometry of  $[(\eta^5\text{-C}_5\text{Me}_4\text{C}_6\text{H}_4\text{C}_6\text{H}_5)\text{Ir}(\text{L1})\text{Cl}]$  (**9**).

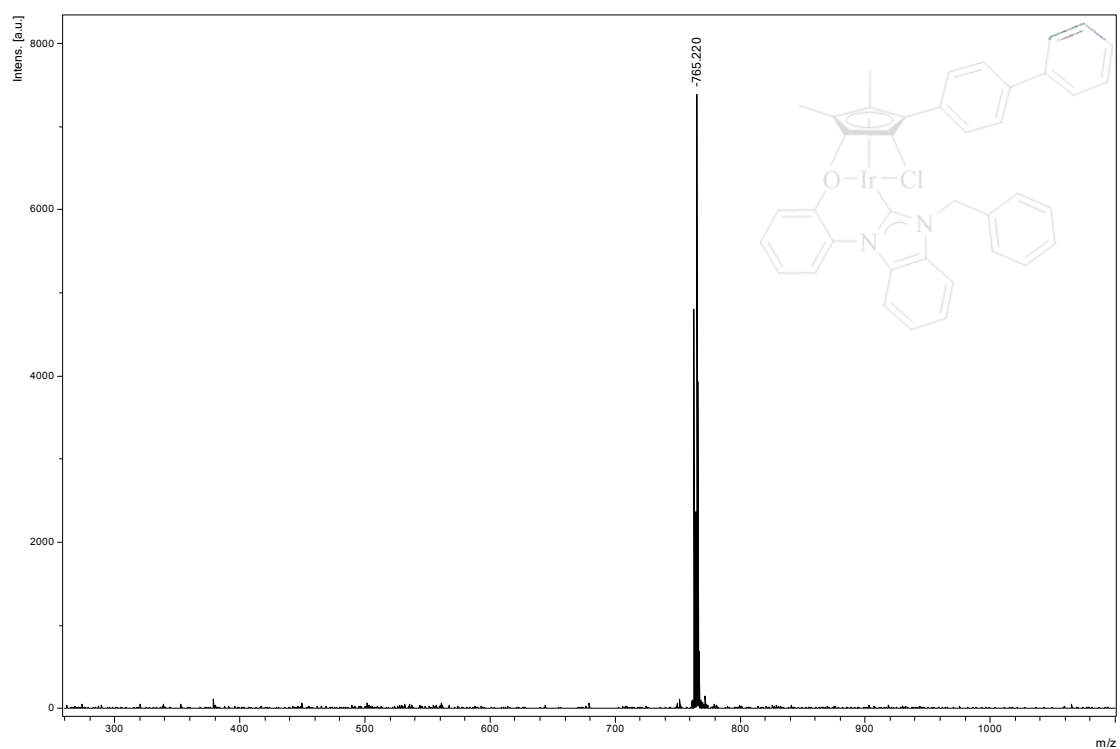


**Figure S60.** The Mass spectrometry of  $[(\eta^5\text{-C}_5\text{Me}_4\text{C}_6\text{H}_5)\text{Ir}(\text{L}2)\text{Cl}]$  (**10**).

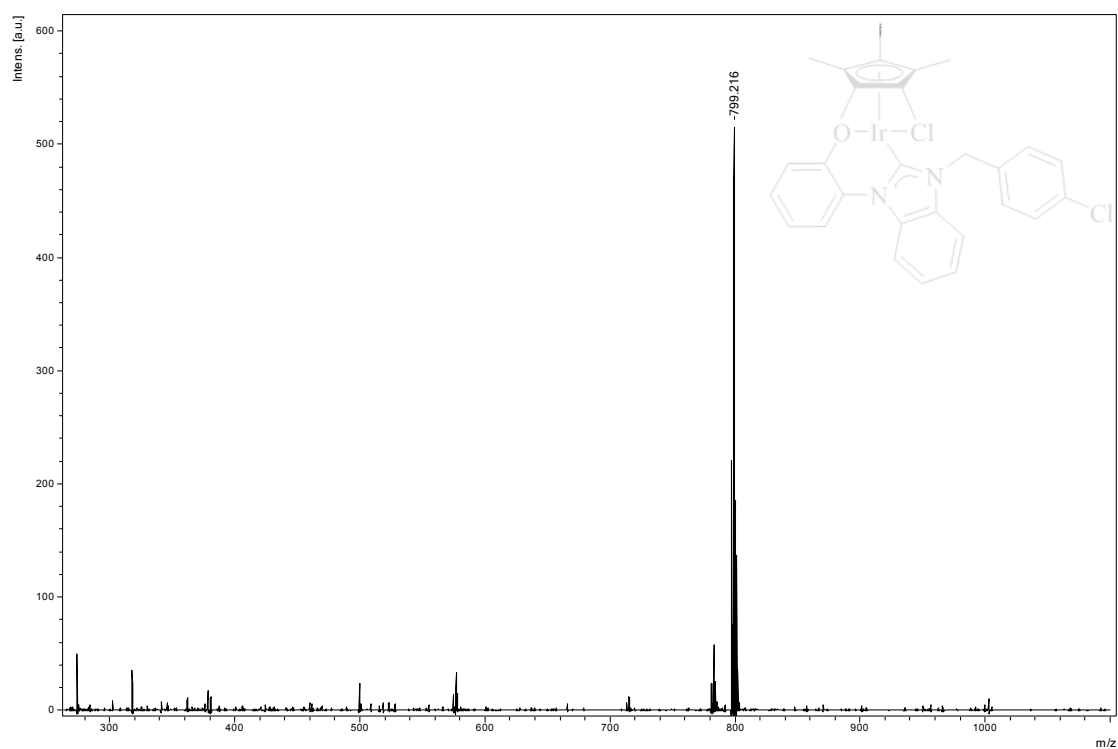


**Figure S61.** The Mass spectrometry of  $[(\eta^5\text{-C}_5\text{Me}_4\text{C}_6\text{H}_5)\text{Ir}(\text{L}3)\text{Cl}]$  (**11**).

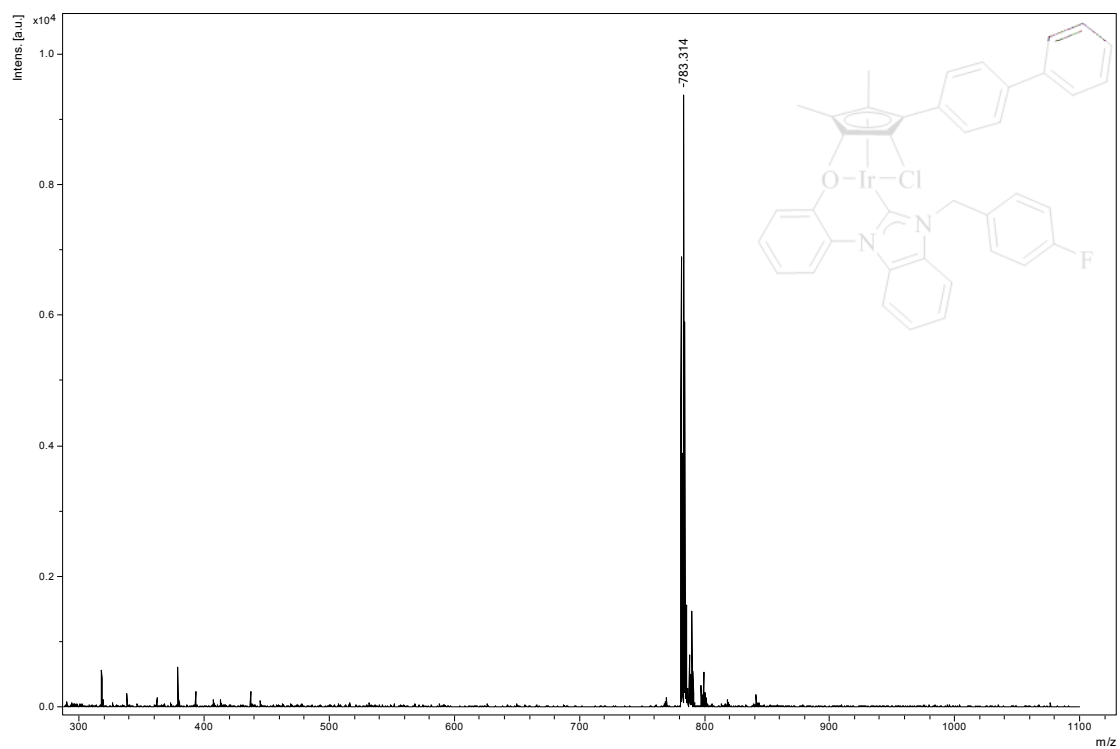


**Figure S62.** The Mass spectrometry of  $[(\eta^5\text{-C}_5\text{Me}_4\text{C}_6\text{H}_5)\text{Ir}(\text{L4})\text{Cl}]$  (**12**).